Doctoral Thesis

Quantitative analysis of cellular behaviour during zebrafish optic cup morphogenesis

María Nicolás Pérez

Director: Juan Ramón Martínez Morales

Tutor: Manuel J. Muñoz

Julio 2014

"La mejor forma de vencer las dificultades
es atacarlas con una magnifica sonrisa"

Baden Powell

A mis padres y amigos

I. Abbreviations **13**

II. Resumen **17**

III. Introduction

1. Morphogenesis 25
   1.1 Polarity and cellular junctions 25
      1.1a Adherens Junctions or Zonula Adherens 27
      1.1b Desmosomes or Macula Adherens 28
      1.1c Focal adhesions or Hemidesmosomes 29
   1.2 Cytoskeleton reorganization and cellular junctions orchestrate cell shape changes 32
   1.3 Mitosis 33
   1.4 Cell migration 34
2. Epithelial morphogenesis 34
3. Apical constriction 36
   3.1 Apical constriction during invertebrate development 37
   3.2 Apical constriction during vertebrate development 38
   3.3 Molecular basis of apical constriction 38
4. Basal constriction 40
5. Eye morphogenesis 43
   5.1 Evagination 43
   5.2 Elongation 44
   5.3 Invagination 44
      5.3a Neural Retina 44
      5.3b Retinal Pigmented Epithelium 46
      5.3c Lens involvement in retina invagination 46
   5.4 Rotation 47
6. Zebrafish as a model organism for eye development 48

IV. Objetives **50**

V. Materials and Methods

1. Cloning into Tol2 destination vectors 53

2. Maintenance of zebrafish (*Danio rerio*) 56
3. Injection of transgene constructs 57
4. Screening of F1 carriers 57
5. Stable transgenic lines 57
6. Mounting of embryos for *in vivo* imaging 59
7. Confocal imaging 59
8. Data processing and analysis 60
   8.1 Image processing with ImageJ
   8.2 Segmentation
   8.3 Intensity measurements
   8.4 Other measurements
9. Transplantation at blastula stages 62
10. RNA synthesis 63
11. Inhibitor treatment 63
12. *Lamc1*MO injections 63
13. Eye phenotypic characterization 64

VI. Results 66

1. Neural retina thickness does not change during optic cup Morphogenesis 67
2. Surface quantification during optic cup folding 69
3. Behaviour of cells at the apical side 71
4. Behaviour of cells at the basal side 73
5. Apical and basal cell surfaces in the retina oscillate in an uncoupled fashion 75
6. Mitosis is not essential for correct retina folding during OCM 76
7. Actin dynamics at the basal feet of retinal neuroblasts 78
8. Basal accumulation of Myosin *foci* is required to the folding during OCM 80
9. Blebbistatin treatment blocks OC folding 83
10. *lamc1* morphant embryos show defects in optic cup folding 88

VII. Discussion 95

1. Neuroepithelial cell shape changes generate the basal

constriction that drives optic cup folding 97
2. Myosin *Foci* Cause Cell Area Decrease and Transient Shortening of Apico-Basal Axis 99
3. Laminin γ Chain Is Essential for the Correct Optic Cup Morphogenesis 99

VIII. Conclusions 103

IX. Supplementary Material 107

X. References 121

XI. Appendix 131

XII. Acknowledgements 147

Contents

Figure 1. Adherens junctions. 28
Figure 2. Focal adhesion binding to the ECM. 31
Figure 3. Quantification of basal behaviour in *Drosophila* follicle cells. 35
Figure 4.Genetic networks required for apical constriction during *Drosophila* gastrulation and vertebrate neural tube formation. 40
Figure 5. Relaxation and contraction states during egg chamber elongation in *Drosophila.* 41
Figure 6. Opo localization and interactions during medaka fish eye morphogenesis. 42
Figure 7. Eye morphogenesis. 45
Figure 8.Tol2 Cloning strategy. 55
Figure 9. Stages of embryonic development in zebrafish. 56
Figure 10. Expression patterns of transgenic lines used. 58
Figure 11. Imaging approach for visualization of apical and basal surfaces of the neural retina. 60
Figure 12. Schematic approach used for image analysis. 61
Figure 13. Schematic approach of embryos for transplantation experiment. 62
Figure 14. Retinal apico-basal axis length does not change significantly during zebrafish optic cup folding. 68
Figure 15. Cell surface area variations during optic cup folding at the apical and basal surface of the retinal epithelium. 70
Figure 16. Cell behaviour at the apical side of the neural retina. 72
Figure 17. Basal constriction during zebrafish optic cup folding. 74
Figure 18. Cell clones in transplanted embryos show uncoupled oscillations at apical and basal surfaces. 76
Figure 19. Mitosis does not play an essential role in basal constriction in zebrafish optic cup folding. 77
Figure 20: Actin accumulation at the basal side of neural retina cells. 79
Figure 21. Myosin accumulates at the basal side of the neural retina during zebrafish optic cup folding. 80
Figure 22. The presence of Myosin *foci* at the basal surface associates with basal cell surface reduction. 81
Figure 23. Myosin *foci* at the basal surface produce a transient decrease of apico-basal axis length. 83
Figure 24. Blebbistatin treatment interferes with optic cup folding. 85
Figure 25. Blebbistatin increases Myosin *foci* stability. 87
Figure 26. Optic cup folding defects caused by *lamc1*MO injection. 89

Figura 27. *lamc1* morphant embryos display retina defects. 90
Figure 28. Myosin *foci* are more stable in *lamc1*MO injected embryos. 91
Figure 29. Myosin *foci* accumulation at the basal retina does not correlate with apico-basal axis length changes in *lamc1*MO injected embryos. 92
Figure 30. A model for actomyosin network behaviour during optic cup folding. 99

I. Abbreviations

Abbreviations

bp	base pairs
DNA	Desoxiribo Nucleic Acid
ECM	Extracellular matrix
EMT	Epithelial to Mesenchymal Transition
ENU	N-ethyl-N-nitrosuourea
ESCs	embryonic stem cells
FAK	focal adhesion kinase
GFP	Green Fluorescent Protein
Hpf	hours *post* fertilization
IKNM	Interkinetic nuclear migration
MET	mesenchymal-to-epithelial transition
MHB	Midbrain-Hindbrain boundary
MHBC	Midbrain-Hindbrain boundary constriction
MO	morpholino oligonucleotides
MRLC	myosin regulatory light chain
NR	neural retina
OC	Optic Cup
OCM	Optic Cup Morphogenesis
OV	optic vesicle
PCR	Polymerase Chain Reaction
PTB	phosphotyrosine binding
RPCs	retinal progenitor cells
RPE	retinal pigmented epithelium
RNA	Ribo Nucleic Acid
wt	wild type

II. Resumen

Durante el desarrollo embrionario las células sufren una serie de procesos morfogenéticos altamente acoplados y regulados para formar tejidos y órganos complejos que darán lugar al individuo adulto. Por tanto, la morfogénesis se define como un conjunto de procesos biológicos que reorganizan las células y los tejidos para constituir todas las formas de vida conocidas.

Los organismos siguen un programa genético que define el orden en el que se suceden los procesos morfogenéticos según un plan corporal conservado. Existen muchos estudios acerca de los mecanismos moleculares que hay detrás de estos procesos altamente regulados (Lecuit *et al.* 2007). Estos procesos hacen que muchas características celulares tales como la forma o la polaridad se modifiquen según la función y/o la localización que las células tendrán en el organismo. De entre las características celulares que se pueden ver afectadas, resaltaremos la polaridad (distribución asimétrica de componentes celulares en la membrana), las uniones celulares (que conectan las células con otras células o con el sustrato y permiten la transmisión de fuerzas de unas células a otras), los cambios de forma, que se deben a la reorganización del citoesqueleto de actomiosina, la migración celular y la división celular, que tiene lugar en la superficie apical de los epitelios (Harris *et al.* 2014; Mammoto *et al.* 2010; Nelson 2009; Sauer 1935). La relación entre todas estas características también se puede modificar durante el desarrollo de un órgano concreto. La alteración de estas características o de la relación existente entre ellas puede conducir a situaciones patológicas (Thiery *et al.* 2009). Por tanto, entender los mecanismos que subyacen al desarrollo y funcionamiento de tejidos y órganos, puede ayudar a prevenir y tratar enfermedades.

Dado que muchos tejidos del organismo adulto son, o fueron epitelios en algún momento del desarrollo, el estudio de las hojas epiteliales, constituidas por células polarizadas que se extienden desde una superficie apical hasta una lámina basal, permite conocer los mecanismos que subyacen a la morfogénesis de los epitelios en diversas especies (Bryant *et al.* 2008; Lecuit *et al.* 2007).

La morfogénesis epitelial depende de la relación entre uniones celulares, cambios de forma y tensión cortical. Estudios recientes han demostrado que los cambios de forma celulares se producen mediante el comportamiento oscilatorio de la red de actomiosina. Dicha red se recluta y se dispersa, bien en la superficie apical o basal de las células, produciendo contracción y relajación de la membrana respectivamente (Gorfinkiel *et al.* 2011).

De entre todos los procesos morfogenéticos, el más conocido en los epitelios animales es la constricción apical.

La constricción apical consiste en una disminución de área en la superficie apical de la célula que hace que éstas cambien su forma columnar inicial a una forma cónica. Sin embargo, la relevancia de la constricción apical reside en que puede producir un cambio irreversible mediante el llamado "mecanismo de trinquete" que da lugar a la invaginación de una hoja epitelial, es decir, el plegamiento de un epitelio plano para formar un órgano con estructura tridimensional (Martin *et al.* 2009; Sawyer *et al.* 2010). Este proceso es responsable de la gastrulación de *Drosophila*, y *Xenopus*, asi como de la morfogénesis del tubo neural y la formación de la lente en vertebrados (Sawyer *et al.* 2010).

Aunque menos conocida que la constricción apical, este fenómeno de contracción (cambio reversible) y constricción (cambio irreversible) también afecta a la superficie basal. Algunos ejemplos de ello podrían explicar el crecimiento de la cámara ovárica de *Drosophila*, el desarrollo del sistema nervioso o la morfogénesis del ojo de vertebrados (Gutzman *et al.* 2008; He *et al.* 2010; Martinez-Morales *et al.* 2009). Y es precisamente la morfogénesis del ojo el sistema elegido como modelo en este trabajo para aclarar los mecanismos que producen la constricción basal.

La morfogénesis del ojo de vertebrados se puede dividir en cuatro fases; evaginación, elongación, invaginación y rotación (Kwan *et al.* 2012). Durante la evaginación, las células que forman el campo óptico en el cerebro anterior migran bilateralmente para formar las vesículas ópticas a ambos lados del embrión (Rembold *et al.* 2006). En el pez cebra se ha visto que hay dos poblaciones celulares distintas; las células marginales que muestran polaridad apico-basal y las células del núcleo que no muestran polaridad (Ivanovitch *et al.* 2013). Para formar las vesículas ópticas, estas células experimentan una constricción apical. Durante la invaginación, por el contrario, el mecanismo sugerido para la formación de la copa óptica es la constricción basal. En embriones del pez medaka, la proteína transmembrana Opo regula la endocitosis de integrinas en el lado basal de las células. Mutantes para esta proteína muestran un fenotipo en el que la retina neural no se pliega y por tanto, no se forma la copa óptica (Martinez-Morales *et al.* 2009). Estos estudios sugieren una relación entre los cambios de forma, la adhesión de las células al sustrato y el plegamiento de la retina.

En esta tesis analizamos de forma exhaustiva el comportamiento celular de la retina neural durante la morfogénesis de la copa óptica, usando el pez cebra como organismo modelo. Los resultados obtenidos de nuestro estudio confirman que la constricción basal que experimentan las células de la retina es el proceso principal que dirige la formación de la copa óptica.

Para analizar el comportamiento de las células se han usado diferentes líneas transgénicas que marcan las membranas de las células de la retina u otros componentes

celulares como la miosina. Con el fin de cuantificar las variaciones de área en las superficies apicales y basales de las células, realizamos películas de microscopia confocal *in vivo* y segmentamos las imágenes obtenidas. La segmentación permite identificar cada célula como una unidad y calcular diversos parámetros tales como el área o el perímetro.

De entre los resultados obtenidos relacionados con los cambios de forma cabe destacar que entre 19 y 20hpf (*hours post-fertilization* del inglés), coincidiendo con el momento en el que se produce el máximo plegamiento (ver Figure 24), las células sufren una disminución significativa de área en la superficie basal. Esa disminución de área se produce tras sucesivas contracciones irreversibles de la membrana de forma similar al mecanismo de trinquete descrito en *Drosophila* (ver Figures 15 y 17). A continuación, entre 20 y 21hpf los neuroblastos incrementan su área en la superficie apical haciendo que las células adopten la forma cónica final (ver Figures 15 y 16).

Con el fin de analizar si esas contracciones y relajaciones de la membrana ocurren simultáneamente en ambas superficies, se llevaron a cabo diferentes experimentos de trasplante de células procedentes de embriones transgénicos a embriones silvestres. Esto permite visualizar neuroblastos transgénicos de forma aislada. Los datos obtenidos revelan que las contracciones de ambas superficies no están acopladas (ver Figure 18).

Para esclarecer los mecanismos moleculares que producen estos cambios de forma en las células, realizamos películas *in vivo* con la línea transgénica que marca la miosina así como inyecciones del ARN de un marcador de actina llamado Utrophin. En el caso de la actina los resultados muestran una correlación positiva entre los cambios de área y la acumulación de actina en la superficie basal. Esto sugiere que la actina no contribuye de forma directa a la reducción de área celular (ver Figure 20). Para la miosina, esos análisis revelaron que durante el plegamiento de la copa óptica, la miosina se acumula en la superficie basal de las células en forma de pequeños focos que aparecen durante unos minutos. La presencia de esos focos en la célula se asocia a la disminución de área en la superficie basal y a acortamientos transitorios del eje apico-basal (ver Figures 21, 22 y 23). Estudios con la droga blebbistatin que interfiere con la actividad ATPasa de la miosina, muestran que en embriones tratados con este compuesto se inhibe el plegamiento de la copa óptica. Además, el blebbistatin incrementa la estabilidad de los focos de miosina en la superficie basal. Sin embargo, en presencia del inhibidor, estos focos de miosina no se asocian a reducciones de área ni al acortamiento del eje apico-basal como ocurre en el caso del silvestre (ver Figures 24 y 25). Estos resultados confirman que la miosina desempeña un papel fundamental en el desarrollo del ojo.

En este trabajo también se abarca la relación de la adhesión a la matriz extracelular con el plegamiento. Para ello se utilizó un morfolino para la cadena γ de la laminina, que es

el principal componente de la matriz. Las injecciones del morfolino produjeron embriones con un fenotipo en el ojo que se caracterizaba por la abertura ventral de la retina, el incremento de la longitud del eje apico-basal y mayor estabilidad de los focos de miosina (ver Figures 26, 27, 28). Nuevamente, este incremento en la estabilidad de los focos no está asociado a acortamientos del eje apico-basal (ver Figure 29).

En conclusión, esta tesis propone que los cambios de forma celulares controlados por el mecanismo de trinquete son responsables del plegamiento de la copa óptica. Además, la localización basal de los focos de miosina y la correcta adhesión a la matriz extracelular a través de la Laminina son esenciales para el adecuado plegamiento de la retina durante el desarrollo del pez cebra.

III. Introduction

1. Morphogenesis

During embryonic development, cells have to be assembled into complex organs. This is enabled by a number of tightly-coupled morphogenetic processes, which regulate the construction of the whole organism. Morphogenesis is, therefore, a set of biological processes that reorganizes cells and tissues and gives shape to all known live forms.

Organisms follow a basic genetic program that defines the sequence in which morphological processes should be carried out according to a conserved body plan. Many studies have investigated the mechanics behind these processes (reviewed in (Lecuit *et al.* 2007)). These are highly regulated mechanisms, which co-ordinately transform individual cell changes into fully organised, tissular structures. Thus, cells display several characteristics such as shape and polarity that are modified according to their function and/or the localization they will have within the body. Among all cellular features that can be affected, we will pay special attention to polarity, cell-cell and cell-substrate adhesion, shape changes, division and migration. The relationship between these features can also be modified during the shaping of specific tissues. Altering these characteristics or the interplay between them can produce congenital malformations (Thiery *et al.* 2009). So, understanding the mechanisms that control these cellular features and their relationships is essential to understand and correct pathological situations.

1.1 Polarity And Cellular Junctions

One of the most important cellular features having a significant impact on morphogenesis is the presence of a polarity axis. This is created by the structural asymmetry of the cellular components in the membrane, specially the localization of: polarity complexes such as Crumbs and Par (Aranda *et al.* 2008; Moreno-Bueno *et al.* 2008; Nelson 2009), some cytoskeleton related proteins (Nelson 2003) and adhesion molecules like integrins and cadherins that regulate cell-cell or cell-substrate contacts (Hynes 1992; Ozawa *et al.* 1989; Ozawa *et al.* 1990). Polarity is part of the cellular differentiation program and is required for processes such as cell migration and cell division to take place. According to their polarity orientation, cells can be divided into epithelial or mesenchymatic cells. Epithelial cells display an apico-basal polarity axis and are attached both to neighbouring cells and to the basement membrane. Mesenchymal cells, in contrast, are able to migrate and are organized along a front-rear axis, according to the direction of migration (Moreno-Bueno *et al.* 2008; Nelson 2009). Both types of cells can convert in the other by either epithelial-to-mesenchymal transition (EMT), which

involves the loss of cell-cell contact as well as the acquisition of directional migration and front-rear polarity, or by mesenchymal-to-epithelial transition (MET) which involves the loss of free mobility and the acquisition of apico-basal polarity and cellular attachments (Moreno-Bueno *et al.* 2008; Nelson 2009). An inappropriate loss of the polarity axis is associated with pathological situations such as cancer (Aranda *et al.* 2008; Moreno-Bueno *et al.* 2008).

Front-rear polarity is present in mesenchymatic cells, and is initiated by the action of some external cues such as the extracellular matrix (ECM) and some growth factors, as well as by the distribution of phosphatidylinositides. Phosphatidylinositide-3,4,5-triphosphate (PtdIns(3,4,5)P3) is enriched in the plasma membrane at the front of the cell, whereas phosphatidylinositide-3,4-bisphosphate (PtdIns(3,4)P2) is enriched everywhere else, including the rear (Nelson 2009).

In contrast, apico-basal polarity presents in epidermal cells, is achieved by the interplay of three polarity complexes with the cytoskeleton and cellular junctions. These complexes are the Scribble complex, the Crumbs complex and the Par complex, which define the basolateral domain, the apical domain and the apicolateral domain respectively (Aranda *et al.* 2008).

- The Par complex is composed by the Par3 and Par6 proteins, the serine/threonine kinase aPKC, and small GTPases such as Cdc42 and Rac1. The complex is involved in the assembly of tight junctions, and in the spatially restriction of the cytoskeleton during cell division. In turn, Par proteins can be regulated intracellularly (i.e. phosporilation of aPKC can either inhibit apoptosis in kidney epithelial cells or determine migration in fibroblast). Each protein is also able to display individual cellular functions such as the regulation of different signalling pathways (Aranda *et al.* 2008; Moreno-Bueno *et al.* 2008).
- The Crumbs complex is localized at the apical side and is formed by the transmembrane protein Crumb (Crb) and the cytoplasmic scaffolding proteins PALS1 and PATJ. They are involved in the formation and maintenance of membrane domain by regulating intracellular transport of proteins (Moreno-Bueno *et al.* 2008; Nelson 2003).
- The Scribble complex, localized at the basolateral membrane, is composed by three proteins: Scribble (Scrib), Disc large (Dlg) and Lethal giant larvae (Lgl). They are involved in the maintenance of the lateral membrane domain (Moreno-Bueno *et al.* 2008; Nelson 2003).

The interplay of polarity complexes, cytoskeleton organization and cellular junctions is crucial during development. Intercellular contacts allow the transmission of mechanical forces generated by individual cells into tissue level, thus having a key role in the morphogenetic processes that shape the organs (Martin *et al.* 2010; Solon *et al.* 2009). The relationship between the polarity complexes mentioned above and the intercellular junctions makes difficult the establishment of an order in the generation of polarity; in some cases, actin filaments are recruited to apical side already marked by the presence of PAR proteins. In other cases, the apical domain is clearly defined by tight junctions which form a barrier that prevents intermixing of membrane protein between apical and basolateral domains (Aranda *et al.* 2008; Mammoto *et al.* 2010; Nance *et al.* 2003). We will pay special attention to some of these junctions:

1.1a Adherens Junctions or Zonula Adherens

Adherens junctions are intercellular contacts that start when lamellipodia or filopodia from neighbouring cells interact through E-cadherin (also known as uvomorulin) (Ozawa *et al.* 1989). E-cadherins are transmembrane proteins structured in clusters at the basolateral plasma membrane that interact with the same type of cadherins from adjacent cells with the extracellular domain (Ozawa *et al.* 1989). Through the intracellular domain, E-cadherins bind with high affinity to β-catenin (a peripheral cytoplasmic protein involved in the junction) (Aberle *et al.* 1994; Ozawa *et al.* 1989; Ozawa *et al.* 1990) forming a stable complex (see Figure 1). This complex recruits F-actin, through catenins, actin binding proteins and several scaffold proteins, to the cellular cortex (Ozawa *et al.* 1990; Yamada *et al.* 2005). The cytoplasmic domain of E-cadherins, as well as the structure of catenins, display a high degree of conservation among species, suggesting that they play a key role during development (Ozawa *et al.* 1989). Upon cadherin binding, the actomyosin network rearranges and form an actin belt through the combined action of formins (i.e. Dia1), Myosin II (Carramusa *et al.* 2007) and the small GTPases Rac1 and RhoA. These GTPases are intracellular proteins that are essential for both; to stabilize cadherins at the intercellular junction and for the clustering of receptors at the contact zone. Rac1 but not RhoA, is also crucial to mediate the formation of actin structures associated with E-cadherin contacts in keratinocytes and fibroblasts (Braga *et al.* 1999; Braga *et al.* 1997).

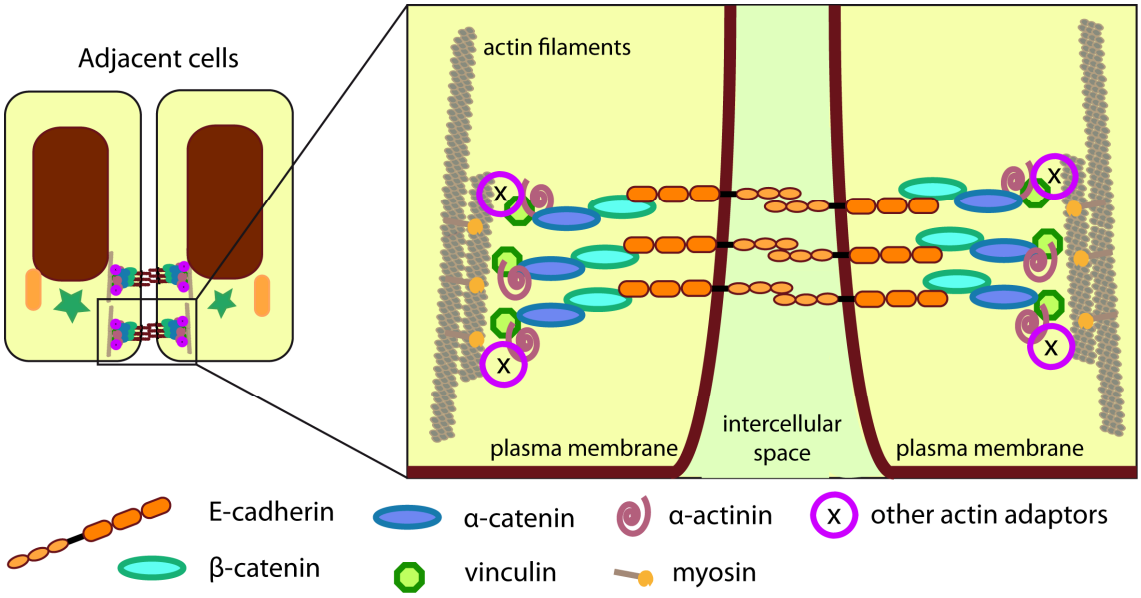

Figure 1. Adherens junctions. Adherens junctions link actin cytoskeleton and E-cadherin by the cytoplasmic complex consisting of β-catenin, α-catenin and some actin binding proteins.

It has been shown that the cytoplasmic anchorage mediated by catenins regulates strength of the cadherin- mediated adhesiveness (Ozawa *et al.* 1990). Furthermore, the formation of these adherens junctions in epithelial monolayers leads to the generation of tensions at the tissue level, which in turn are needed to control cellular rearrangements in a developing epithelium. Morphogenetic tension is created by the actomyosin network contractibility generated *in situ* as adherens junctions form. Moreover, only formin mediated actin polimerization but not the actin nucleator Arp2/3 complex plays a role in tension generation, at least, in MDCK monolayers (Harris *et al.* 2014).

The presence of adherens junctions but also cell-junction remodelling in a developing epithelium can modulate surface tension allowing morphogenetic processes such as cell intercalation or epithelial bending (Lecuit *et al.* 2007).

1.1b Desmosomes or Macula Adherens

Desmosomes are one of the main macromolecular cell surface attachment sites that mediate the interaction between filaments at cell-cell and cell-substrate contacts. They are formed after the initial contact between two cells or between cell and substrate; and are mediated by cadherins (desmoglein and desmocollin), which nucleate a plaque of proteins. At this point, all desmosomal components are recruited to the membrane to shape the mature desmosomal plaque; plakophilin, plakoglobin and/or β-catenin form the outer plaque and desmoplakin constitutes the inner plaque. Afterwards this complex stabilizes

the interaction between adjacent cells and intermediate filaments (Acehan *et al.* 2008; Gallicano *et al.* 1998).

However, although desmosomes link intermediate filaments contacts between neighbouring cells, the presence of desmosomes in a embryonic epithelium does not correlate with the generation or transmission of the tissular tensions needed to shape an organ, suggesting that they do not play a pivotal role in shape changes of epithelia during early development (Harris *et al.* 2014). Moreover, as they do not seem to be regulated by the same molecular components as other junctions, it is likely that they are involved in different cellular processes (Braga *et al.* 1997).

1.1c Focal Adhesion or Hemidesmosomes

Focal adhesions are junctions between cells and the basement membrane and are mediated by integrins, a wide family of cell surface receptor proteins. They are αβ transmembrane heterodimers with a globular extracellular head and a small intracellular domain. Through the extracellular domain, integrins bind to molecules belonging to the extracellular matrix (ECM), especially laminins (see box 1). Through the intracellular tail, especially through the β subunit, they bind to actin adaptors such as talin, vinculin or α-actinin (see Figure 2). Many combinations of α and β subunits can form different integrin heterodimers, but the α5β1 integrins are the major ECM receptors engaged at focal adhesions. Thus, they constitute a major player into the transmission of external forces to the cell. One of the major function of integrins is, therefore, the regulation of mechanical properties such as stiffness or contractile forces, mediating cytoskeletal interactions at the inner face of the plasma membrane where integrin-dependent focal adhesions are located (see Figure 2) (Hynes 1992; Mierke 2013; Tamkun *et al.* 1986). In consequence, focal adhesions are involved in a number of morphogenetic processes such as migration and inflammatory response where a tight coupling of integring recycling and focal adhesion establishment is required.

Box 1: The Extracellular Matrix and its components. Laminins.

The ECM is a relatively or completely insoluble assembly of proteins surrounding cells that form structures such as the basement membrane, interstitial matrices, etc. The basement membrane is, thus, a type of ECM, which is essential in epithelia organization, providing a locus for adhesion of epithelial cells and contributing to the definition of the apico-basal polarity. All basement membranes are composed by a core network of cross-linked type IV collagen, laminins, nidogen (a laminin binding glycoprotein) and perlecan (a huge heparan sulfate glycoprotein) (Hynes 1992; Yurchenco 2011). Laminins are heterotrimeric components of the basement membrane. They are composed by three short arms with at least an α, a β and a γ chains, and a globular domain that binds to several cellular receptors including integrins (see Figure 2). Integrin binding requires the presence of the γ1 laminin chain, although it is not known whether integrins interact in a direct or indirect fashion with this chain (review in (Hohenester *et al.* 2013; Yurchenco 2011)). This interaction between integrins and the γ1 chain of laminins is required in many processes but overall in those implied at early stages during development. When specific laminin chains are missed, the basement membrane fails to form. In zebrafish embryos it has been shown that laminin is essential for notochord development. Removal of laminin γ1 chain prevents formation of basement membrane surrounding the notochord and as a result a failure in notochord cells differentiation (Parsons *et al.* 2002).

Whether initial focal contacts disassemble or progress to become mature focal adhesions, depends on Rho-regulated myosin contractility and the interplay between Rho and Rac, which are members of the Rho GTPases family. Whereas Rac is involved in the formation of new focal contacts by ruffling activity in the membrane allowing the movement, Rho regulates the maduration of pre-existing focal complexes to form more stable focal contacts. Furthermore, Rac and Rho exhibit mutually antagonism effects in their pathways (Braga *et al.* 1997; Rottner *et al.* 1999).

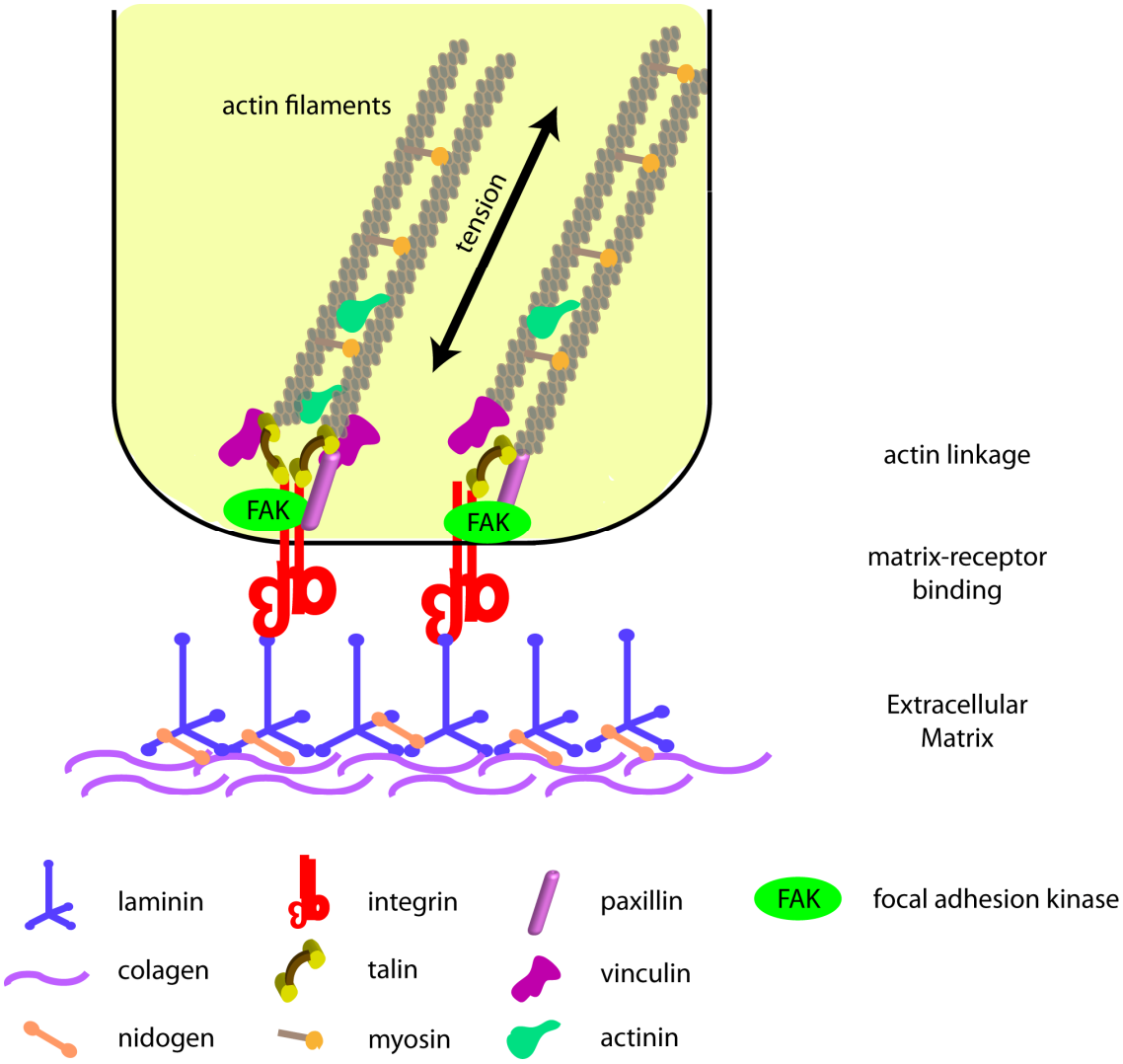

Figure 2. Focal adhesion binding to the ECM. Schematic drawing of focal adhesion attachment to the ECM and linkage with actin filament by different actin adaptors such as vinculin, talin, paxillin and actinin. These bindings result in the generation of mechanical forces.

It has been shown that mature focal adhesion disassembly depends on focal adhesion kinase (FAK) and dynamin (Ezratty *et al.* 2005). More recent studies showed that during cell migration, the formation and disassembly of focal adhesions are tighly coupled to the recycling of integrins through endocytic processes (Caswell *et al.* 2006). In migrating fibroblasts it has been demonstrated that microtubules-induced focal adhesion disassembly is regulated by clathrin and some clathrin adaptors such as Dab2 and ARH. These adaptors link α5β1 integrins and clathrin to form endocytic vesicles. Then, integrins travel through endocytic compartments after focal adhesion disassembly (Ezratty *et al.* 2009).

In medaka embryos, it has been shown that Opo, a transmembrane protein, competes with integrins to bind clathrin adaptors. This competition regulates the recycling of integrins, which is crucial for optic cup folding (Bogdanovic *et al.* 2012). This will be explained in detail below.

1.2 Cytoskeleton Reorganization And Cellular Junctions Orchestrate Cell Shape Changes

Isolated cells tend to have a spherical shape to reduce their surface tension, which is determined by differences in intercellular adhesion and cytoskeletal organization at the cellular cortex (Lecuit *et al.* 2007; Mammoto *et al.* 2010). The cortex is a cross-linked actin network lying beneath the plasma membrane. It is attached to the inner side of the membrane, and therefore, it plays a central role in cell shape control. Its protein composition confers two essential properties to the cellular cortex; mechanical rigidity and high plasticity (Salbreux *et al.* 2012). Furthermore, the cellular cortex is able to respond to Myosin II activation (see box 2) and modify the cellular visco-elasticity, defined as a balanced between the ability to recover original shape after a deformation and the resistance to flow due to molecular interactions. In addition, individual cells sense changes in physical forces and transduce them into intracellular signals that drive alterations in cell shape, polarity, migration and other processes. These changes can be also produced by transcriptional changes (Lecuit *et al.* 2007; Mammoto *et al.* 2010).

Box 2: Myosin and its activation

Myosin is a hexamer formed by two myosin heavy chains (MHCs), two myosin light chains and two regulatory light chains (RLCs). The head domain of the MHC subunits contains the ATPase activity and interacts with actin (Tan *et al.* 1992). Myosin heads bind to actin network and exert contractile forces on it by phosphorilation of it RLCs by Rho kinase that in term controls the contractile activity of myosin (Dawes-Hoang *et al.* 2005).

When cells are integrated into tissues, the presence of cellular junctions decrease surface tension and facilitate cell shape changes (Lecuit *et al.* 2007). In a polarized epithelium, during tissue morphogenesis, actomyosin network is recruited to the apical side in an oscillatory manner (Gorfinkiel *et al.* 2011) to produce tissular changes such as invagination. We will go through it in further detail below.

In concordance with this, tensional forces generated by the actin cytoskeleton, are also resisted by these adhesive tethers and by internal cytoskeletal structures such as microtubules that compress resulting in a force balance that ensure tissue and organ shape stability (Mammoto *et al.* 2010).

In summary, the final shape of the cell depends not only on the organization of the actomyosin network, but also on the establishment of a balance between axis polarity within the cells and the distribution of transmembrane proteins within the plasma membrane that mediate the contact with the ECM or contacting cells (Lecuit *et al.* 2007).

1.3 Mitosis

In a proliferating epithelium, where cells are polarized, mitosis takes place at the apical pole. However, nuclei are not fixed at this surface during tissue development, but mitotic events at the apical side are followed by a basal descent of the nucleus, which will ascent back to the apical surface every mitotic cycle. This process is known as interkinetic nuclear migration (IKNM) (F.C. Sauer 1935). This displacement is divided into two different phases: the first phase is characterized by a persistent and rapid movement and the second phase, that precedes the next mitotic event, in which nuclei show stochastic movements (Norden *et al.* 2009). It has been suggested that IKNM influences mitosis of neuroblast through Notch signalling, which is polarized toward the apical side of the epithelial sheet (Del Bene *et al.* 2008; Murciano *et al.* 2002). Moreover, there are many studies showing different mechanisms to explain this process; in zebrafish neural retina, the actomyosin network is the main driving force (Norden *et al.* 2009), however the microtubules and their motors proteins are also involved (Del Bene *et al.* 2008).

Although proliferation has a major impact on the increase in volume and size of epithelia and organs, many publications have shown that mitosis does not play a role in shape changes during epithelial development (Gutzman *et al.* 2008; Krupke *et al.* 2014; Kwan *et al.* 2011). In *Xenopus*, when proliferation is inhibited, retinal cells differentiate normally although the resulting eyes are smaller than those in untreated embryos (Harris *et al.* 1991). During zebrafish optic cup morphogenesis (OCM), again, embryos treated with mitosis inhibitors display optic vesicles with fewer and larger cells than controls, but morphogenesis occurs normally, as reflected by organized eyes containing neural retina (NR) and retinal pigmented epithelium (RPE) enwrapping the lens (Kwan *et al.* 2011). All these studies together indicate that in epithelia, morphogenesis proceeds independently from proliferation. An exception to this general rule has been described in sea urchin embryos. In this model, when ciliary band cells are treated with DNA synthesis inhibitors

to block mitosis and indirectly prevent cytokinesis, cells apically constrict (Krupke *et al.* 2014)

1.4 Cell Migration

Directional migration is a key process involved in embryonic development, wound healing, cancer, etc. There are two types of movements: the first involves collective migration, where cells maintain their cohesive contacts and the whole tissue moves in a coordinated fashion. The second involves the migration of individual or small group of cells through the ECM and implies the modification of their adhesive properties. Migrating cells undergo epithelial to mesenchymal transition (EMT), consisting in the loss of cell-cell contacts and the modification of apico-basal polarity and the reorganization of the endocytic and exocytic trafficking pathways (Locascio *et al.* 2001; Nelson 2009). In both cases, this process depends on cell attachment to the ECM through focal adhesions. Focal adhesions, as it has been explained above, provide the connection between the ECM and the actin cytoskeleton and serve as traction points. As cells migrate, integrins are trafficked at the front of the cell to form focal adhesions and are disassembled at the rear. The mechanisms that spatially regulate the assembly and disassembly of these focal adhesions are still poorly understood (Ezratty *et al.* 2009), although it is clear that the mutual antagonism between Rac and Rho is involved in the generation of cell movement. Rac promotes ruffles in the membrane, that lead to the formation of new focal contacts through existing complexes at the front of the cell and encourages the turnover of pre-existing contacts (Rottner *et al.* 1999).

Once the migration has finished and cells reach their final fate, they may undergo a reverse mesenchymal to epithelial transition process (MET).

2. Epithelial Morphogenesis

Given that many adult tissues are epithelial or were epithelial during their ontogeny, the study of epithelial sheets, formed by polarized cells that extend from an apical surface to a basal lamina, has considerably contributed to better understand the mechanisms underlying morphogenesis in several species. Throughout development, cells undergo impressive changes and collective movements to create complex three-dimensional organs in a process referred as epithelial morphogenesis (Bryant *et al.* 2008; Lecuit *et al.* 2007). How individual cellular properties can be translated into tissue changes still remains unclear.

Epithelial morphogenesis during embryonic development depends on the interplay between cell junctions and cortical tension. Changes in either adhesion to the substrate or to neighbouring cells, or in surface tension can result into variations in the mechanical response, that in term, contribute to cell shape changes. These changes allow tissue morphogenesis through processes such as cell intercalation and tissue bending (Lecuit *et al.* 2007).

Box 3: Oscillatory behaviour during epithelial morphogenesis

In the last few years, many studies of cellular behaviour have led to a new understanding of tissue development. Oscillatory cell shape changes combined with the contractile activity of the actomyosin network seem to drive epithelial morphogenesis in many organs (Gorfinkiel *et al.* 2011).

In the *Drosophila* embryo, intercalating cells in the germ-band undergo an oscillatory behaviour with contraction and expansion phases without area constriction, that allows cell intercalation and, as a consequence, axis elongation. Although oscillations are an intrinsic cellular property, the anisotropy of these oscillations required a tightly junctional system. The formation of an actin meshwork at the medial cellular cortex followed by the recruitment of Myosin II produces this cellular activity in germband cells. Moreover, contacting cells predominantly oscillate in antiphase, although others behaviours are also allowed (Fernandez-Gonzalez *et al.* 2011).

Other morphogenetic movements produce the constriction of epithelial sheets by shrinking, either the apical or the basal side of cells, causing bending (Gutzman *et al.* 2008; Solon *et al.* 2009). Many studies have proposed a hypothesis to solve the question about how invagination is produced and to explain the mechanics of the process (Davidson *et al.* 1995). In polarized epithelia, it is clear that the molecular motors provide the forces needed to lead cell and tissue reorganization (see Figure 3), which are required to shape a complex organ (He *et al.* 2010; Martin *et al.* 2009), and there are many examples that try to explain the recruitment of these motors.

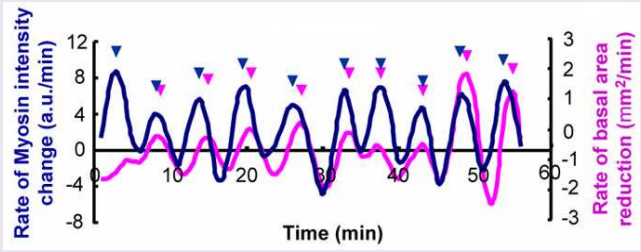

Figure 3. Quantification of basal behaviour in *Drosophila* follicle cells. Rate of myosin intensity changes (blue) and rate of basal area changes (pink). Adapted from (He *et al.* 2010).

Among the morphogenetic processes above described, the best-known event in animal epithelial sheets is the apical constriction (Sawyer *et al.* 2010).

3. Apical Constriction

Apical constriction is a cellular shape change caused by the shrinking of the apical surface. Apical constriction has been described in many vertebrate and invertebrate tissues and it is a basic mechanism at early stages of development (Sawyer *et al.* 2010). A classical examples of it can be found in sea urchin embryos, where ciliary band formation relies on an apical constriction of the cells, a process that results in a highly packed array of cilia needed for larval swimming and feeding (Krupke *et al.* 2014; Strathmann 1971). However, the relevance of apical constriction is linked to the fact that it results in epithelial invagination, which is the bending of a cell sheet by inward folding of the tissue. This is the case during sea urchin (Davidson *et al.* 1995; Kominami *et al.* 2004), *Xenopus* (Hardin *et al.* 1988; Holtfreter 1943) and *Drosophila* gastrulation (Costa *et al.* 1994; Sweeton *et al.* 1991), as well as chick inner ear development (Meier 1978) and vertebrate neural tube formation (Lowery *et al.* 2004; Schoenwolf *et al.* 1984). Although there are some common features conserved between organs and species in apical constriction events, the mechanics of the process differ widely between organisms and between tissues within the same organism (Sawyer *et al.* 2010). In principle, a few cells can lead the invagination by suffering apical constriction. In *Drosophila* gastrulation, constricting cells undergo shape changes to drive the bending of the invaginating epithelial sheet (Sweeton *et al.* 1991). How these changes are regulated is still unclear. However, there are many hypotheses that try to explain these alterations; variations in tension within the cellular membrane or in adhesion between cells could induce cell shape changes. Many studies in different species have shown cells with a smaller and/or flattened apical surface, bigger basal surface, and in some cases, elongated along their apicobasal axes, as tissue invagination happens (Leptin *et al.* 1990; Sweeton *et al.* 1991). In several organisms these cells are known as bottle cells, which were originally cuboidal cells transformed into wedge-shaped (Davidson *et al.* 1995). In other species such as *Caenorhabditis elegans*, the constriction occurs without forming clear bottle shape cells (Nance *et al.* 2002).

From a molecular point of view, it is commonly accepted that the actomyosin network generates the mechanical forces required to produce apical constriction. As it was previously mentioned, the organization of actin filaments interacting with Myosin II motor units changes in constricting cells (Hildebrand 2005; Plageman *et al.* 2010; Roh-Johnson *et al.* 2012). However, there are two facts that support the idea by which a tight regulation of

the dynamic linking actomyosin meshwork and apical cell-cell contacts should trigger the constriction. Firstly, cell-cell contact complexes formed by E-cadherin-βcatenin-αcatenin have slower mobility rates than actin filaments at the membrane level (Yamada *et al.* 2005). Secondly, the actomyosin network is already contractile at the apical cortex before any cell shape change takes place. Some examples of this process have already been described in *Drosophila* and *C.elegans* (Roh-Johnson *et al.* 2012; Solon *et al.* 2009).

3.1 Apical Constriction During Invertebrate Development

During *Drosophila* gastrulation, the slow apical flattening and the fast stochastic phases required to produce the ventral furrow during mesoderm invagination (Oda *et al.* 2001; Sweeton *et al.* 1991) are correlated with weak and strong constriction pulses that lead to invagination. These pulses are produced by an actin filament meshwork apically localised, in which Myosin spots are constrained forming an organised network on the ventral surface of the embryo. When Myosin is fluorescently labelled, these spots repeatedly increase in intensity. Moreover, when apical constriction begins, there is a reorganization of adherens junctions that involves junctions below the apical cortex disappearing, while new adherens junctions emerge at the cell edge. These new junctions are the sites where new pulsed of constriction are generated. The actomyosin network is stabilised at these junctions to pull inward and produce the bending (Martin *et al.* 2009). So, these junctions serve as structures through which epithelial tension is transmitted. Besides, knocking down some of the core adherens junctions components such as E-cadherin, α-catenin or armadillo disrupts epithelial tension, suggesting that a supracellular actomyosin network is generated through cell-cell contacts producing a tissue-wide meshwork (Martin *et al.* 2010).

In *Drosophila* dorsal closure, an actin cable formed in leading edge amnioserosa cells provides the forces needed to pull on the surrounding epithelial cells. The force generated in an individual constricting cell is also transmitted by intercellular contacts producing a constriction in the neighbouring cells. This transmission of forces produces a wave of constriction/relaxion states that occurs with a minimal tissular tension. The maintenance of tissular tension is achieved through myosin-mediated sliding of actin filaments and it is necessary to ensure the closure (Solon *et al.* 2009). This process, by which oscillating cells reduce their surface in an irreversible manner producing apical constriction has been referred as “ratchet mechanism” (Martin *et al.* 2009; Solon *et al.* 2009).

Generally, when neighbouring cells behaviour was analysed, most of the cells preferentially oscillate in antiphase (Martin *et al.* 2009; Solon *et al.* 2009). In *Drosophila,*

differences in oscillatory behaviours have been identified. While in the onset of dorsal closure cells start oscillating by mechanical interaction between neighbouring cells, and the supracellular actin cable is generated parallel to the cell interface (Solon *et al.* 2009); during the formation of the ventral furrow in gastrulation, oscillations seem to be an autonomous property of cells, and the supracellular actomyosin cable is instead oriented perpendicularly to cell interface (Martin *et al.* 2010).

3.2 Apical Constriction During Vertebrate Development

In vertebrates, the process occurs similarly to what has been observed in the fly. During development, several cell shape changes convert a flat neural plate into the final neural tube, and also drive the embryonic lens placode to turn into the differentiated lens (Hendrix *et al.* 1974; Schoenwolf *et al.* 1984). These cell changes have been studied in different organisms but in all cases, the conversion of columnar cells into wedge-shape cells and the rearrangement of the actomyosin network are both required (Chauhan *et al.* 2011; Hildebrand 2005; Plageman *et al.* 2010; Schoenwolf *et al.* 1984).

The development of the neural tube and the lens have been analysed in detail. During lens placode invagination, the actin-binding protein Shroom3 induces apical constriction by the recruitment of contractile complexes to the cell apex. This recruitment is necessary in lens pit cells to undergo the cylindrical-to-wedge shape transition (Plageman *et al.* 2010).

During neural tube closure, Shroom3 localises to apical adherens junctions and regulates cellular shape changes as occurs in lens cells (Hildebrand 2005).

3.3 Molecular Basis of Apical Constriction

Many genes have been implicated in the understanding of apical constriction, but further investigations are required to complete the gene regulatory networks involved in this process. In sea urchin embryos, *Eph-Ephrin* signalling is necessary for actomyosin reorganization and it also regulates apical constriction of ciliary band cells through phosphorilated FAK (Krupke *et al.* 2014). In *Drosophila* gastrulation, constricted cells express the patterning gene *twist* that acts through its target gene *folded gastrulation* (*fog*), which is apically polarized. These genes are implicated in the localization of Myosin to the apical side. Additionally, in the fly, the cytoskeletal regulator *RhoGEF2* is recruited at the apical side, either through the transmembrane protein T48 or through *fog*/*concertina* (*cta*) signalling pathway, where it is required for apical localization of adherens junctions

and for the contraction of Myosin, both needed to orchestrate final apical constriction (Costa *et al.* 1994; Dawes-Hoang *et al.* 2005; Kolsch *et al.* 2007; Leptin *et al.* 1990; Oda *et al.* 2001; Sweeton *et al.* 1991) (see Figure 4). Moreover, *RhoGEF2* and *Abelson kinase (Abl)* also contribute to recruit F-actin at the apical surface by independent mechanisms (Fox *et al.* 2007). More recently, other participants such as the *Drosophila afadin* homologue *Canoe* have been shown to provide a mechanical link between adherens junctions and the actomyosin network during apical constriction (Sawyer *et al.* 2009).

Vertebrates share with invertebrates some of the molecules involved in the regulation, but there are also additional players. In mice, during lens and neural tube formation, Shroom3, an actin-binding protein activated by *pax6*, is necessary and sufficient to recruit both F-actin and Myosin II at the tip of adherens junctions, showing again the tight coupling between junctions and actomyosin reorganization (Hildebrand 2005; Plageman *et al.* 2010) (see Figure 4). Shroom3 acts by binding to *Mena/Vasp* proteins through a proline-rich domain, and this binding facilitates the recruitment of actin apically responsible of cell shape changes needed to produce the final constriction (Plageman *et al.* 2010). During lens apical constriction, a balance between the activities of small GTPases Rac1 and RhoA is required to modulate cell shape changes. Each GTPase can regulate both the apical width and the height of a cell. Rac1 binds to Arp2/3 (an actin nucleator) to generate Y-branched F-actin networks, which are needed to induce cell elongation, and suppresses the formation of phospho-myosin regulatory light chain (MRLC). On the other hand, RhoA-dependent formation of apical phosphor-MRLC is required to mediate apical constriction. RhoA is able to block Rac1-dependent basal localization of Arp2/3 (Chauhan *et al.* 2011).

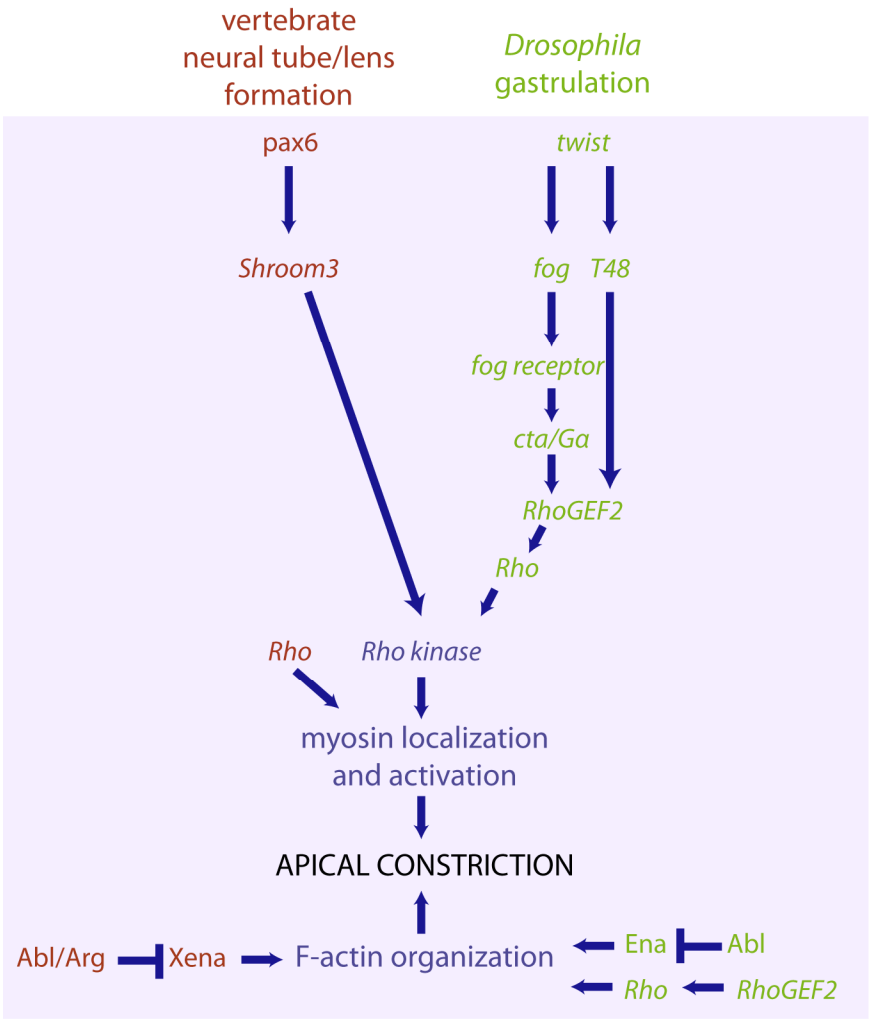

Figure 4. Genetic networks required for apical constriction during *Drosophila* gastrulation and vertebrate neural tube formation. For simplicity, connections between actomyosin network and adherens junctions recruitment are not shown here. (Chauhan *et al.* 2011; Fox *et al.* 2007; Hildebrand 2005; Kolsch *et al.* 2007; Plageman *et al.* 2010; Sweeton *et al.* 1991) and references in text). Adapted from (Sawyer *et al.* 2010).

4. Basal Constriction

Although the bending at apical surfaces is the most common type of constriction, this similar shape changes may also happen at the basal side of animal epithelia.

During basal constriction columnar cells from an epithelial sheet shrink their basal surface and adopt a wedge shape (Gutzman *et al.* 2008; He *et al.* 2010; Martinez-Morales *et al.* 2009). Although much less studied than apical phenomena, there are already some established examples for basal "constriction" and "contraction".

In *Drosophila* follicle cells, basal "contraction" takes place to produce the elongation of the egg chamber. In contrast to other tissues such as *Drosophila* dorsal closure that follow

a ratchet mechanism, in the elongation of the egg chamber, the average basal area does not vary because area changes are temporary. As opposed to "constriction" events in which area changes are progressive and permanent, this is referred as "contraction" behaviour. Follicle cells undergo periodic cycles of contraction and relaxation produced by cyclic accumulation of Myosin on a polarized actin network (see Figure 3 and 5). When the ROCK inhibitor Y-27632 is used, the amplitude of these oscillations is diminished indicating that Myosin accumulation causes membrane oscillations. Furthermore, cadherin-mediated cell-cell adhesion and integrin-mediated adhesion of follicle cells to the extracellular matrix (ECM) are required to the proper egg chamber elongation as shown in interference experiments with different adhesion molecules (He *et al.* 2010).

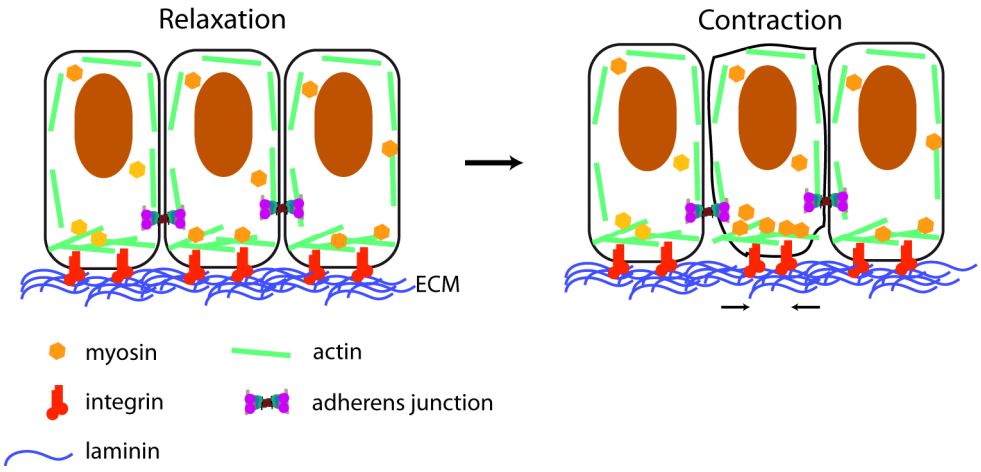

Figure 5. Relaxation and contraction states during egg chamber elongation in *Drosophila.* Cells oscillate between a relaxed and a contracted state. When follicle cells are contracting, Myosin is recruited to the basal side of the epithelium.

In contrast to contraction phenomena, the inward folding of an epithelial sheet requires a constriction mechanism.

Midbrain-hindbrain boundary (MHB) is a bend that appears during the development of the vertebrate brain and constitutes the first well-documented example of constriction at the basal surface (Gutzman *et al.* 2008). As the nervous system develops, a number of prominent furrows emerge along its anterio-posterior axis; the deepest bend is known as the MHB constriction (MHBC). At the beginning of MHBC in zebrafish, the neuroepithelium is composed by columnar shape cells. By 24hpf, cells localised at the sharp point become shorter and undergo basal constriction. In addition, the authors describe apical expansion of the neuroblasts, although it is not well known whether both mechanisms are interconnected. In the same study, the authors show that Laminin, a major component of

the basement membrane, is required for proper basal constriction of MHB. In this study, an increase in the amount of actin was observed at the basal side of the neuroblast in fixed embryos. However, further investigations are needed to conclude whether the actomyosin network has a role in MHBC (Gutzman *et al.* 2008).

Another example of basal constriction in vertebrates may occur during the morphogenesis of the optic cup (OCM). During the folding of the retinal epithelium in medaka, the transmembrame protein Opo acts as a key regulator of focal adhesions trafficking at the basal feet of neural retina cells. In a large-scale ENU (*N-ethyl-N-nitrosuourea*) screen in medaka, *opo* was identified as a recessive lethal mutation that causes defects in eye morphogenesis and other epithelial tissues like fins, heart, brain and neural crest-derived structures (Loosli *et al.* 2004; Martinez-Morales *et al.* 2009). In the developing eye, this protein is localized at the basal surface where cytoskeletal organization depends on integrin-mediated contacts. Work from our laboratory showed that Opo interacts with the clathrin adaptors Numb and Numbl, and thus negatively regulates integrin endocitosis. When Numb and Numbl bind to Opo, integrin-mediated focal adhesions are stabilised and retina folding proceeds normally (see Figure 6). Besides, the scaffold protein Paxillin links integrin-mediated adhesions with the cytoskeleton and accumulates at the basal surface of retina cells in *opo* (Bogdanovic *et al.* 2012; Martinez-Morales *et al.* 2009). *Opo* mutants display a phenotype characterized by a ventral opening in the eye, which is the product of inappropriate retinal folding. In addition, preliminary results pointed to expanded basal feet in the mutant neuroblasts. Although these results suggest that optic cup morphogenesis may constitute another example of basal constriction, this has not been formally proved. Therefore, in the present work we aim to investigate this issue further and to elucidate the role that the actomyosin network and the ECM play during optic cup folding, using zebrafish as an *in vivo* model organism.

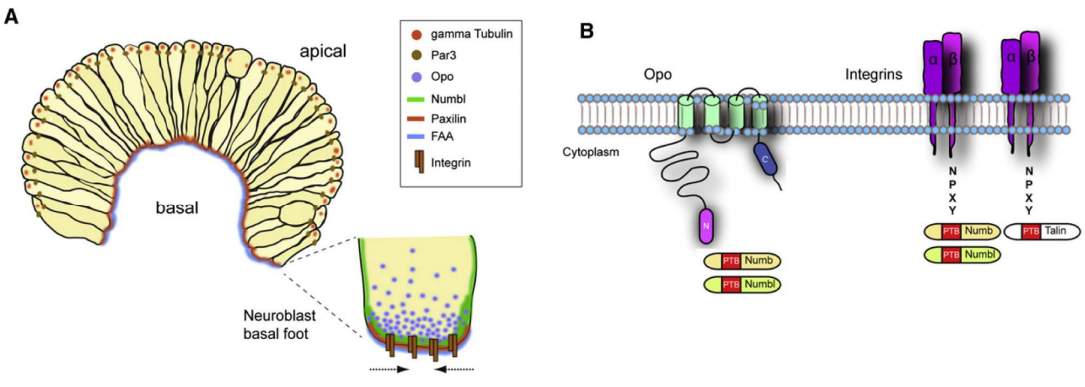

Figure 6. Opo localization and interactions during medaka fish eye morphogenesis. A) Representation of neuroblast basal foot during optic cup folding. B) Schematic diagram showing Numb/Numbl interaction with Opo and integrins. Adapted from (Bogdanovic *et al.* 2012).

5. Eye Morphogenesis In Zebrafish

Vertebrate optic cup morphogenesis (OCM) can be divided into four steps: evagination, elongation, invagination and rotation (Kwan *et al.* 2011). Each step is individually described in the text below.

5.1 Evagination

Previous works in vertebrates show that the onset of eye morphogenesis takes place during neurulation when the retinal progenitor cells (RPCs), expressing the homeobox gene *rx3*, constitute the eye field at the anterior end of the embryonic neural tube (Adelmann 1929; Rembold *et al.* 2006). The *rx* homeobox transcription factors are essential for eye morphogenesis, and *rx3* mutants in both teleosts, zebrafish and medaka embryos lack eyes (Loosli *et al.* 2003; Loosli *et al.* 2001). In rx3 mutants, RPCs show an aberrant behaviour and migrate to the midline to form the neural keel instead of evaginating to form the optic vesicles (OV) (Rembold *et al.* 2006).

As eye development proceeds, cells from the eye field evaginate bilaterally, forming the optic vesicles. In medaka, it has been suggested that evagination is produced as a result of coordinated individual RPCs migration that has been considered the main driving force in OVs formation (Rembold *et al.* 2006). However, recent studies in zebrafish have shown that two different cell populations are clearly distinguished in the eye field before the onset of the evagination (Ivanovitch *et al.* 2013). The marginal cells, localised basally in the eye field, acquire precocious apico-basal polarity and undergo cell shape changes to establish a pseudoestratified neuroepithelial organization. The other population, the core cells are localized apically in the eye field and do not display apico-basal polarity at early stages. Later on, these cells undergo mesenchymal-to-epithelial transition (MET) that is concomitant with the intercalation between marginal cells, and contributes to later stages of OV evagination (see Figure 7) (Ivanovitch *et al.* 2013). Furthermore, Laminin1, an ECM component crucial for the establishment of an epithelium (Yurchenco 2011), and pard6γb, a polarity protein, are both involved in the organization and maintenance of epithelial apico-basal polarization required for OV evagination (Ivanovitch *et al.* 2013). These

findings demonstrate the relevance of polarity and ECM components at early stages of eye morphogenesis.

Once the RPCs have evaginated, the resulting OVs in teleosts are flattened and formed by two epithelial layers clearly separated by the optic lumen; the lateral layer from which the prospective neural retina (NR) will be developed and the medial layer that will become the retinal pigmented epithelium (RPE) (Li *et al.* 2000).

The optic stalk that connects the vesicles with the neural tube is thick and short. The overlying ectoderm thickens to form the epithelium of the lens placode that remains in close contact to the presumptive NR during OCM (Li *et al.* 2000).

a. Elongation

The OV acquires flipper-like shape by elongating the epithelium in a cell movement called "pinwheel", which consists on the posterior displacement of cells from NR posteriorly and laterally and the shift of RPE cells medially and anteriorly causing net posterior growth. Prospective lens cells undergo movements with the same direction and speed as underlying NR cells, although they do not contact directly (Kwan *et al.* 2011).

b. Invagination

5.3a Neural Retina (NR)

During invagination, ingression of some cells from the medial layer to the lateral layer takes place around the anterior and posterior border between the two layers as the organ is forming (Kwan *et al.* 2011; Li *et al.* 2000). This movement is known as "rim movement". Additionally, prospective NR cells undergo an anterior rotation (Kwan *et al.* 2011).

In medaka embryos, as it has been mentioned above, the main driving force of NR invagination has been suggested to be the basal constriction of the NR cells (see Figure 6 and 7). This morphogenetic event is orchestrated by a tight regulation of integrin-mediated cell-ECM contacts in the presence of Opo protein (Martinez-Morales *et al.* 2009). It has been previously shown that during development there is a balance between the turnover of integrins and the stabilization of focal adhesions. The disassembly of focal adhesions, through the endocytosis of integrins, is a clathrin-dependent process. Some members of the phosphotyrosine binding (PTB) family of clathrin adaptors (such as Dab2, Numb and ARH) are recruited to the cellular basal feet to mediate the endocytosis of

integrins in a FAK and dynamin-dependent manner (Calderwood *et al.* 2003; Ezratty *et al.* 2009).

Opo competes with integrins for the binding of Numb/Numbl through their PTB site, thus interfering with integrin turnover. When Opo binds to these clathrin adaptors, focal adhesions are stabilised and integrins basally recruit the actomyosin network producing OC folding. Accordingly, in *opo* mutants, the excessive endocytosis of integrins drives to a defective adhesive function, an impaired recruitment of the actin adaptor proteins such as paxillin, and as a consequence a failure in OCM responsible of the phenotype. Additionally, when a dominant negative marker torso^{D}/βcyt (Martin-Bermudo *et al.* 1999) was used to interfere with integrins function, an *opo*-like phenotype was observed indicating that tension cannot be exerted correctly when integrin function is impaired (Bogdanovic *et al.* 2012; Martinez-Morales *et al.* 2009).

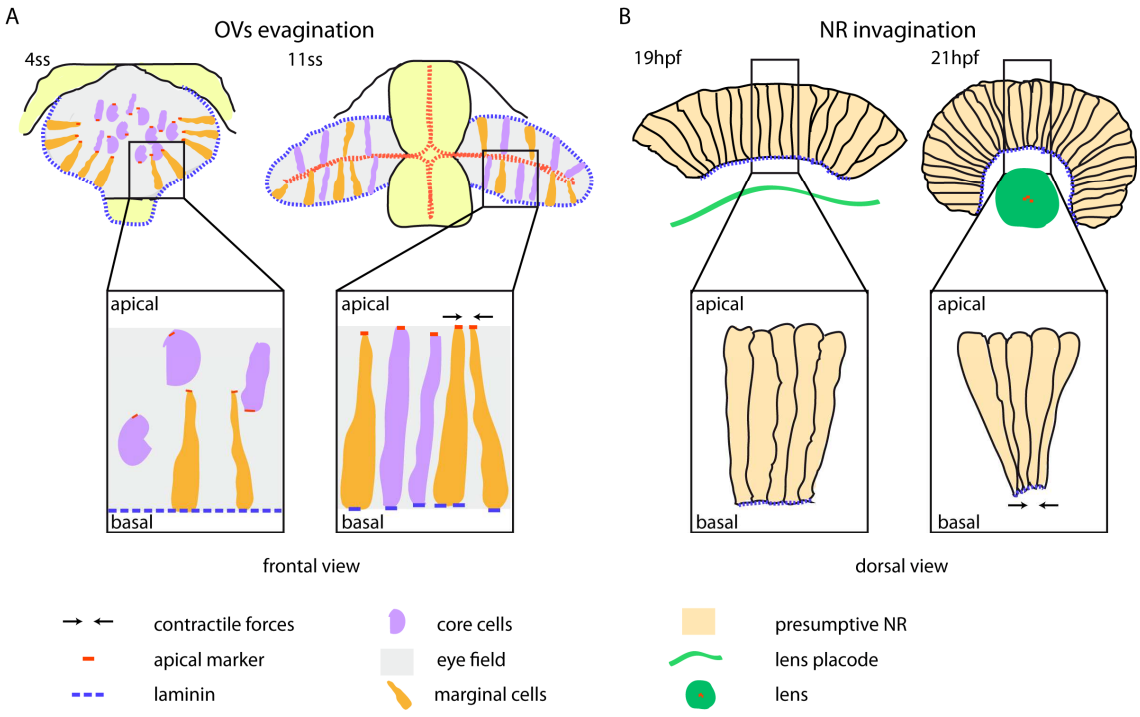

Figure 7. Eye morphogenesis. A) Optic vesicles evagination. At early stages, cells from the marginal zone of eye field display apico-basal polarity and are in contact with the basal lamina while cells in the core do not. During evagination, core cells intercalate between marginal cells. Their apical domain remains attached to the midline and the basal domain extend to reach the basal lamina. At the end they are indistinguishable from marginal cells. Cells undergo apical constriction to shape optic vesicles. Adapted from (Ivanovitch *et al.* 2013). B) Neural retina invagination. Proposed basal constriction mechanism during optic vesicle morphogenesis. At 19hpf, neuroblasts apical and basal surfaces are similar. Then, cells undergo basal constriction to shape the optic cup.

5.3b Retinal Pigmented Epithelium

The RPE arises from the medial layer of the OV. During invagination, the presumptive RPE shrinks dramatically becoming a flat epithelium. Cells adopt a squamous shape and spread, to cover the back of the NR (Li *et al.* 2000). Little is known about how these morphological changes take place *in vivo*.

Genetically, all the cells that compose the early OV express the same transcription factors, including the *microphthalmia-associated transcription factor (Mitf)*, the *orthodenticle-related transcription factors (Otx*) and the *paired-box transcription factors (Pax)*. But soon their expression patterns become restricted to the RPE (is the case for *Mitf* and *Otx*) or disappear from this territory (e.g. *Six3 or Rx*2), to allow the differentiation of this epithelium (Martinez-Morales *et al.* 2004). *Mitf* is required for RPE cell fate and it is also essential in pigment cell development (Fuhrmann 2010). In *Otx* mutant mice, there is a failure in RPE differentiation, and the lack of RPE is associated with an increase of the presumptive NR and optic stalk territories (Martinez-Morales *et al.* 2001). Other morphogens such as Bone Morphogenetic Proteins (BMP) and Hedgehog-related proteins and partners of their signalling pathways are co-expressed in the RPE. Additionally, as the RPE has reduced mitotic activity, some molecules involved in RPE differentiation and inhibition of cell cycle such as connexin43 (Cx43), cyclin-dependent kinase (Cdk) inhibitor p27kip1, are also expressed in this epithelium (Martinez-Morales *et al.* 2004; Martinez-Morales *et al.* 2001).

Other works in explants culture of chick OVs have demonstrate that the adjacent extraocular mesenchyme is involved in RPE specification because is required for the induction of *Mitf* expression (Fuhrmann *et al.* 2000; Kagiyama *et al.* 2005; Mochii *et al.* 1998). Furthermore, in mouse OVs explants culture, the absence of the adjacent extraocular tissue alters *Mitf* expression (Fuhrmann 2010).

Once the invagination has concluded, both epithelia enwrap the lens forming the adult vertebrate eye (Kwan *et al.* 2011; Li *et al.* 2000).

5.3c Lens Involvement in Retina Invagination

Previous studies in mice showed the presence of filopodia from the NR and the surface ectoderm during OC folding. Filopodia are cytoplasmic structures formed by parallel actin filaments and are usually anchored at their tips by cadherin-catenin, or integrin-dependent focal adhesions. These filopodia act as physical tethers that pull the lens, to regulate the accurate invagination of the presumptive NR and lens; thus coordinating the

inter-epithelial distance during the folding. The formation of filopodia is dependent on the small GTPase Cdc42 and the effector protein IRSp53 (insulin receptor substrate) that recruit actin filaments through actin nucleators such as the Arp2/3 complex. Furthermore, actin-myosin contraction depends on Myosin phoshorilation, and the presence of phosphorilated Myosin in filopodia seems to regulate filopodia length variations and help regulate inter-epithelial distance. Interference experiments on the actin-myosin network resulted in abnormal folding of epithelia, by altering the degree of curvature (Chauhan *et al.* 2009). These findings suggest that the physical contact between the neuroepithelium and the surface ectoderm during the folding is involved in the coupling of both tissues to shape the eye, but does not interfere with NR self-organizing programs.

Other work in mouse embryonic stem cells (ESCs) showed that isolated cells are able to shape a retina without interaction with other tissues; by adding selected basement membrane matrix components. The resulting retina is patterned along its proximal-distal axis. The proximal portion differentiates into the RPE and the distal portion bends inward to form the embryonic optic cup. Thus, this work suggests that an intrinsic self-organization program involving stepwise and domain-specific regulation of local epithelial properties is responsible for OC folding (Eiraku *et al.* 2011).

However, studies in chick embryos showed that ablation of pre-lens ectoderm results in a failure of OC folding (even if BMP and FGF are added), despite the correct differentiation of retina cells into NR and RPE. In contrast, when lens ectoderm is ablated, a bilayered optic cup with inner and outer layers is formed. These results demonstrate that early OVs require a temporally-specific association with pre-lens ectoderm, independent of BMP and FGF signalling. It is also clear that once the intrinsic retina organizing program has begun, the optic cup can form in the absence of a lens (Hyer *et al.* 2003).

c. Rotation

Between 24-36hpf, the right eye rotates clockwise and the left counter clockwise to place the pupil-forming choroid fissure ventrally, and to reach its final position in the embryo. This rotation seems to be an active motion independent of the cephalic flexure that takes place at the same stage (Kwan *et al.* 2011).

6. Zebrafish As A Model Organism For Eye Development

For this project, zebrafish was selected as a model organism for several reasons. First, its small size, the large amount of eggs that delivers *per* week, the transparency of its offspring, its rapid development (in 3 days the larvae hatch and start swimming). These features, together with an important number of additional embryological advantages, make the zebrafish an excellent model to study morphogenesis and other biological aspects. Eye development, driven by a neuroepithelial folding, constitutes an excellent model to analyse basal constriction in a vertebrate context, thanks to its accessibility and optimal visualization. To gain insight into the mechanisms governing OCM, we generated transgenic lines that label the membranes of the retina neuroblasts, to follow cell shape changes during OC folding. Taking advantage of recent technological advances in live imaging (review in (Keller 2013)), we have monitored and analysed in detail zebrafish retina folding. Moreover, we studied the relationship between the actomyosin network and cell shape changes and their connection with the ECM.

IV. Objectives

To gain insight into the mechanisms underlying eye morphogenesis through the dynamic analysis of shape changes in individual cells, this thesis focuses in the accomplishment of the following objectives:

- To analyse quantitatively neuroblasts behaviour during optic cup folding.

- To explore actomyosin network dynamics in retina neuroblast during optic cup invagination.

- To investigate the role of Laminin γ1 during retina folding.

V. Materials and Methods

1. Cloning into Tol2 Destination Vectors.

The sequence for the retina-specific *vsx2.2* medaka promoter (Martinez-Morales *et al.* 2009) was cut from an available construct with KpnI/NotI (Takara Bio Company) and sub-cloned into the 5'entry vector of the Multisite Gateway-based System using T4 DNA ligase (M1804 Invitrogen). The sequence of the fluorescent tracer protein *lyn-tdtomato* (von Hofsten *et al.* 2008) was also cut from plasmids using XbaI/NotI (Takara Bio Company), and then cloned into the middle entry vector by conventional cloning.

Finally, each middle entry constructs, together with the 5' and 3'entry vectors (containing a poly(A) tail), were recombined (LR clonase11791020, Invitrogen) with the destination vector (see Figure 8) (Kwan *et al.* 2007). The resulting constructs thus drive the expression of the *lyn-tdTomato* marker (Love *et al.* 2011) in the neural retina membranes and in the neural tube, or caaxGFP in the neural retina membranes. As a transgenesis control, these constructs also drive cytoplasmic GFP expression in the heart driven by the promoter of the cardiac myosin light chain gene (see Figure 8).

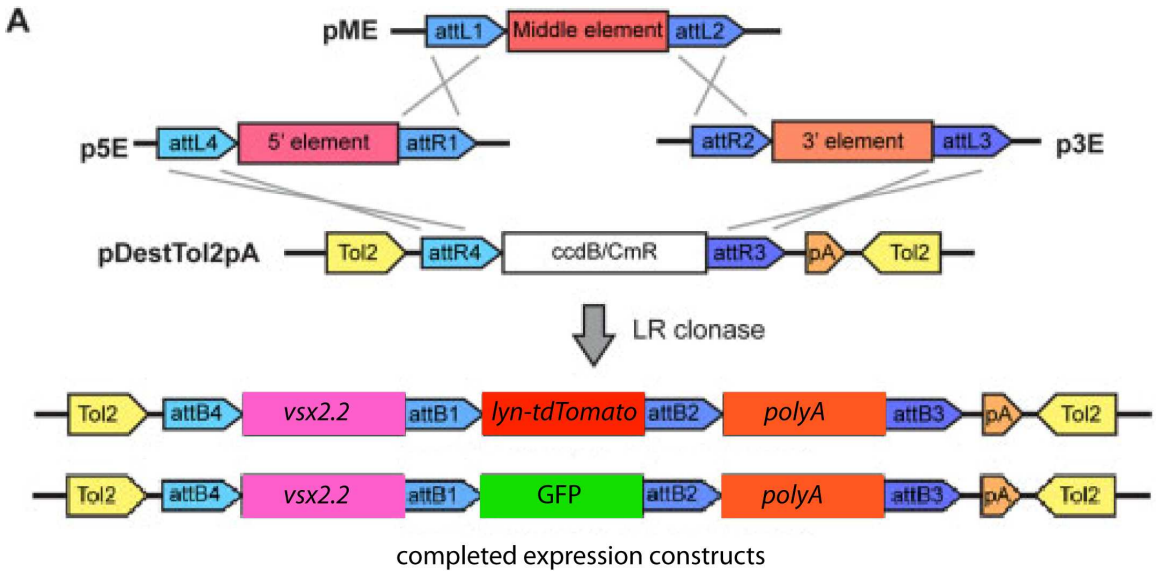

Figure 8.Tol2 Cloning strategy. A) Diagram of the 3-part LR recombination reaction used to generate the expression construct, using three entry clones (5' element + middle element + 3' element) and the pDestTol2pA/pA2 destination vector. The completed constructs contain the Tol2 transposase target sites (yellow), the recombination sites attB4, attB1, attB2 and attB3 (blue), the *vsx2.2* medaka promoter (pink), the *lyn-tdTomato* marker (Love *et al.* 2011) or the GFP marker (green) and the poly(A) tail (dark orange). Modified from (Kwan *et al.* 2007).

2. Maintenance of Zebrafish (*Danio rerio*)

Adult AB/Tübingen (AB/Tu) zebrafish were maintained under standard conditions according to the procedures described in (Kimmel *et al.* 1995) and in the Zebrafish Model Organism Database (http://zfin.org; (Sprague *et al.* 2003). All developmental stages are reported in hours post-fertilization (hpf) at 28.5ºC; according to the standard staging tables (Kimmel *et al.* 1995). Embryos were grown in E3 medium.

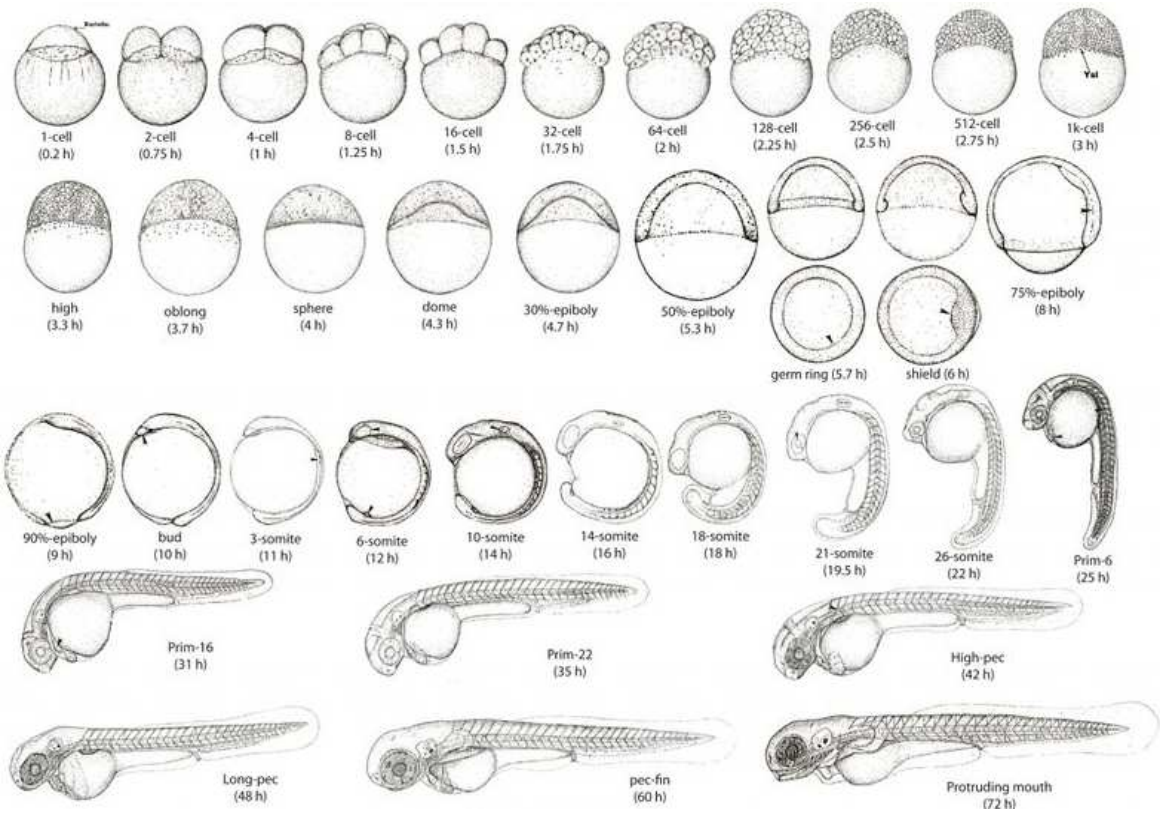

Figure 9. Stages of embryonic development in zebrafish. From one cell stage to 72 hpf. Adapted from (Kimmel *et al.* 1995).

Fish crosses for injection experiments or transgenic lines maintenance, were performed as it follows: On the day prior to microinjection, adult wild type fishes were separated according to sex into two different 3 litre tanks. On the following morning, immediately after lights were switched on, males and females were placed together into a 5 litre tank. Newborn eggs were physically separated from adults by a grid (Kimmel *et al.* 1995).

3. Injection of Transgene Constructs

Eggs were injected at one cell stage using a manual microinjector (Narishige) and glass needles (Glass Capillary Filament 1.0mm x 58mm, 6´´ CIBERTEC601500), previously prepared using a horizontal puller (Sutter instrument model P-97). Each embryo was injected with 3-5nl of a solution containing a final concentration of 25nM of the construct, 25nM of Tol2 mRNA and 0.1% of inert dye phenol red (Sigma-Aldrich) to enhance visualization of the solution within the cytoplasm.

After injection, embryos were incubated at 28,5ºC. As experimental control, an equal number of uninjected sibling embryos were also incubated.

GFP and *lyn-tdtomato* expression patterns were analysed at 24, 48 and 72 hpf with a fluorescent stereoscope. Embryos showing a homogenous GFP pattern in the heart, confirming the insertion of the construct in the genome, were grown into adulthood in the fish facility, to be screened as putative founders at the F1 generation.

4. Screening of F1 Carriers

Once the F0 or "putative founder" generation of injected fish reached adulthood, fish were individually outcrossed with wild-type partners. Embryos with *lyn-tdtomato* expression in neural retina cells and GFP in the heart or GFP in neural retina cells and GFP in the heart were identified, raised in the facility, and considered the F1 generation for each line; *Tg(vsx2.2:GFP-caax*) and *Tg(vsx2.2:lynTdTomato*). These lines were maintained by incrossing animals from the same generation.

5. Stable Transgenic Lines

The following stable transgenic lines were used in this study:

1.- The *Tg(vsx2.2:GFP-caax*) line was generated by fusing the medaka *vsx2*.2 promoter (previously known as *vsx3*) (Martinez-Morales *et al.* 2009) and GFP-caax (green fluorescent protein), as a reporter protein that localises to the cell membrane. The resulting expression pattern for this line is therefore GFP expression in the neural retina membranes. As a control of transgenesis this line also expresses cytoplasmic GFP in the heart (Kwan *et al.* 2007) (see Figure 10).

2.- The transgenic line *Tg(vsx2.2:lyntdTomato*) was generated by fusing the medaka *vsx2.2* promoter (Martinez-Morales *et al.* 2009) and *lyn-tdTomato* as a reporter protein that also localises to the cell membrane. This line expresses *lyn-tdTomato* in the neural

tube cell membranes and in the neural retina membranes and GFP (as a control of transgenesis) in the heart (Kwan *et al.* 2007) (See Figure 10). This additional expression domain in the neural tube is in concordance with the expression pattern of the gene *vsx2.2* (http://zfin.org). In fact, we could also observe this expression in some founders of the *Tg(vsx2.2:GFP-caax)* line. However, in order to obtain a retina specific transgenic line, we selected those founders which insertion did not drive GFP expression in the neural tube.

3.- The *Tg(βactin:Myl12-GFP)* line was provided by C.P. Heisenberg's laboratory (Maitre *et al.* 2012) and contains the ubiquitous *β-actin* promoter fused to myosin12GFP (see Figure 10). This line labels non-muscle myosin12 in the whole body of the fish.

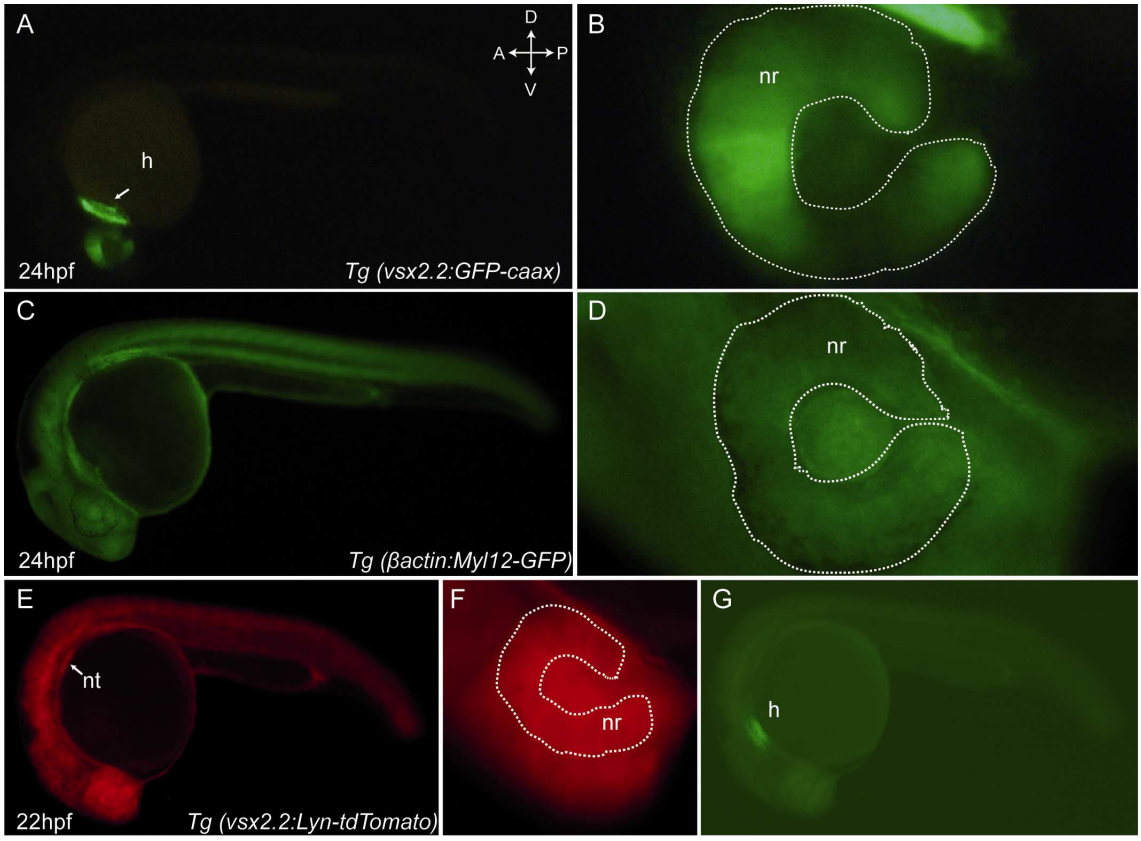

Figure 10. Expression patterns of transgenic lines used. A-G) Fluorescent stereoscope images showing expression patterns at 24 and 22hpf respectively. Arrowhead: heart (h) and neural tube (nt). Neural retina (nr). Dashed line: neural retina.

6. Mounting of Embryos for *in vivo* Imaging

Embryos were selected at the appropriate developmental stages and then dechorionated with forceps, embedded in 100µl of 0,5-1% low melting point agarose type IV (Sigma-Aldrich), and mounted onto a 35mm petri dish (WPI -- FD3510-100 Fluorodish). Embryos were carefully oriented to the appropriate position. Once the agarose had solidified, the agarose bed containing the embryo was covered with E3 medium (Rembold *et al.* 2004) (see Figure 11).

7. Confocal Imaging

Time-lapse imaging was performed at room temperature using an inverted confocal microscope (Leica SP5) with a 20X multi-immersion objective. Different parameters were used for specific time-lapses:

7.1 Apical and basal surface of the retinal epithelium: the laser scanned areas of 119,15 x 119,15µm (0,2327µm pixel $^{-1}$) every 15 sec. The use of the resonant scanner allowed the acquisition of images with high temporal resolution. Image Z-stacks were acquired using 1µm steps over a total depth of 3 µm. Optical sections within stacks were chosen at a distance of 2-3 µm apart from the basal feet of retina cells (for basal areas) and a similar distance from the apical surfaces (for apical areas) (see Figure 11, D-F).

7.2 Apico-basal axis (central retina): Images were recorded with the galvano laser (image resolution being, in this case, paramount over temporal resolution) every 20s by scanning areas of 221,47 x 221,47µm (0,4325 µm pixel $^{-1}$). Image Z-stacks of the central retina were acquired using 2 µm steps over a total depth of 20µm. A greater range for depth ensured cells of interest would be imaged in focus regardless of whether their positions shifted. (see Figure 11, C).

7.3 Transplanted neuroblasts in wild type retinas. Image Z-stacks were recorded with the resonant laser every 8s by scanning areas of 119,15 x 119,15µm (0,2327µm pixel $^{-1}$) with 1 µm steps over a total depth of 7 µm. Stacks were selected in the central plane of the neuroblast, to ensure that the comparison between different neuroblast would always be performed within the same part of the cell.

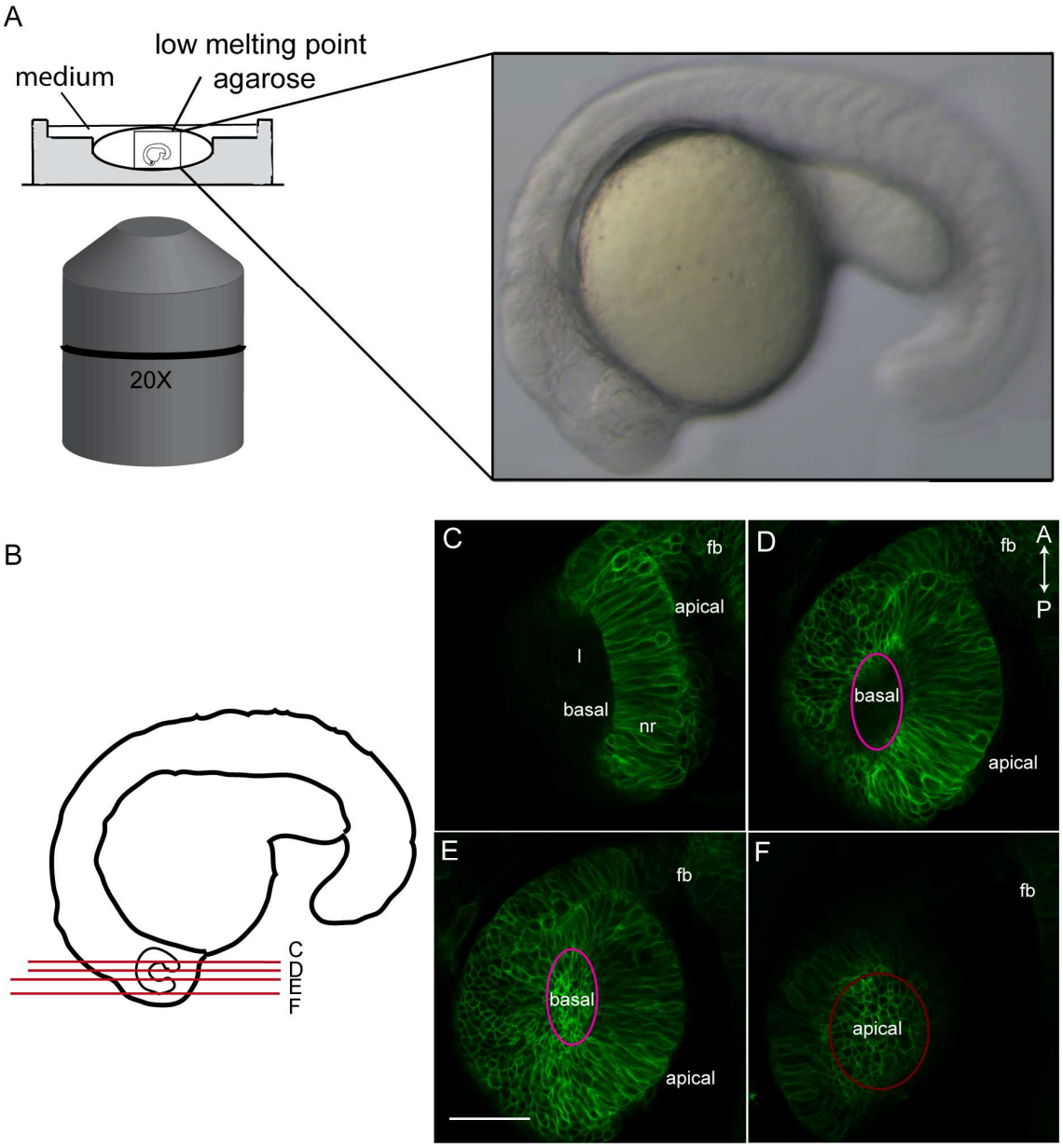

Figure 11. Imaging approach for visualization of apical and basal surfaces of the neural retina. A) Illustration of mounted embryos positioned for visualization. B) Illustration of confocal microscopy planes selected for a standard z-stack in a timelapse movie. C-F) Confocal microscopy images showing images from a Z-stack of the retina. Pink circles label basal cell surfaces. Brown circle labels apical surfaces. Forebrain (fb), neural retina (nr), lens (l). Scale bar: 50 µm.

8 Data Processing and Analysis

8.1 Image processing with ImageJ

ImageJ is a freely available imaging processing software (Wayne Rasband, National Institute of Health, Maryland, http://rsb.info.nih.gov/ij/). We used Version 1.46d to obtain

maximum intensity projections (MIP) of image Z-stacks. An ImageJ macro was also utilized for quantifications of signal intensity during specific experiments. In this case, a background region of interest (ROI) was selected. The resulting mean value of this area, plus an additional value (equal to the standard deviation multiplied for a scaling factor (1.0)) was subtracted for each slice, in order to obtain unbiased intensity measurements. An area of 2,327μm (0,2327μm pixel $^{-1}$) was used to delimitate each point and to quantify its intensity pixel mean value.

8.2 Segmentation

Processed images were segmented to indentify each cell as an individual unit with its own parameters, and then, the area of each identified cell was tracked through time. Both segmentation and tracking were done using Packing Analyzer V2.0 software provided by Susanne Eaton's laboratory (Max Plank Institute of Molecular Cell Biology and Genetics, Dresden, Germany), (Aigouy *et al.* 2010). This software is able to efficiently detect the cell membrane, which is required to obtain accurate area measurements. The programme also allowed us to examine individual images and correct the automatic segmentation whenever necessary. Once cell areas were quantified (see Figure 12, A-D), the rate of area change was calculated as the first derivative.

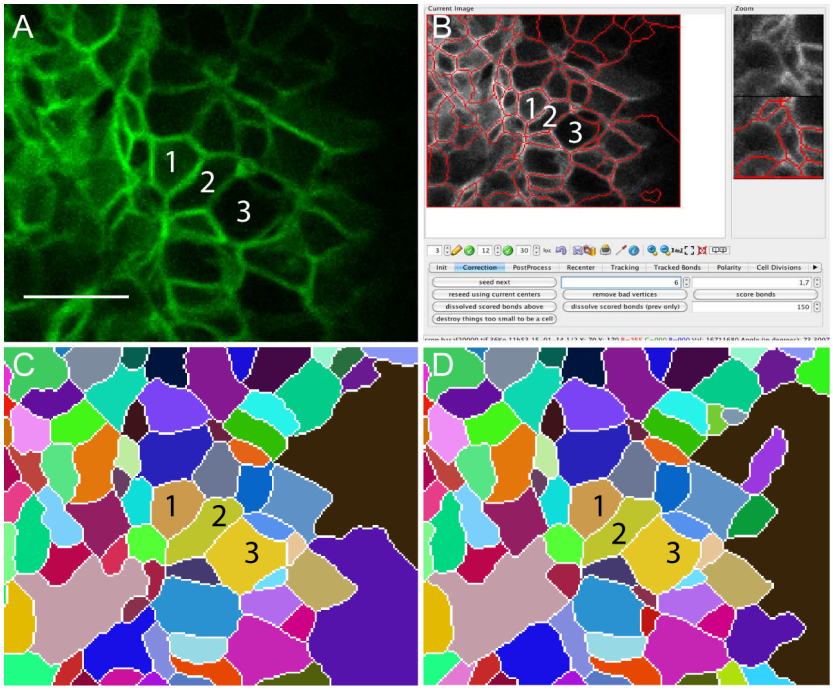

Figure 12. Schematic approach used for image analysis. A) Original confocal microscopy image showing basal cell feet of retinal epithelium cells, marked with GFP at 20hpf. Three

individual cells are selected and labelled 1, 2 and 3. Scale bar: 10 µm. B) Segmentation with Packing Analyzer V2.0 (Aigouy *et al.* 2010). C-D) Example of cell area tracking for cells 1-3.

8.3 Intensity measurements

Segmented and tracked images were then processed with a MATLAB script. This script used cell data obtained from Packing Analyzer V2.O (Aigouy *et al.* 2010) and quantified pixel intensity mean value for each cell. Intensity changes rates were calculated as the first derivative to detect intensity changes through time.

8.4 Other measurements

Apico-basal axis length, cellular distance, opening angles and basal and apical cell length (in transplantation experiments) were also quantified using ImageJ software.

Cross-correlation analysis was performed using a MATLAB script design in our laboratory by Franz Kuchling.

9 Transplantation at Blastula Stages

Fertilized *Tg(vsx2.2:GFP-caax*) and wt eggs were incubated at low density (50 eggs per dish) at 28ºC. At around 4hpf, eggs were dechorionated by pronase treatment (375µg/ml) and carefully washed with E3 medium, avoiding contact of embryos with air, as dechorionated embryos of such early stages are quite fragile. Then, donor embryos at sphere stage were placed into a column within a set agarose mold; and host wt embryos of the same stage were placed in the adjacent column (see Figure 13). Cells from the blastula cap of donor embryos were collected with a glass needle (Borosilicate Glass Capillaries GC100-10;1.0mm x 58mm, 6´´HARVARD APPARATUS 30-0016) and implanted into the caps of host embryos. After cell transfers were completed, host and donor embryos were incubated at 28ºC until they reached the desired developmental stage. GFP positive embryos were selected then and prepared for *in vivo* live imaging.

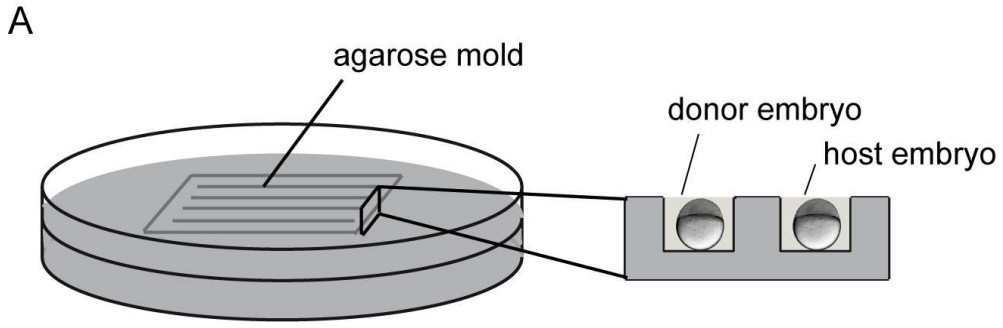

Figure 13. Schematic approach of embryos for transplantation experiment. A) Petri dish with an agarose mold and position of both, donor and host embryos.

10 RNA Synthesis

To visualize actin dynamic, we used a vector containing utrophin, which is a well-known cytoplasmic protein that binds laterally with its actin-binding domain to cortical actin filament (Hong *et al.* 2013; Tinsley *et al.* 1992). The plasmid Pcs2+UtrGFP, already available in our laboratory, was used to synthesize the utrGFP RNA. The construct was first linearized with NotI (Takara Bio Company) and purified. The lineal DNA was transcribed with the SP6 enzyme (Roche Applied Science) and then digested with Turbo DNAse (DNAseI, Boehringer Mannheim) to remove any traces of DNA. The mRNA was precipitated with 4M LiCl and quantified. The utrGFP RNA was injected into *Tg(vsx2.2:lyn-tdtomato*) embryos at one cell stage (200pg per embryo).

11 Inhibitor Treatment

Embryos were mounted for *in vivo* imaging at the confocal microscope (as described in section 6) and covered, accordingly, with E3 medium, E3 with DMSO or E3 with blebbistatin. Blebbistatin is a highly specific inhibitor of ATPase activity of myosin (Kovacs *et al.* 2004). It was diluted in DMSO and used in a final concentration of 150 μM.

When required, embryos at 18.5hpf were first incubated at 28ºC for one hour in E3 medium with added blebbistatin. Embryos were also protected from light during treatment, as blebbistatin is a light-sensitive molecule. Control embryos were incubated in the same conditions with E3 and DMSO. After treatment, embryos were mounted for *in vivo* imaging.

12 Lamc1MO Injections

The antisense *lamc1*morpholino oligonucleotides (MO) was purchased from Gene Tools, LLC. Lamc1MO 5'-TGTGCCTTTTGCTATTGCGACCTC-3' blocks translation, as it is complementary to the 5'sequence of laminin γ 1 RNA (Langheinrich *et al.* 2002; Parsons *et al.* 2002).

The lamc1 MO was injected into *(vsx2.2:GFP-caax)* and *Tg(βactin:Myl12-GFP*) embryos at one cell stage (see section 3 for injection protocol details), at a concentration of 0,7 – 1 pmoles per embryo. It has been shown that MO injections tend to trigger unspecific tissue apoptosis in zebrafish embryos, and it is therefore recommended to co-inject the *p53*morpholino 5'-GCGCCATTGCTTTGCAAGAATTG-3' (Langheinrich *et al.* 2002), which counteracts this effect. We co-injected it with *lamc1*MO at a concentration of 0,5 pmoles per embryo. Control embryos were injected in parallel with *p53*MO alone. Injected and control non-injected embryos were incubated at 28ºC until required and then mounted for live imaging.

13 Eye Phenotypic Characterization

Injected and control embryos were analysed at 24hpf. Digital photographs were taken using a fluorescent stereoscope coupled with a camera (SZX16-DP72, Olympus); using the same set parameters for sensitivity, magnification and exposition in both transmitted light and fluorescent conditions. Eye opening angles, retina width and diameter of the otic vesicle were measured for each embryo; using ImageJ 1.46d (Wayne Rasband, National Institute of Health, Maryland, http://rsb.info.nih.gov/ij/). Retina width values were normalized with the otic vesicle size of each individual embryo. Over 200 embryos, including their respective controls were analyzed for each phenotypic condition.

VI. Results

As it was mentioned in the Introduction, epithelial sheets may constrict at both cell surfaces to shape different organs. In many examples, these constrictions require cell shape changes including variations of cell area surface and changes along the apico-basal axis (review in (Sawyer *et al.* 2010)). Previous works in our lab suggest that in medaka embryos, neural retina cells undergo basal constriction to form the optic cup. This bending is regulated by Opo protein, which interacts with clathrin adaptors to regulate polarized endocytosis and thus integrin localization at the neuroblasts basal feet. However, little is known about the cell shape changes that occur during this process (Bogdanovic *et al.* 2012; Martinez-Morales *et al.* 2009).

In this thesis, we use zebrafish neural retina to explore cell behaviour in a comprehensive manner during optic cup morphogenesis. The data presented here confirm formally that retinal precursors undergo basal constriction as the main cellular process driving this morphogenetic event. However, before describing at a cellular level the constriction, it is necessary to describe quantitatively the general geometry of the retinal epithelium as it folds.

1. Neural Retina Thickness Does Not Change During Optic Cup Morphogenesis

It has been shown that during *Drosophila* gastrulation, the ventral furrow and the posterior midgut cells invagination proceeds through several cell shape changes, including cell elongation and a subsequent shortening of the apico-basal axis (Sweeton *et al.* 1991). In order to address whether similar cell shape changes occur in a vertebrate context, we studied the behaviour of the epithelium during optic cup folding. As a first step, we measured epithelium thickness, which could be indicative of changes in retinal neuroblasts width. To this end, we perform in vivo time-lapses using a reporter, *Tg(vsx2.2:GFP-caax*), in which cell membranes are GFP-tagged, thus facilitating the measurements of such width changes (see Methods section 7 and 8.4). We then quantified in three different retinae the apico-basal axis length, at anterior, middle and posterior positions and at two time-points (19 and 22hpf, corresponding to optic cup folding (see figure 14). Initial length was calculated as the mean value obtained from the first five frames, and final length as the mean value for the last five frames. The final value corresponds to the mean of all three measurements at one time-point.

Even though the volume of the whole organ increases dramatically during these stages due to the architecture of the organ itself (Kwan *et al.* 2011), during optic cup folding we did not observe significant changes in retina thickness (according to the student t-test

analysis) at the anterior, centre or posterior sides (see Figure 14). The average width remained within a range of 45 to 50 µm.

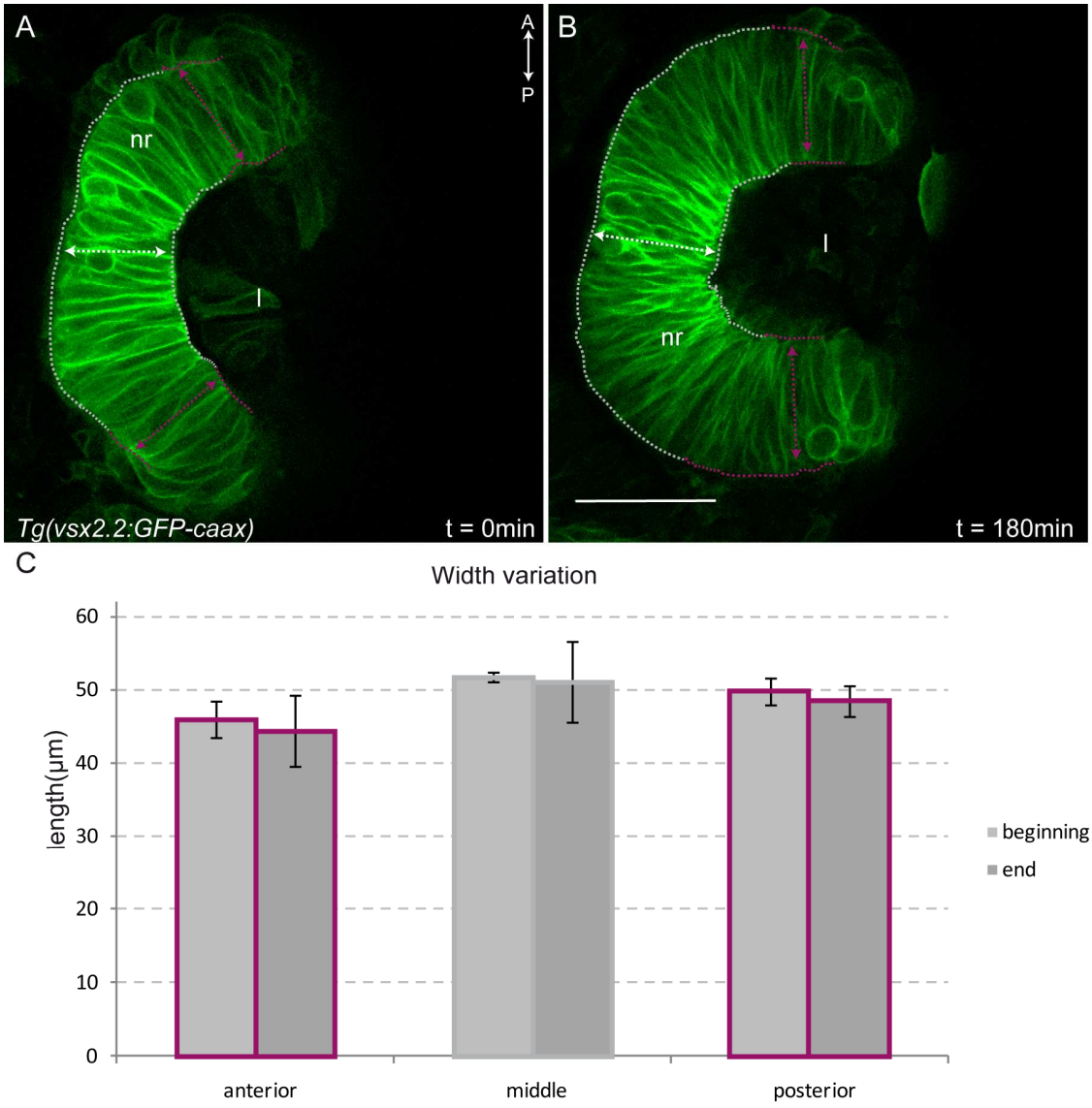

Figure 14. Retinal apico-basal axis length does not change significantly during zebrafish optic cup folding. A-B) Confocal microscopy time-lapse images showing initial (A) and a late (B) steps of eye cup morphogenesis in *Tg*(vsx2.2:GFP-caax) embryos (membranes: green) (dorsal view). Arrowheads: apico-basal axis length in the anterior (purple), middle and posterior (purple) neural retina. Neural retina (nr), lens (l). Scale bar: 50 µm. C) Quantification of apico-basal axis length variation at different time points during optic cup folding. Error bars indicate standard error of the mean. p= 0,8 p= 0,91 and p=0,68 for anterior, middle and posterior neural retina respectively.

2. Surface Quantification During Optic Cup Folding

Once we established that no significant changes in width occur along the apico-basal axis during OCM, we aimed to explore area variations at the apical and basal surfaces. To address this question, confocal *in vivo* time-lapse imaging was performed with *Tg(vsx2.2:GFP-caax*) embryos (see Methods, Sections 6 and 7) at 19, 20 and 21hpf, in a set of 6 retinae (3 retinae for each side, apical and basal). The 19hpf stage was chosen because at this point, the neuroepithelium has just started folding and the polarity of the neuroblasts can be easily visualized at this point, from a dorsal view. At stage 20 hpf OCM has progressed more than 50% and by 21hpf, the optic cup is almost completely folded. As the architecture of the organ itself was changing through time, images were acquired as separate movies for the different stages, so that the focal plane could be adjusted. Around 100 cell areas were measured in total (see Methods section 8) for each side (see Supple. Table 1, 2 3 and 4.).

Area changes through time were calculated as the difference between the initial and the final surface for each cell, at the different stages analysed. For cell size, statistical significance was determined using a student's t-test, where significance was assumed when $p<0.05$. Mitotic cells were not taken into account during quantifications to reduce bias in the measurements.

At 19hpf, around 40% of the surface areas measured at the apical side were increasing, 30% did not suffer any change and the remaining 30% were decreasing in size (See Figure 15, A). At 20hpf, once the neuroepithelium is 50% folded, an increase in the number of cells that remain unchanged was detected, as well as in the number of those that increase their surface area. At 21hpf, when the morphogenetic process is almost finished and the cells have reached their final shape, there are more cells that do not change their surface area (Figure 15, A). In contrast to the apical side, at the basal side the surface areas decreased in more than 70% of the cells during stage 19hpf. This corresponds with the moment when the most severe bending of the tissue takes place according to angles measurements (see Figure 24). The remaining 30% did not undergo significant changes or underwent a no significant increase in surface area. As development proceeds, the percentage of cells reducing their basal surface decreases and the number of stabilized cells increases basally (Figure 15, B). Quantitatively, the percentage of cells with apical areas ranged between 20-35 $\mu m^{2,}$ is increasing through the process, while the percentage of cells with basal surfaces larger than 20 μm^2 decreases (figure 15, C and D). These variations indicate that apical and basal surfaces are changing and thus cells are progressively forced to acquire a wedge shape. Although we have measured changes in

both surfaces, between 19hpf and 20hpf, when the most severe bending is taking place, we observed a significant (*p<0,01*) reduction of the basal (from 25µm² to 18 µm²) but not in the apical areas in most of the cells. Later on, a small but significant (*p<0,05*) enlargement of the apical side can be also detected (figure 15, C' and D').

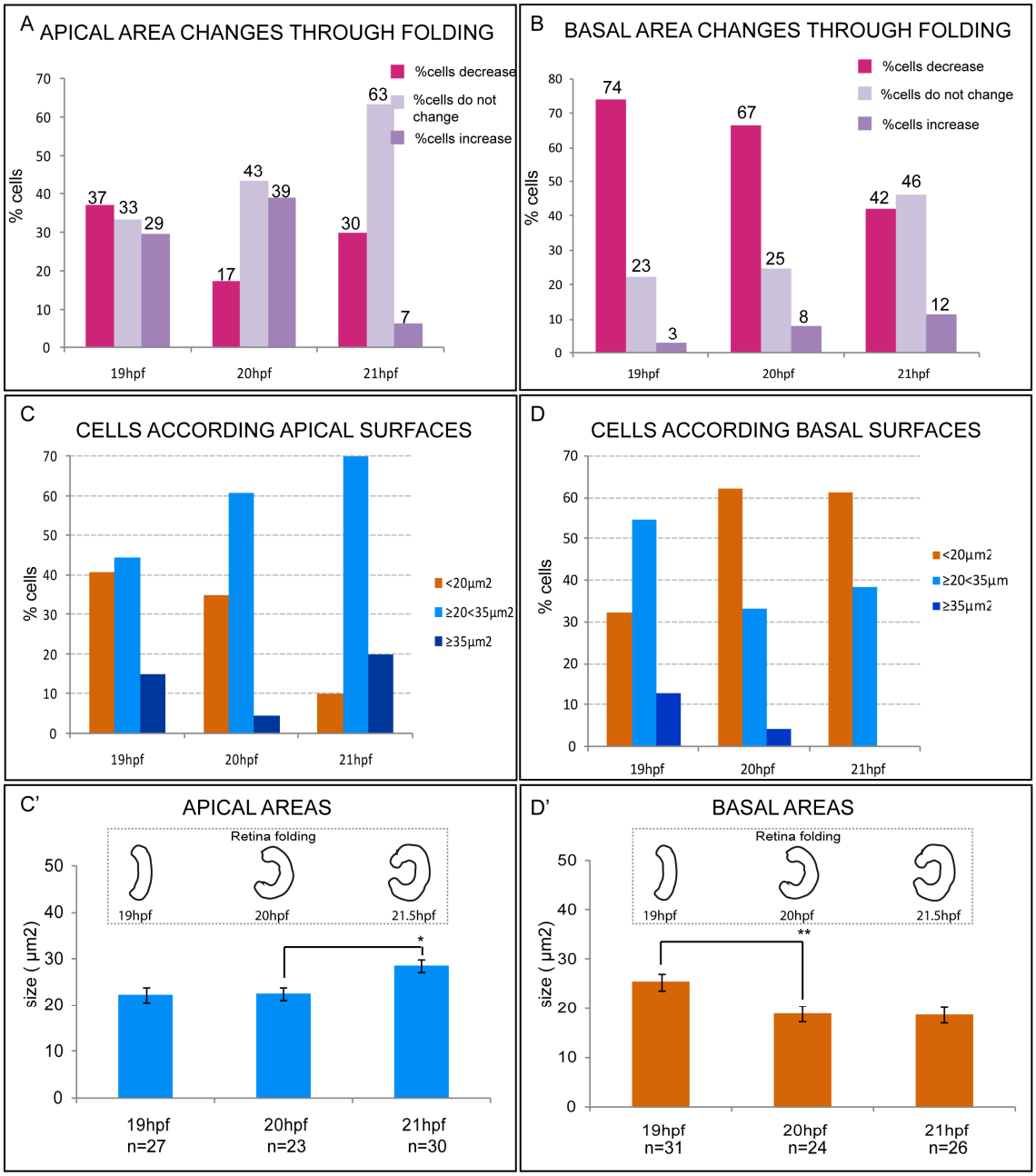

Figure 15. Cell surface area variations during optic cup folding at the apical and basal surface of the retinal epithelium. A,B) Quantifications of percentage of area changes at apical (A) and basal (B) surfaces at 19, 20 and 21hpf. C,D) Quantifications of percentage of cells according to the size of their apical (C) and basal (D) surfaces at 19, 20 and 21hpf. Specific percentages are displayed for each column. C'-D') Illustrations of retina folding degrees at the corresponding stages,

and charts showing mean cell area sizes at 19, 20 and 21hpf of the apical (C') and basal (D') surfaces. The significance of the increase in the mean apical areas and the basal constriction are indicated with asterisks. Error bars show the standard error of the mean. (C') *p<0,05* and (D') *p<0,01;* Student t-test.

3. Behaviour of Cells At The Apical Side

To study cell behaviour at the apical side, confocal *in vivo* time-lapse imaging was performed at the apical surfaces of retina cells (see Methods section 7 and 8) in *Tg(vsx2.2:GFP-caax*) embryos at 20hpf. A total of 40 cells were analysed from a set of 3 different retinae. Area change rates were calculated as the first derivative. The Pearson correlation coefficient was calculated for 40 pairs of adjacent cells to quantify whether at one point in time, either cell of the pair is constricting or relaxing.

Our results show that cells were in a dynamic state; apical area rate measures indicate that the behaviour of the cells is oscillatory (increasing and decreasing their apex surface). Furthermore, to find out whether there is a correlation in contractions between neighbouring cells, the Pearson correlation coefficient (R) was calculated. The R coefficient of the 75% of measured cells was comprised between -0,5 and 0,5 (see Suppl. Table 5) showing that cells had an asynchronic activity (figure 16, E).

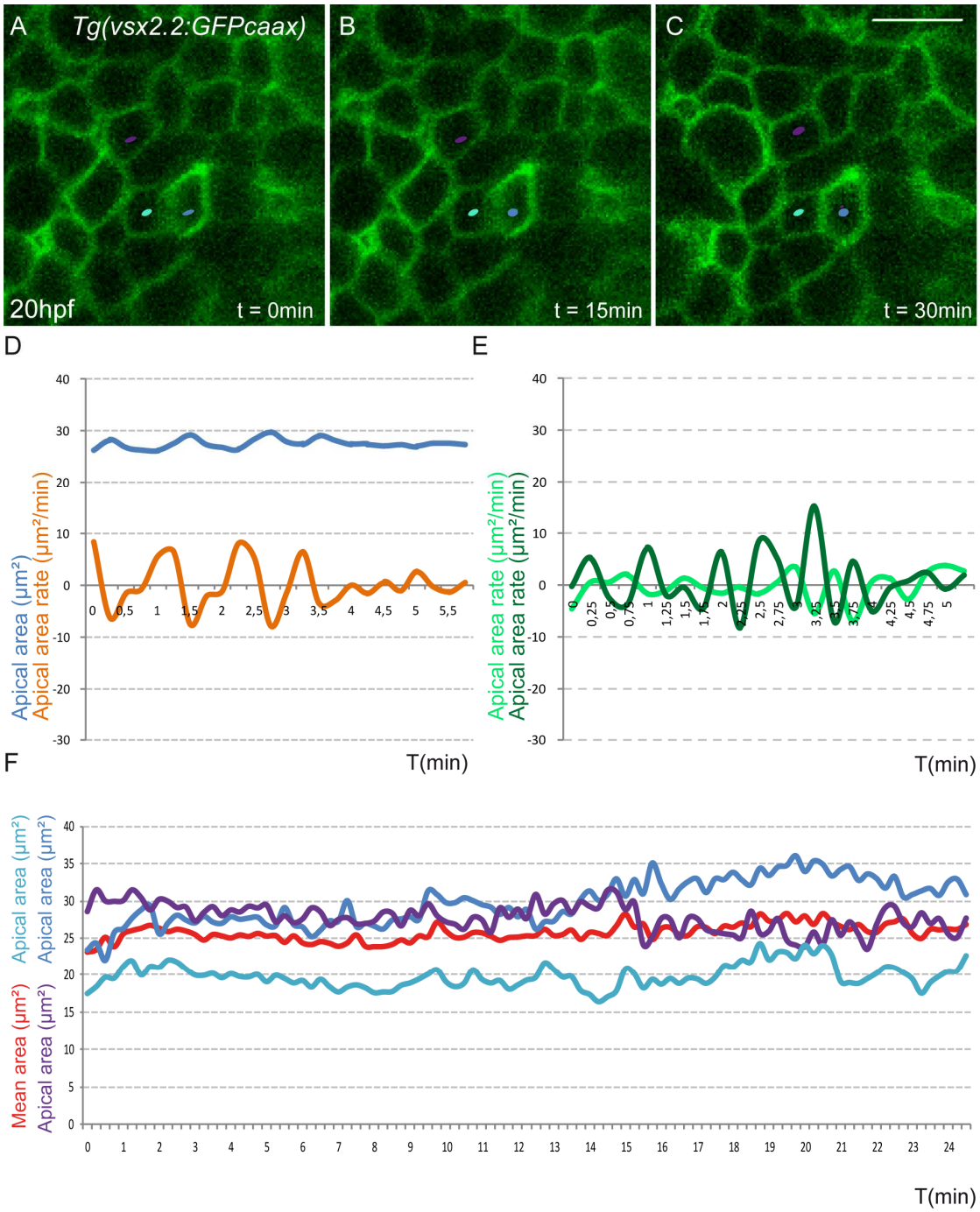

Figure 16. Cell behaviour at the apical side of the neural retina. A-C) Confocal microscopy time-lapse images showing apical cell surface in *Tg*(VSX2.2:GFP-caax) embryos (membranes, green). Coloured dots mark area changes in different neuroblast. Scale bar: 10 µm. D) Quantification of apical rate and apical area changes through time in an individual cell. E) Graphic showing asynchronic activity in neighbouring cells. F) Quantification of apical area behaviour of contiguous neuroblasts and their mean value.

These findings indicate that the apical behaviour of the cells during eye morphogenesis is dynamic and that contiguous cells do not oscillate in phase.

4. Behaviour of cells at the basal side

To explore the behaviour of cells at the basal side during OCM and compare it with the apical one, confocal *in vivo* time-lapse imaging was performed at the basal surfaces of retina cells (see Methods section 7 and 8) in *Tg(vsx2.2:GFP-caax*) embryos at 20hpf. A total of 100 cells were analysed from a set of 8 individual retinae. Surface area rates were calculated as the first derivative.

We find that cells at the basal side are oscillating (increasing and decreasing their areas), as was the case for the apical side. Both, the basal area of the cells and their constriction rate were plotted (Figure 17, D). To establish whether there is a correlation in the contractile behaviour of adjacent cells, the Pearson correlation coefficient (R) was calculated. As was the case for the apical side, contiguous cells at the basal side showed asynchronic activity (Figure 17, E and Suppl. Table 6). This suggests that cells were also not in phase at the basal side. Moreover, almost 70% of the cells analyzed showed a decrease in basal surface area (Figure 17, F). This is consistent with an irreversible progressive constriction of the cell surfaces, a ratchet-like behaviour similar to what has been previously described in apically-driven morphogenetic processes in *Drosophila* (Martin *et al.* 2009; Solon *et al.* 2009).

Together, these findings suggest that cell areas are dynamic at both the apical and the basal side, and that optic cup folding is mainly driven by the constriction of the basal side.

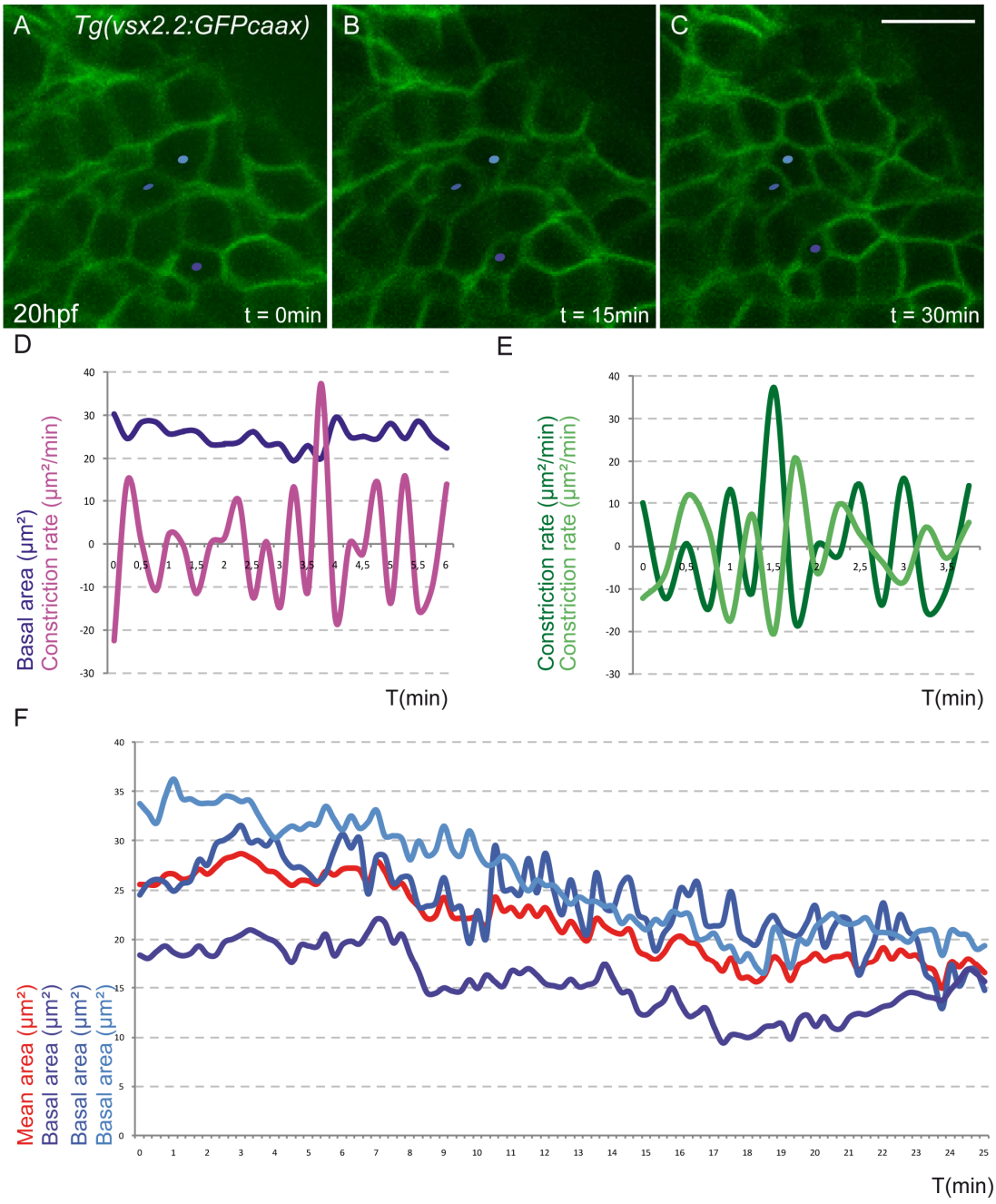

Figure 17. Basal constriction during zebrafish optic cup folding. A-C) Confocal microscopy time-lapse images showing the basal cell surface in *Tg*(VSX2.2:GFP-caax) embryos (membranes, green). Coloured dots mark area changes in different neuroblasts. Scale bar: 10 µm. D) Quantification of the constriction of an individual cell's basal surface. E) Pulsed constriction is asynchronous in neighbouring cells. F) Quantification of the basal constriction of contiguous neuroblasts and their mean value showing the decrease in area through time.

5. Apical and Basal Cell Surfaces in the Retina Oscillate in an Uncoupled Fashion

To quantify whether apical and basal surfaces were contracting and relaxing simultaneously or not in an individual cell, transplantation experiments were performed (see Methods section 9). Cells from *Tg*(*vsx2.2:GFP-caax*) embryos at blastula stage were transplanted into wild type embryos in order to visualize the behaviour of individual neuroblast. Then, GFP positive embryos were mounted and prepared for in vivo time-lapse imaging (Methods section 6, 7.3 and 8).

From the recordings obtained, the lengths of both apical and basal retina surfaces were measured. A 40 min window during optic cup folding was selected from each time-lapse, in three individual transplantation experiments. The rates of length variation for both surfaces were calculated as the first derivative to obtain length changes through time (see Figure 18). The Pearson correlation coefficient for the rates of basal and apical length variations was calculated for each cell, to check whether increases and decreases of length at one side could be correlated with changes of length in the other surface. For all neuroblasts analysed, the R coefficient was -0,5 and 0,5 (see Supple. Table 7), indicating that there was no correlation between the dynamics of retina cell area changes in both surfaces. Therefore, our results indicate that apical and basal surfaces were contracting and relaxing mostly in an independent manner.

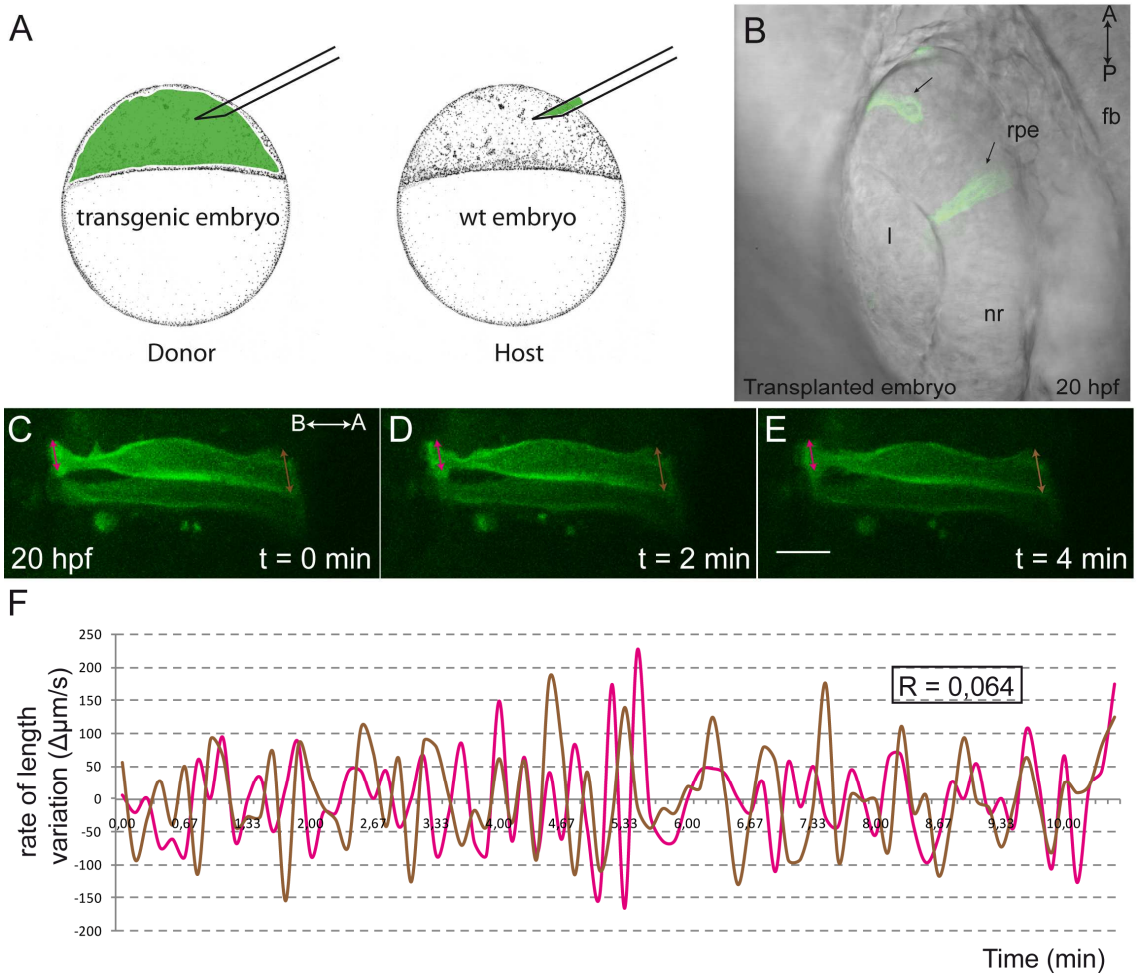

Figure 18. Cell clones in transplanted embryos show uncoupled oscillations at apical and basal surfaces. A) Scheme of transplantation experiment. Cells from a transgenic (membranes green) donor embryo are transplanted to a wild type host embryo at sphere stage. B) Confocal microscopy image showing GFP expression of transplanted cells at 20hpf. Arrowheads: individual cells. Forebrain (fb), retinal pigmented epithelium (RPE), neural retina (nr), lens (l). C-E) Confocal microscopy time-lapse images of a transplanted cell clone. Arrows indicate basal (pink) and apical (brown) length variation. Scale bar: 10 μm. F) Quantification of the basal (pink) and apical (brown) rate of length variation for an individual clone. R (Pearson correlation coefficient).

6. Mitosis Is Not Essential For Correct Retina Folding During OCM

The role of mitosis during eye formation has already been studied in some vertebrates. In *Xenopus,* inhibition of cell division does not affect retinal differentiation (Harris *et al.* 1991). Additionally, optic cup morphogenesis in zebrafish is not severely impaired when embryos are treated with proliferation inhibitors; eyes are smaller in size and have less

number of cells and lower density, but they invaginate correctly; suggesting that mitosis is dispensable for the basic program of OCM (Kwan *et al.* 2011).

As mitosis in a proliferating epithelium is strictly restricted to the apical surface (Sauer 1935), we expected to observe changes in the distance between cells surrounding a mitotic event. To test whether apical divisions contribute to the expansion of the apical retina, we measured the distance separating the two flanking cells that surround a central mitotic cell (see Figure 19, A-D). These measurements were obtained during mitosis for both apical and basal sides, in a total of 10 mitotic cells identified in different retinae.

If mitosis does not have indeed a role during OCM, the distance between two different cells surrounding a mitotic cell should recover after mitosis, to avoid an apical expansion of the retina.

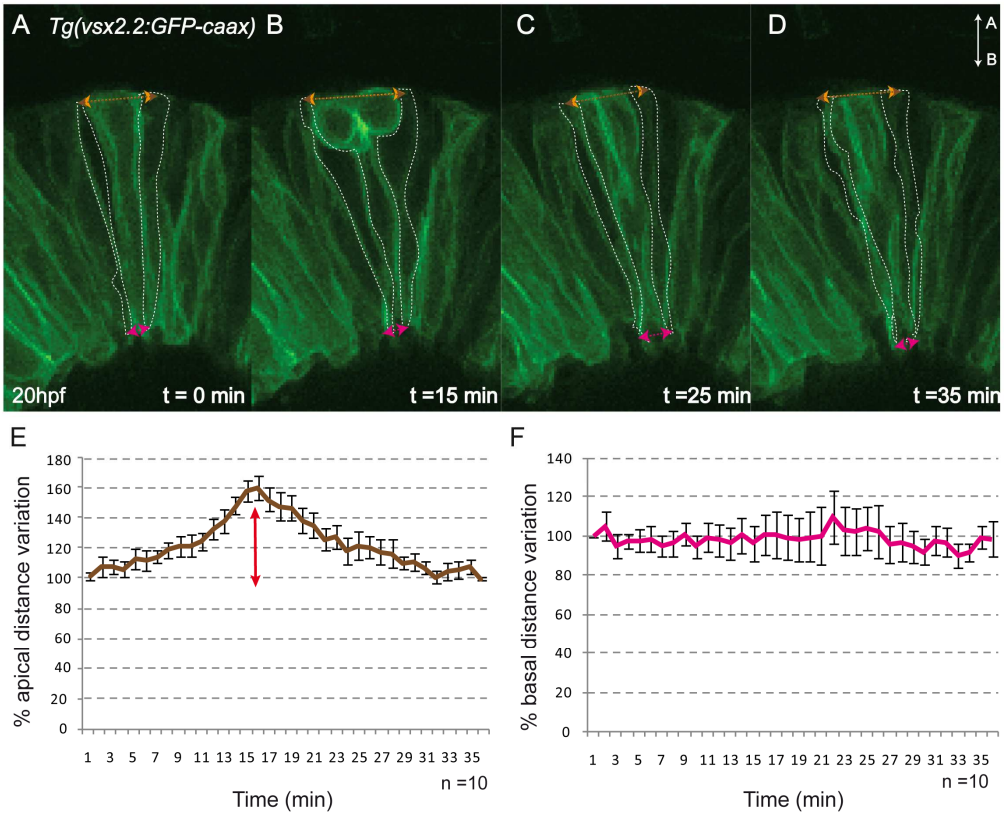

Figure 19. Mitosis does not play an essential role in basal constriction in zebrafish optic cup folding. A-D) Confocal microscopy time-lapse images showing a mitosis at 20hpf in a *Tg*(vsx2.2:GFP-caax) retina (membranes, green). Dashed lines mark surrounding cells. Arrows indicate distance variation (brown apical, pink basal). E-F) Quantification of percentage of distance variation on the apical (E) and basal (F) sides. Error bars indicate standard error of the mean.

As shown in Figure 19, E and F respectively, a transient increase in the percentage of apical and basal distance variation was detected during the mitotic event (on the apical

side) (E) and once the new cell has been intercalated (on the basal side) (F). However, the original distance between cells is roughly recovered after 25 minutes. This shows that mitosis does not interfere with principal aspects of basal constriction during zebrafish optic cup folding.

7. Actin Dynamics at the Basal Feet of Retinal Neuroblasts.

Previous works in Drosophila have shown the role of the actomyosin network in apical constriction (Hunter *et al.* 2013; Martin *et al.* 2010). Furthermore, many studies have demonstrated that cell shape changes responsible for constriction proceed in pulses driven by the oscillatory activity of the actomyosin network (review in(Gorfinkiel *et al.* 2011)). Therefore, to analyse actin behaviour and to verify whether similar oscillatory activity leads OC folding, we used the RNA of the polymerized actin marker UtrGFP (See Methods section 10). The RNA was injected into one-cell stage in *Tg(vsx2.2:lyntdTomato*) embryos, a transgenic line that labels neural retina membranes. The microinjected embryos were then incubated at 28ºC until they reached the proper developmental stage, and un-injected sibling embryos were also incubated as a control. Several, independent experiments were carried out and included in the analysis. Embryos that displayed GFP expression were then mounted for in vivo time-lapses (See Methods section 6 and 7). Basal area changes and actin variations were quantified after segmentation for each cell. To detect whether there is a relationship between actin accumulation and basal area changes, a cross-correlation analysis was performed.

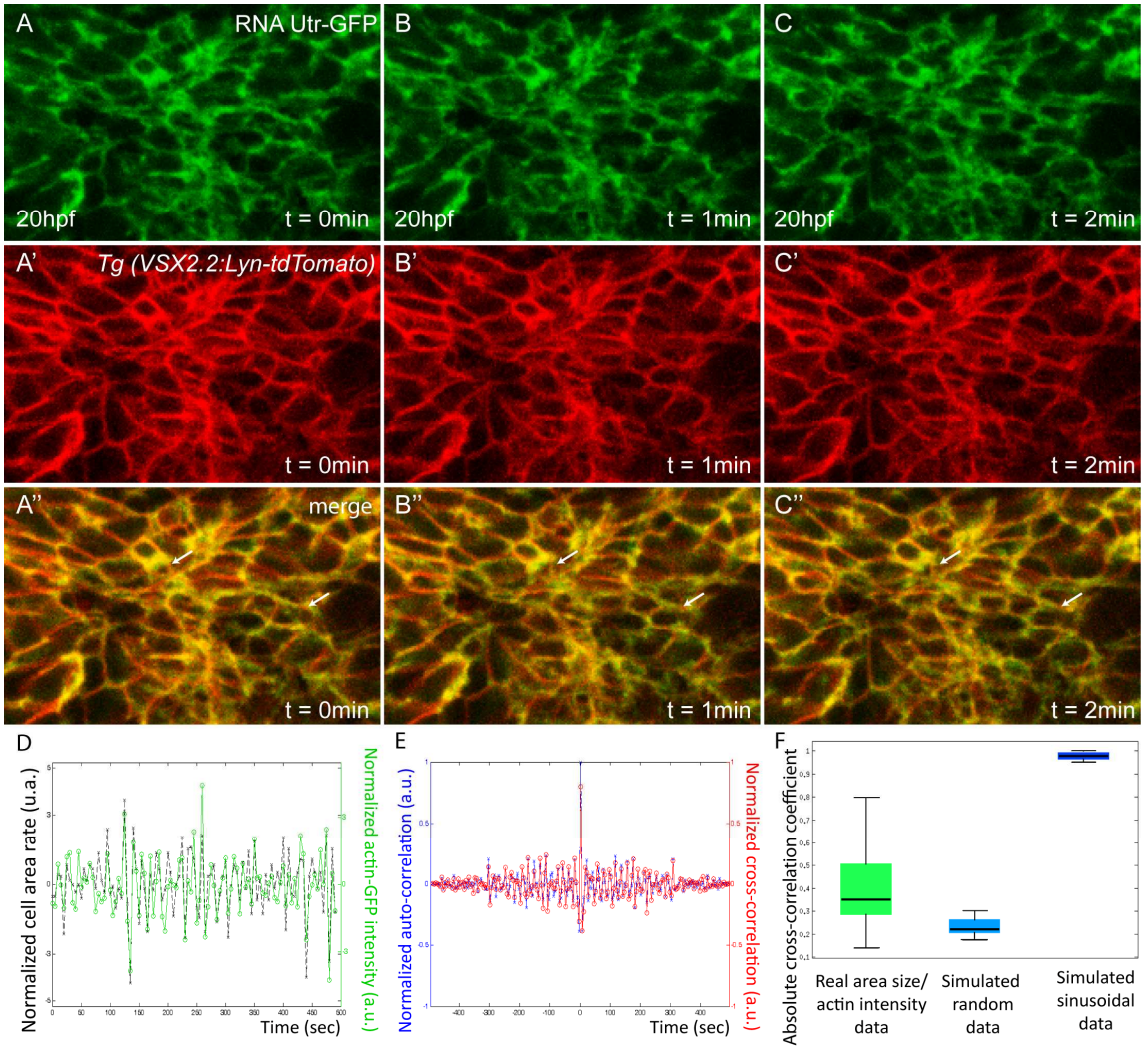

Figure 20: Actin accumulation at the basal side of neural retina cells. A-C) Confocal microscopy time-lapse images showing basal cell surfaces and Utrophin accumulation. A-C)(green: Utrophin-GFP). A'-C') (red: membranes).A''-C'') merge. E) Graphic showing cross correlation coefficient. F) Cross correlation coefficient for real, simulated random and simulated sinusoidal data. Arrows show actin accumulation.

Our results show that the presence of actin at the basal feet of neural retina cells fluctuates during OC folding (see Figure 20 A-H). Cell area rate and Utr-GFP accumulation rate were plotted in Figure 20, D showing that larger cell areas coincides with high Utr-GFP intensity levels. The cross correlation coefficient was calculated for cells from three different experiments. We observed a dominantly positive correlation between actin accumulation and basal area changes, indicating that within the experimental sampling rate of 5 seconds, both phenomena occur simultaneously. In order to evaluate our results we compared our experimental data with simulated random and sinusoidal signals of similar statistical properties. The box plot shows that the coefficients of simulated random

data are significantly lower than our observations in vivo, and that the coefficients of simulated sinusoidal data are close to one. This indicates that the majority of cells display a significant correlation between actin accumulation and basal area changes.

8. Basal accumulation of Myosin *foci* is required to the folding during OCM.

Previous studies in *Drosophila*, and in *C.elegans* have shown that the presence of discrete Myosin accumulations coalescing continuously at the apical cortex can cause apical constriction (Martin *et al.* 2010; Roh-Johnson *et al.* 2012). Thus, to observe the role of Myosin activity during OCM, we performed confocal *in vivo* time-lapses of Myosin localisation using embryos of the Myosin reporter line Tg(*β-actin:Myo12-GFP*).

The images obtained show an accumulation of Myosin, detected as *foci* (transient accumulations) at the basal side of the neural retina (see Figure 21) while the optic cup is folding. These accumulations are transient, displaying initially low fluorescence intensity, which progressively increases to finally disappear after a few minutes (see Figure 21, F-J).

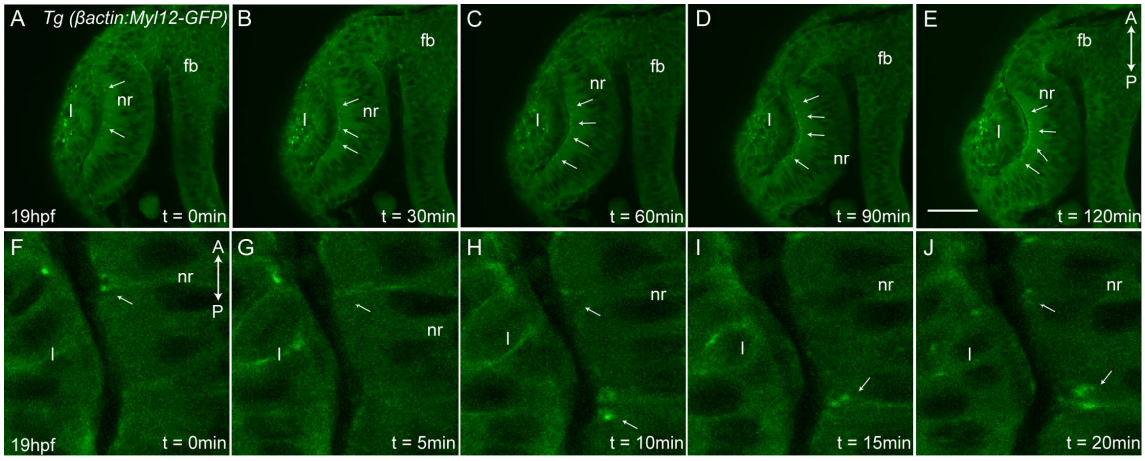

Figure 21. Myosin accumulates at the basal side of the neural retina during zebrafish optic cup folding. A-J) Confocal microscopy time-lapse images showing zebrafish eye morphogenesis in *Tg* (βactin:Myl12-GFP) embryos (myosin green) (dorsal view). Arrowheads: Myosin accumulation. Forebrain (fb), neural retina (nr), lens (l). Scale bar: 50 μm.

To explore the function of Myosin *foci* during the basal constriction, we quantified basal area changes (see Methods) in a random selection of neuroblasts from different retinae and analysed them for the presence of Myosin *foci* (Figure 22), which were quantified by measuring pixel intensity levels.

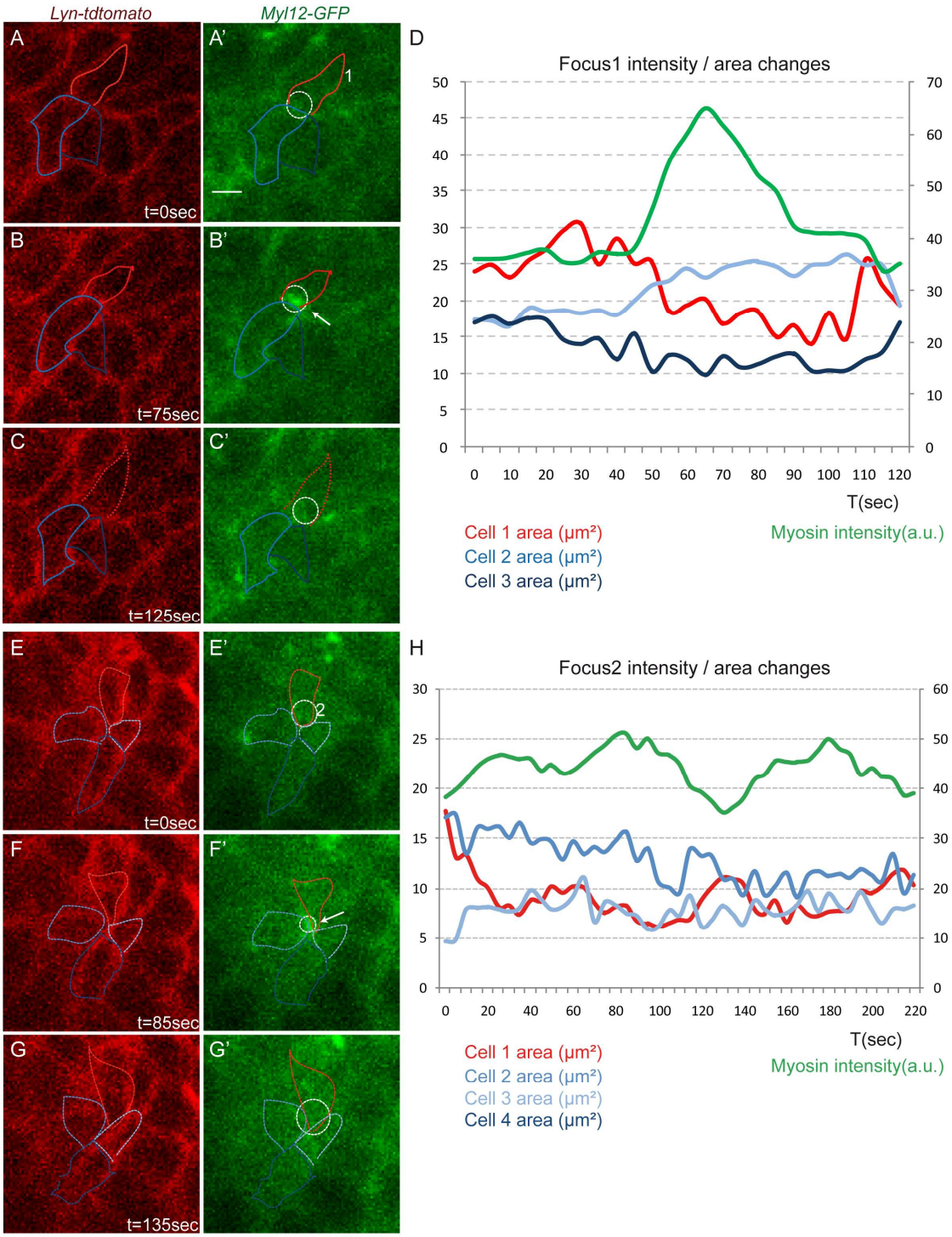

Figure 22. The presence of Myosin *foci* at the basal surface associates with basal cell surface reduction. A-C, E-G) Confocal microscopy time-lapse images showing basal cell surfaces and Myosin accumulation for two different *foci* (red: membranes, green: myosin). Coloured, dashed lines mark a cell with a *focus,* and the surrounding cells. White dashed circles mark Myosin individual *foci* 1 (Solon *et al.* 2009) and 2 (E-G). Scale bar: 5 µm. D and H) Quantification of foci 1

(D) and 2 (H) intensity and basal area changes shows the association between the increase of Myosin intensity and basal area reduction in the cell containing the focus.

Our results, summarized graphically in Figure 22, D and H, show that the presence of a Myosin accumulation coincides with a decrease in the basal area of the neuroblast containing the *focus*. Furthermore, the increase of Myosin *foci* fluorescence in a cell precedes its own constriction (Figure 22, D and H). This finding is consistent with previous observations in *Drosophila*, where a periodic accumulation of the actomyosin network correlates with basal cell area contraction at the basal surface in follicles cells, as well as with apical constriction of ventral furrow cells powered by pulses of actin-myosin contraction during gastrulation (He *et al.* 2010; Martin *et al.* 2009). In 70% of the cells measured, the initial surface area was not recovered after the constriction, once the *focus* had been disappeared. However, no significant reduction was detected in the adjacent cells, suggesting that Myosin accumulation is directly coupled to basal surface reduction.

To address how transient Myosin accumulations affect the whole cell epithelium in the context of the OC basal constriction, we performed *in vivo* time-lapse imaging along the apico-basal axis (see Methods section 23) and measured changes in axis length whenever a Myosin *focus* appeared. Apico-basal axis length was measured as the distance between apical and basal surfaces in the frames where the Myosin *focus* was present. For each *focus*, the data obtained were quantified as the mean value of three independent measurements for the same time-point.

We find that there is an association between the presence of Myosin *foci* and a transient decrease of the apico-basal axis length (Figure 23). Axis length is recovered once the *focus* disappears (Figure 23, G), and the width of the epithelium does not change during eye morphogenesis as it was mentioned above (Figure 14). This is consistent with a previous observation showing transitory changes in apico-basal axis during OCM in medaka embryos (Supple. Figure 1) (Martinez-Morales *et al.* 2009) .

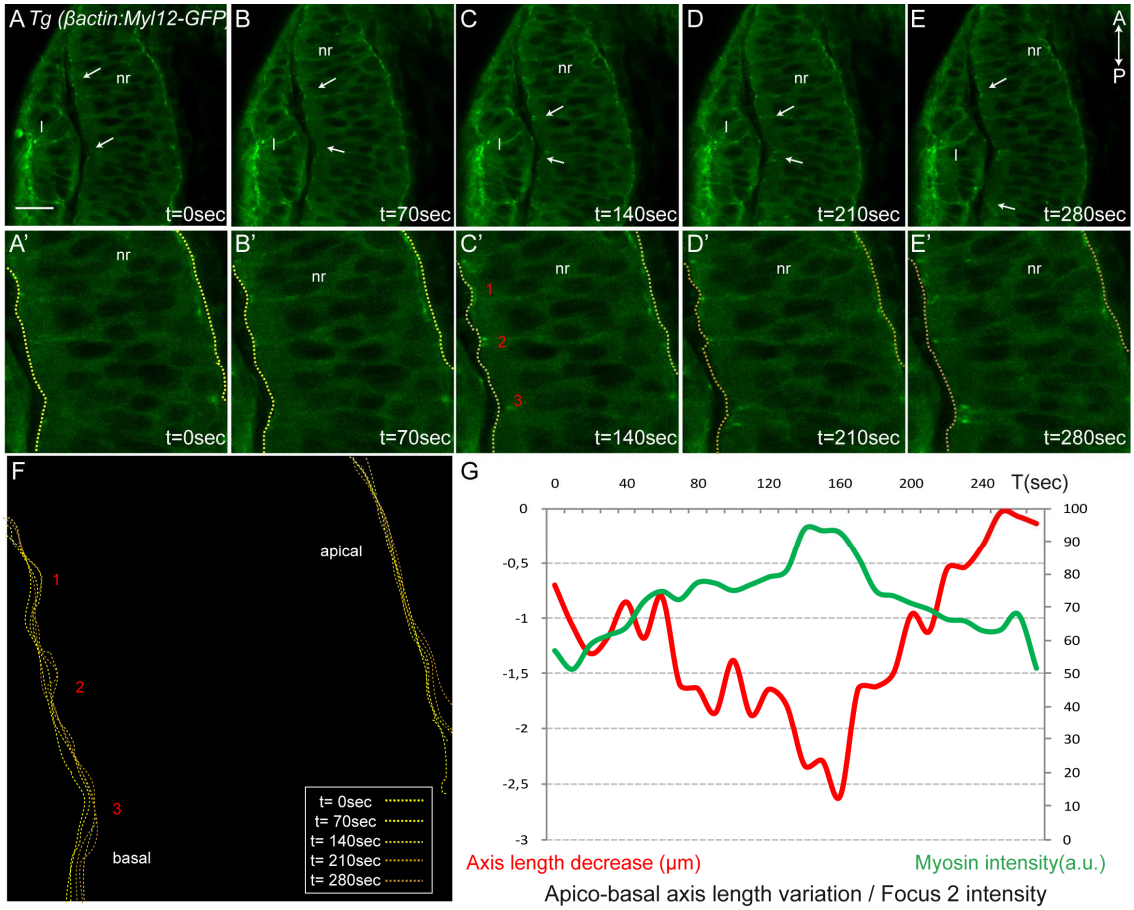

Figure 23. Myosin *foci* at the basal surface produce a transient decrease of apico-basal axis length. A-E) Confocal microscopy time-lapse images showing optic cup folding at 20hpf in *Tg* (βactin:Myl12-GFP) embryos (Myosin green). Arrowheads indicate Myosin *foci*. Neural retina (nr), lens (l). Coloured dashed lines mark apical and basal surfaces changes through time. Scale bar: 20 µm. F) Chart showing a decrease in the apico-basal axis length for three different *foci*. G) Graph showing the association between the increase of Myosin accumulation and the decrease in apico-basal axis length for the *focus* 2. For axis length decrease, 0 is considered the initial distance.

Together, these results suggest that, during OCM, Myosin recruitment at the basal cellular cortex may contribute to the generation of forces acting to induce both the transient shortening of the apico-basal axis, as well as the basal constriction. Both phenomena may in turn contribute to the folding of the epithelium.

9. Blebbistatin treatment blocks OC folding

To determine whether OCM is a Myosin dependent process we decided to interfere with its function using the drug Blebbistatin: a small molecule inhibitor that blocks Myosin II heads by forming a complex with low affinity (Kovacs *et al.* 2004).

To test our hypothesis, Tg*(vsx2.2:GFP-caax*) embryos at 19hpf were treated with blebbistatin (see Methods section 11) in three separate experiments. Images in Figure 24 show how the neuroepithelium folds in control embryos but fails to do so in blebbistatin-treated siblings. Thus, to analyze the results in a quantitative manner, the opening angles of the optic cup were measured once, every hour, (Figure 24, A-H) during the time-lapse movies acquired for the whole morphogenetic event. The angle in control retinae decreased with time, as is expected during a successful folding event. However, in blebbistatin-treated embryos the folding process was at first slowed down, as indicated by opening angles not changing as quickly as in non-treated embryos (Figure 24, E-F); thus resulting in a failure in optic cup closure (Figure 24, G-H). This experiment indicates that normal optic cup folding requires Myosin activity. Significant differences were not detected between untreated and DMSO- treated control embryos (data not shown); supporting the finding that it is the Myosin inhibitor that is responsible for the phenotype observed, and not the experimental setup.

To study the interference of blebbistatin in the actomyosin network at cellular level, embryos at 18hpf were first incubated with blebbistatin for one hour and analysed by *in vivo* time-lapse imaging at 19hpf. Images of basal surfaces from a total of 50 cells, in several untreated and blebbistatin-treated embryos, were segmented and basal area reduction rates and amplitudes were calculated. The amplitude was calculated as the mean of the distance between the highest and the lowest value per oscillation for at least fifty consecutive oscillations. Basal areas from blebbistatin-treated embryos were significantly bigger ($p < 0,01$) than control ones at time-point zero (19hpf) suggesting that the blockage of the contractile machinery resulted in a relaxation of the cellular cortex. After 25 minutes, basal areas from control embryos had undergone a significant reduction (around 30%) while basal areas from blebbistatin-treated embryos did not show relevant changes; indicating that cells treated with the inhibitor are less contractile than cells in untreated retinae. Furthermore, when area changes were represented through time (see Figure 24, N), differences in the global basal surface area as well as contractile patterns were evident. This becomes more obvious when the amplitude of basal area reduction rates were compared (see Figure 24, O). The amplitude of the membrane oscillations was significantly reduced ($p < 0,0001$; Figure 24; P) in blebbistatin-treated cells, indicating that Myosin activity is required for the oscillatory activity of the cell.

This is in agreement with previous observations in *Drosophila* follicle cells, where the use of the ROCK inhibitor Y-27632 results in the lost of basal myosin (He *et al.* 2010).

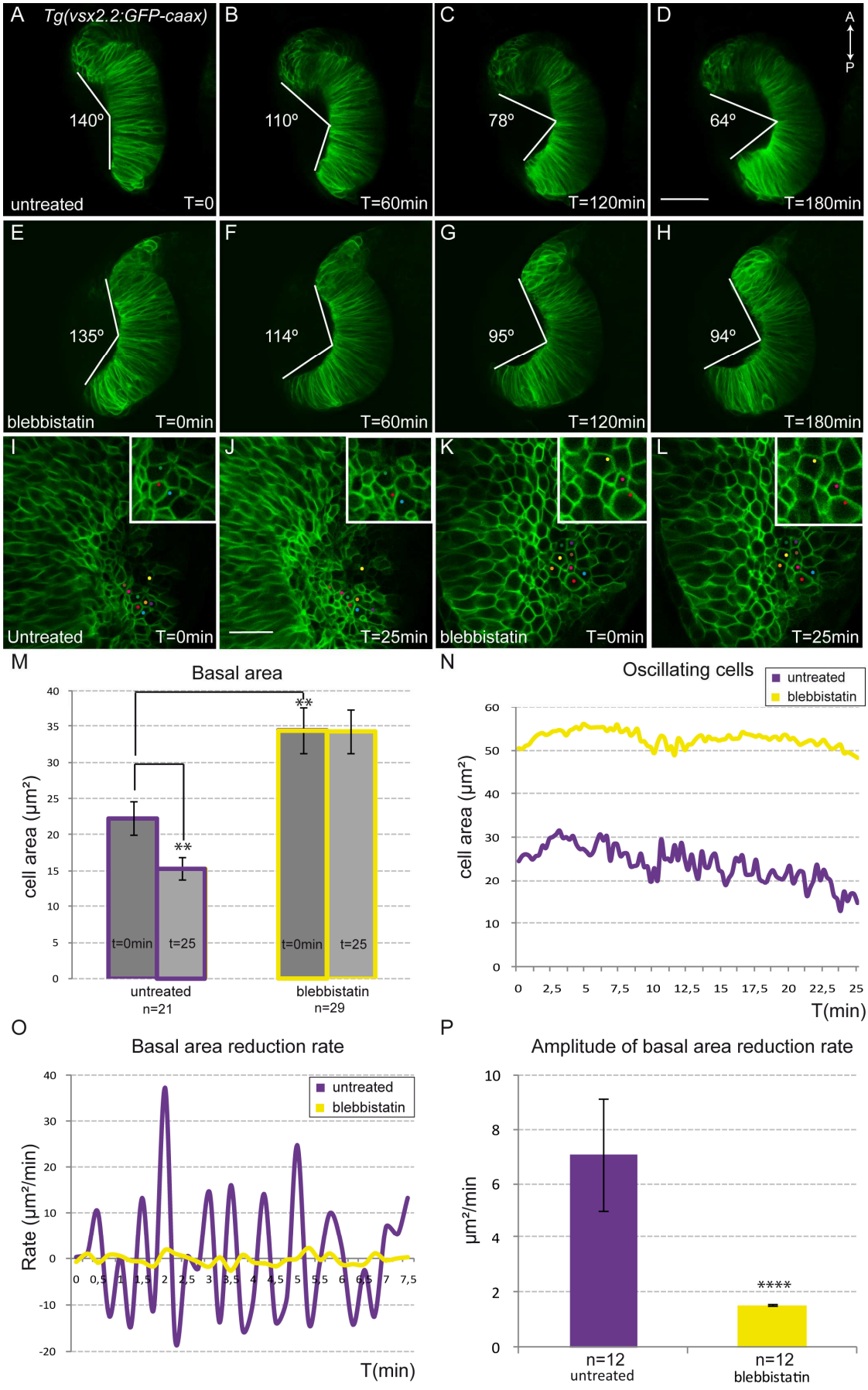
A Tg(vsx2.2:GFP-caax)
140º
untreated
T=0
B
110º
T=60min
C
78º
T=120min
D
A
P
64º
T=180min
E
135º
blebbistatin
T=0min
F
114º
T=60min
G
95º
T=120min
H
94º
T=180min
I
Untreated
T=0min
J
T=25min
K
blebbistatin
T=0min
L
T=25min
M
Basal area
cell area (µm²)
t=0min
t=25
untreated
n=21
blebbistatin
n=29
N
Oscillating cells
untreated
blebbistatin
cell area (µm²)
T(min)
O
Basal area reduction rate
untreated
blebbistatin
Rate (µm²/min)
T(min)
P
Amplitude of basal area reduction rate
µm²/min
****
n=12
untreated
n=12
blebbistatin

Figure 24. Blebbistatin treatment interferes with optic cup folding. A-H) Confocal microscopy time-lapse images showing optic cup folding in *Tg*(*vsx2.2:GFP-caax*) embryos (membranes, green) (dorsal view). A-D) Untreated and E-H) blebbistatin treated embryos. Basal angles mark changes in retina folding through time. Scale bar: 50 μm. I-L) Confocal microscopy time-lapse images at the basal side of the neural retina showing cell area variations. Coloured dots mark individual cells. Insets show a cluster of cells. I-J) Untreated and K-L) blebbistatin treated embryos. Scale bar: 20 μm. M) Quantification of basal areas at 19hpf and 25min later in both untreated and blebbistatin treated embryos. Error bars indicate standard error of the mean. *p<0,01* according to Student t-test. N) Graph showing different oscillating cells (purple, untreated cell and yellow, blebbistatin treated cell). O) Graph showing basal area reduction rate (purple, untreated cell and yellow, blebbistatin treated cell). P) Quantification of amplitude of basal area reduction rate in both, untreated and blebbistatin treated embryos. Error bars indicate standard error of the mean. *p<0,0001* according to Student t-test.

According to the previous results (see Figure 24), blebbistatin interferes with optic cup folding. To confirm that this interference is due to the inhibitory effect of the compound when it binds to the Myosin-ADP-Pi complex, Tg (*βactin:Myl12*-GFP) embryos at 18hpf were incubated for one hour either with E3 or DMSO as negative controls or, alternatively, with blebbistatin at 150μM. Figure 25 A-L shows Myosin *foci* localized at the basal surface in untreated, DMSO and blebbistatin-treated retinae respectively. We observed that Myosin *foci* remained static in blebbistatin- treated retinae, while *foci* in control retinae have a dynamic behaviour, appearing and disappearing in a short period of time. Therefore, Myosin *foci* stability was quantified at the basal side of the neural retina; measured as the extension of time during which an identified accumulation of Myosin was observed. The box plot (Figure 25, N) shows the dispersion of the data in the three treatment conditions (untreated, DMSO and blebbistatin), with median values for *foci* stability similar for untreated and DMSO embryos (4 minutes aprox.). This observation was consistent with our previous results, where no differences in the folding angle between controls were detected (see Figure 24). Interestingly, the median value of *foci* stability in blebbistatin-treated embryos was significantly increased (17 minutes; *p< 0,0001)*. Similar results were obtained when we compared mean values instead. (see Supple. Table 8).

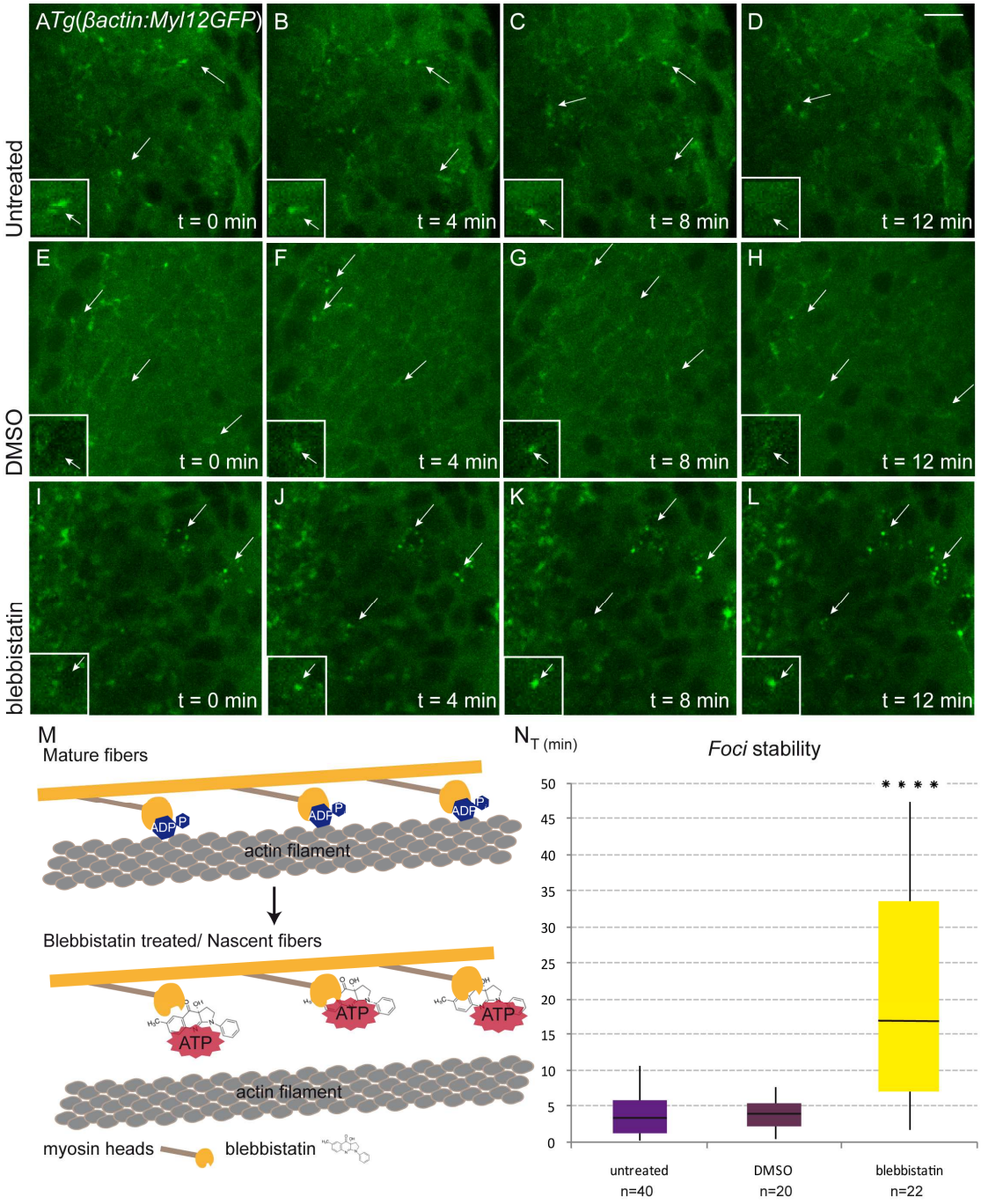

Figure 25. Blebbistatin increases Myosin *foci* stability. A-L) Confocal microscopy time-lapse images showing Myosin *foci* at the basal side of the retina cells. Insets show individual Myosin *focus* through time. Arrowheads: Myosin *foci*. A-D) Untreated, E-H) DMSO and I-L) blebbistatin treated embryos. Scale bar: 10 µm. M) Scheme showing the mechanism of blebbistatin inhibition. The compound interferes in the binding of Myosin heads with actin, by interacting with the Myosin II ATPase (Kovacs *et al.* 2004). N) Quantification of the distribution for *foci* stability in untreated, DMSO and blebbistatin treated embryos respectively. Data in charts are displayed as box plots showing the median, 1st and the 3rd quartile are represented by the box maximum and minimum values. *p< 0,0001* according to a Student t-test.

These findings confirm that blebbistatin can interfere with optic cup folding by blocking Myosin turnover at the basal side of the neuroepithelium.

10. *lamc1* morphant embryos show defects in optic cup folding

Basement membrane proteins provide the scaffold onto which individual cells organize themselves to shape a complex organ. Laminins are large extracellular proteins and a major constituent of basement membranes (Streuli *et al.* 1995). We thus reasoned that they might play an important role in the attachment of the neural retina to the basement membrane during the folding. In fact, Integrin-mediated attachment has been proved to be essential during vertebrate eye folding (Bogdanovic *et al.* 2012; Martinez-Morales *et al.* 2009).

To explore cellular behaviour upon Laminin interference in the folding retina, a *laminin c1* morpholino (*lamc1*MO) directed against the predicted start site of the translation of the Laminin *γ1* chain was used (Parsons *et al.* 2002). To evaluate the effects of *lamc1* knockdown, the MO was injected into one-cell stage in Tg(*vsx2.2:GFP-caax*) embryos, a line that labels neural retina membranes. Several, independent experiments were carried out and included in the analysis. To avoid unspecific apoptosis effects, the *p53* morpholino (*p53*MO) was coinjected with *lamc1*MO at 100μM (Langheinrich *et al.* 2002). Control embryos were either injected with *p53*MO at 100μM or not injected.

The analysis of the resulting phenotypes showed that *lamc1*MO affects eye development when compared to control siblings. Injected embryos displayed malformations previously reported, including a notochord phenotype (i.e. consequence of failures during notochord cells differentiation) and the displacement of the lens and other phenotypic features (Dolez *et al.* 2011; Ivanovitch *et al.* 2013; Parsons *et al.* 2002). In addition, morphants display two main morphological eye defects: malformation of the optic cup with retinal opening angles and an increase in retina width. When retinal opening angles were quantified in *lamc1*MO injected embryos at 24hpf, around 45% of the embryos displayed opening angles in the retina ranging between 21º to 130º (see Figure 26). This contrasts sharply with the measurements obtained from control embryos, showing openings in a range of 0º to 20º (Figure 26, Suppl. Table 9).

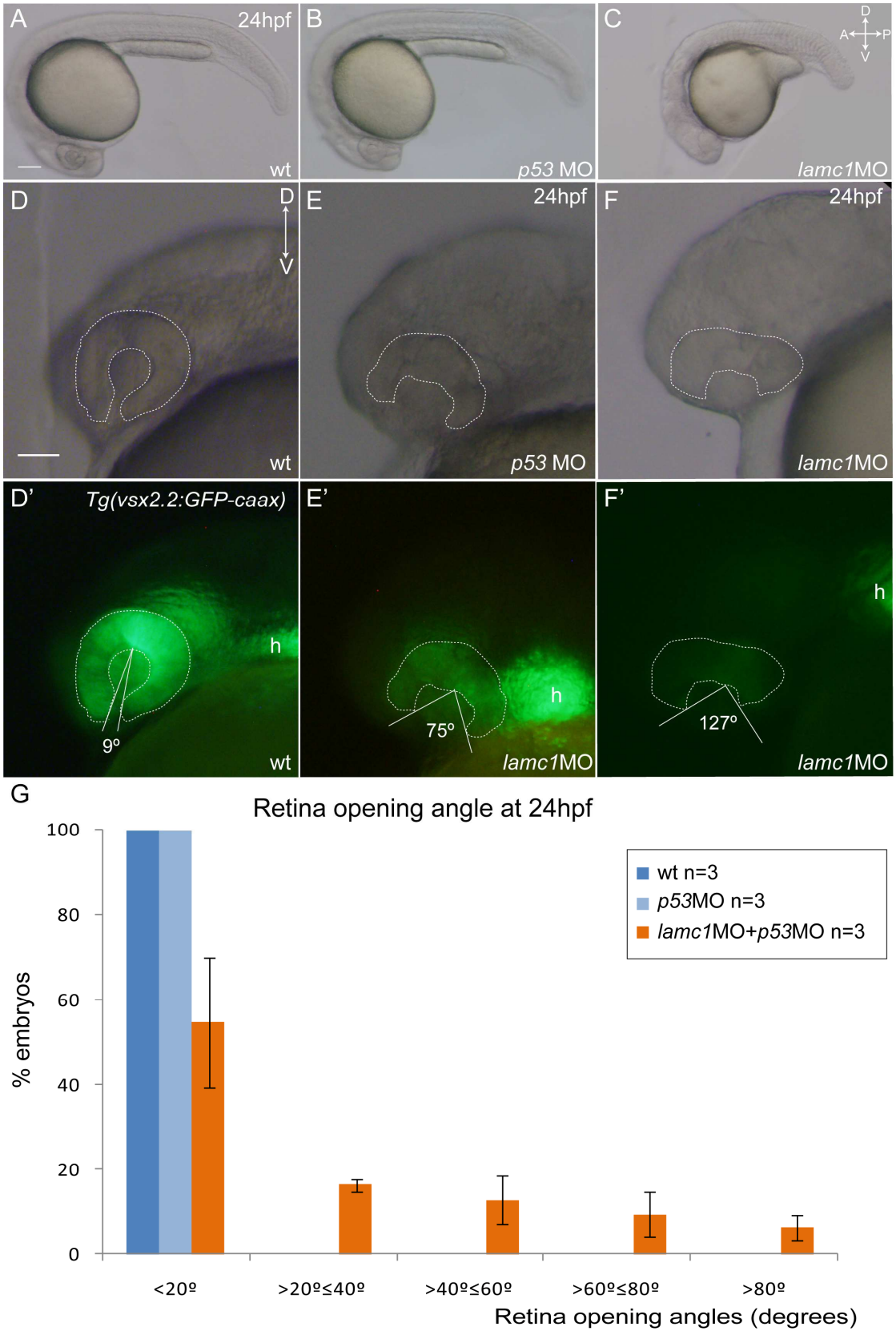

Figure 26. Optic cup folding defects caused by *lamc1*MO injection. A-B) Wild type and *p53*MO-injected control embryos. C) *lamc1*MO injected embryo at 24hpf. Scale bar: 500µm. D-D') wild type control embryos showing no eye defects. E-F') *lamc1*MO embryos showing opening

retinae higher than 60º. Heart (h). G) Quantification of retina opening angles in controls and *lamc1*MO morphants embryos at 24hpf.

To quantify retina width variation, apico-basal axis length was measured as the distance between the apical and basal surface in *lamc1*MO-injected embryos and its respective controls at 24hpf. Data were normalized with ear diameter, which did not vary between control and morphant embryos. A large proportion of *lamc1*MO morphant embryos showed a severe phenotype displaying wider retinae than wild type embryos (See Figure 27, C and Supple. Table 10).

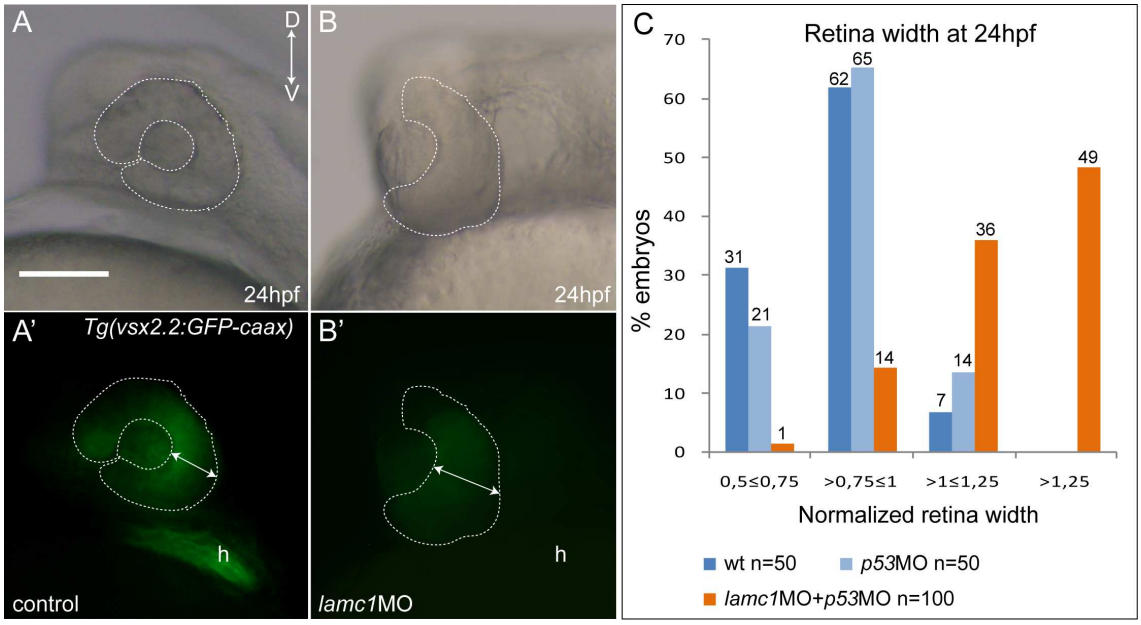

Figura 27. *lamc1* morphant embryos display retina defects. A-A') wild type control embryos showing no eye defects. B-B') Eye defects in *lamc1*MO injected embryos. Heart (h). C) Quantifications of normalized retina width in *lamc1*MO injected embryos and control embryos. Percentages for each column are indicated above.

Here we show that the Laminin γ1 chain is necessary for the proper folding of the optic cup and that its knockdown results in retinal morphological defects. This is in concordance with previous studies demonstrating the role of laminins in the maintenance of the neuroepithelium morphology during optic vesicle formation (Ivanovitch *et al.* 2013).

As mentioned, focal adhesions localize basally and play a pivotal role in the morphogenesis of epithelial sheets. Integrins, which are transmembrane proteins, serve as Laminin receptors and recruit scaffold proteins that link the extracellular matrix with the cytoskeleton (Hynes 1992). Taken into account the phenotype that *lamc1*MO morphants

display, Tg(*βactin:Myl12GFP*) embryos were injected (see Methods 12) to analyze Myosin function in this context.

Basal accumulation of Myosin and *foci* stability were analysed in uninjected, *p53*MO- and *lamc1*MO-injected embryos. As in blebbistatin analyses, the results are presented in a box plot to show the wide dispersion of the data. Myosin *foci* from control embryos (uninjected and *p53*MO-injected embryos) have a stability of around 4min, however, in morphant embryos the *foci* are significantly more stable (*p<0,001*). As a consequence, the number of *foci* visualized at the basal surface in morphants embryos is higher than in control embryos.

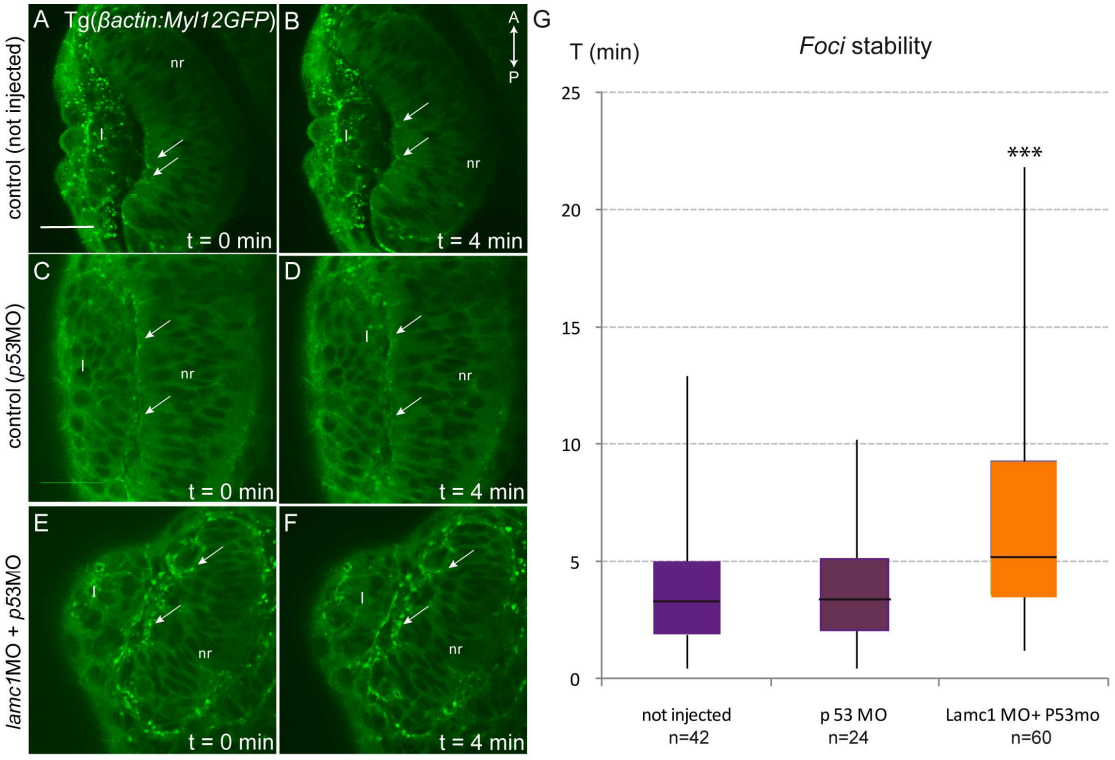

Figure 28. Myosin *foci* are more stable in *lamc1*MO injected embryos. A-F) Confocal microscopy time-lapse images showing zebrafish eye morphogenesis in *Tg*(*βactin:Myl12-GFP*) embryos at 20hpf (Myosin green) (dorsal view). Arrowheads mark Myosin *foci*. Neural retina (nr), lens (l). Scale bar: 30 µm. A-B) Not injected embryo. C-D) *p53*MO injected embryo. E-F) *lamc1*MO+*p53*MO injected embryo. G) Quantification for Myosin *foci* stability in uninjected, *p53*MO injected and *lamc1*MO+*p53*MO injected embryos. Data in charts are displayed as box plots showing the median, 1st and the 3rd quartile represented by the box maximum and minimum values. *p<0,001* according to Student t-test analysis.

To investigate whether the increase of Myosin intensity correlates with a displacement of the basal lamina in *lamc1*MO morphants, as we observed in wild type embryos, (see

section 23 above for details) the apico-basal axis length in cells containing Myosin *foci* were measured (see Figure 28). For each *focus*, the measurements were obtained as the mean value of three different data in the same timepoint.

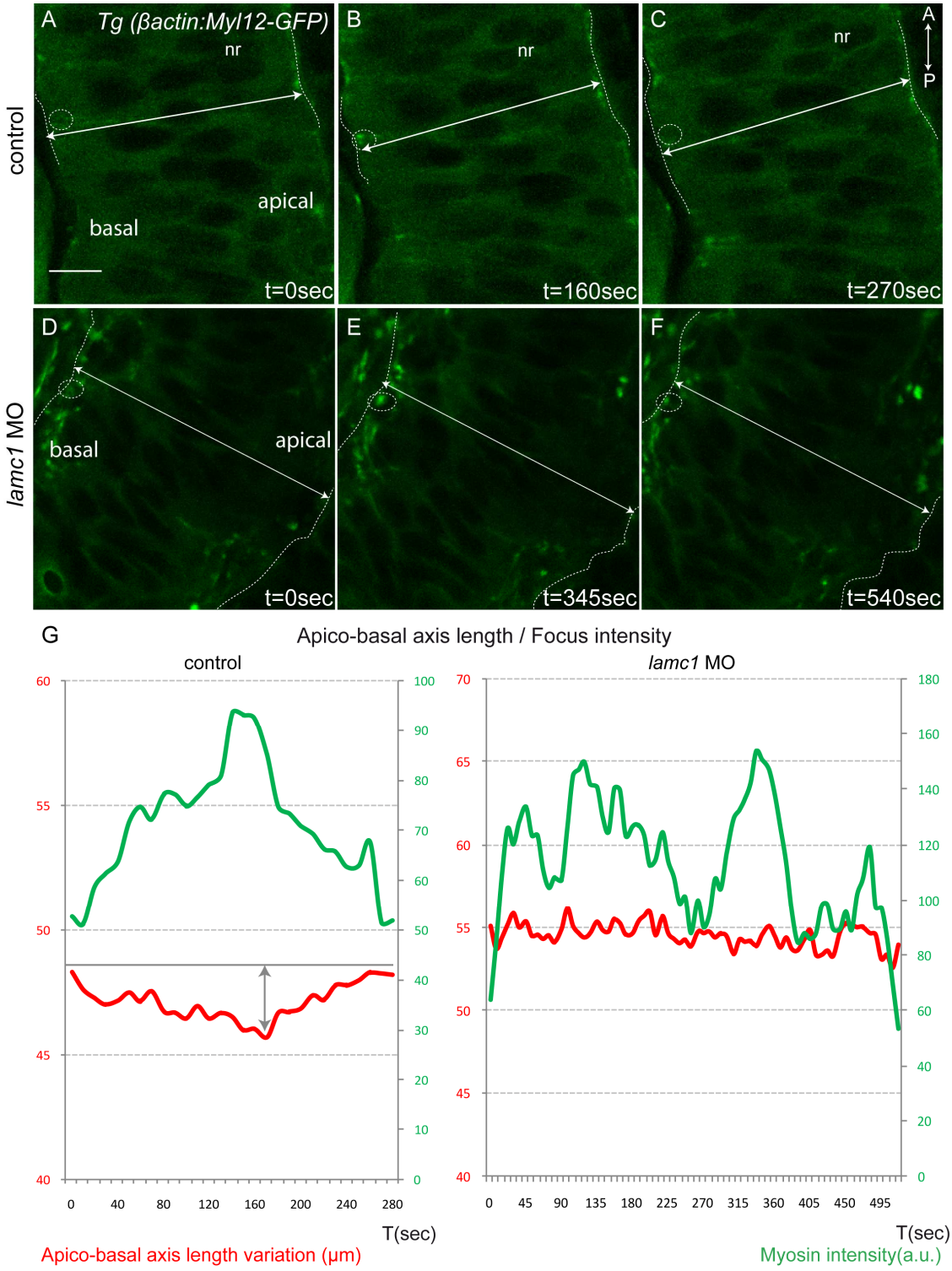

Figure 29. Myosin *foci* accumulation at the basal retina does not correlate with apico-basal axis length changes in *lamc1*MO injected embryos. A-F) Confocal microscopy time-lapse

images of transgenic embryo (Myosin green) Dashed lines mark basal and apical surfaces. Dashed circles mark Myosin *focus*. Neural retina (nr). Scale bar: 10 μm. A-C) Not injected embryo (control). D-F) *lamc1*MO injected embryo. G) Quantification of Myosin *focus* intensity associated with a decrease of the apico-basal axis length in the control (left) and with no associated with apico-basal axis length changes in the *lamc1*MO injected embryo (right). Arrowheads mark length variation. Gray line marks initial apico-basal axis length.

The results showed no association between changes in apico-basal axis and the presence of Myosin accumulation in *lamc1* morphants. This is in contrast to the cellular behaviour in wild type retinae.

Together, these findings suggest that Laminin γ1 chain knockdown disturbs the mechanism by which the optic cup folds, by altering the anchor needed to stabilize focal adhesion, and as a consequence transmit the morphogenetic forces exerted by the acto-myosin apparatus.

VII. Discussion

In this study, we provide new insights into the mechanisms regulating optic cup folding. First, we show that Myosin is the driving force behind the cell shape changes in the retina required for correct eye morphogenesis. Additionally, we provide evidence suggesting that the attachment of neuroblasts to the ECM is essential for the proper invagination of the neural retina. Most importantly, we have performed a careful analysis of cell behaviour in the retinal neuroepithelium, which shows the first example of a ratchet mechanism controlling basal constriction in vertebrates.

1. Neuroepithelial cell shape changes generate the basal constriction that drives optic cup folding

The formation of complex organs such as the eye requires the coordinated orchestration of cellular movements and shape changes. They should integrate developmental patterning information with resulting forces to ensure a spatial and temporal regulation of each morphogenetic event. For instance, the bending of an epithelial sheet is an essential event during important processes such as gastrulation, neural tube formation, etc (Gutzman *et al.* 2008; Leptin *et al.* 1990).

A considerable effort has been made to compare some of the mechanisms involved in inward epithelial folding, and it seems that a widespread array of cellular shape changes operate in different organisms. The folding involves permanent changes in cellular shape that seem to be coupled to oscillations of the cellular membrane. When this oscillatory process is coupled to an irreversible reduction of the cellular apex then is referred as "ratchet mechanism" (Martin *et al.* 2009; Solon *et al.* 2009) (see Introduction). Cells that originally have columnar or cubical-like shape shrink irreversibly either at the apical or the basal surface (Gutzman *et al.* 2008; Leptin *et al.* 1990). Additionally, these cells may undergo an expansion of the opposite surface, adopting a final conical shape. In many systems these changes are also accompanied by changes in cellular length, although it is not clear yet whether variations at the apical and basolateral surfaces are coupled with changes in apico-basal axis. During *Xenopus* and *Drosophila* gastrulation, bottle cells lengthen at the same time as they are constricting (Hardin *et al.* 1988; Sweeton *et al.* 1991). In contrast, during zebrafish optic vesicle evagination, cells constrict apically and shorten as they move distally (Ivanovitch *et al.* 2013).

In this work, we have recorded the contraction behaviour of neural retina cells during optic cup folding using time-lapse microscopy. We quantified *in vivo* cell area changes at the apical and the basal surfaces as well as any apico-basal length variations during invagination. In addition, we have performed transplantation experiments to isolate

individual neuroblasts and investigate whether variations at the apical and the basal surfaces correlate. We ended our analysis by measuring the contribution of cell proliferation to the process of optic cup morphogenesis (OCM).

Our data show that cell areas at both surfaces are oscillating, which involves periodical increases and decreases of cell areas during OC folding. At the basal surface, these oscillations are accompanied by a significant and irreversible reduction of their basal area (see Results Figure 15). Other authors have suggested that these oscillations are essential for the ratchet mechanism (Martin *et al.* 2009; Solon *et al.* 2009). Additionally, there is a small expansion of apical area surfaces. Our findings reveal that cell areas are dynamic and in constant fluctuation, but the final result is the acquisition of a conical shape, as has been shown in other systems (see Results Figure 16 and 17).

Our analyses also reveal that the oscillatory behaviour observed at the basal surface occurs independently of the oscillations occurring at the apical side (see Results Figure 18). This could be explained by the cellular morphology of the retinal precursors. The neuroblasts are relatively long cells (ca. 50μm) and the apical and basal domains are thus spatially quite separated. Furthermore, these domains could be subjected to different tensional forces, as the basal surface is attached to the ECM and the apical surface is constrained by an actin belt at junctional complexes, allowing different degrees of resistance to physical forces.

Our quantification of apico-basal axis length during invagination, did not revealed any change along this axis (see Figure 14). Our results are at odds with previous works. The cellular elongation showed by(Picker *et al.* 2009), which we failed to find, could be explained because apico-basal axis elongation in retina cells may happen earlier in eye morphogenesis, probably when neuroblasts reach their positions within the flat epithelium before invagination starts. Therefore, our failure to identify this behaviour may simply be due to the restricted time window we focused in. Further quantifications at earlier developmental stages are thus required to establish if this is the case.

Our findings also show that proliferation does not contribute to the acquisition of wedge shape required for invagination, as our measurements of distance between neighbouring cells during mitotic events confirm (see Results, Figure 19). Our results in this case are in agreement with previous works, which show that proliferation is not a crucial factor. This is the case during sea urchin ciliary band formation (Krupke *et al.* 2014), and zebrafish OCM (Kwan *et al.* 2011).

2. Myosin *Foci* Cause Cell Area Decrease and Transient Shortening of Apico-Basal Axis

The coupling of the periodic accumulation of actomyosin network with the oscillation of the cell membrane has been proposed as a mechanism responsible for shape changes during epithelial morphogenesis in many organs. Given that retinal neuroblasts display an oscillatory behaviour, we aimed to explore actomyosin dynamics during optic cup folding.

When we examined Myosin activity through *in vivo* time-lapses, we found that it is mainly localised at the basal surface of NR during OC folding and accumulated as *foci*: transient and discrete spots that flow across the cortex, before dispersing (Martin *et al.* 2010). Furthermore, we observed that the presence of these *foci* is associated with a transitory reduction of apico-basal axis length and an irreversible decrease in basal cell surface (see Figure 22 and 23; Supple. Figure 1). This is in agreement with observations in other morphogenetic models in which periodic myosin accumulations either at the basal or the apical surfaces drive the constriction (He *et al.* 2010; Martin *et al.* 2010). In contrast, actin analysis showed that there is a positive correlation between actin accumulation and area changes (see Figure 20). The main function of actin at the cellular cortex is the maintenance of the cellular architecture. This actin network confers mechanical properties to the cellular cortex that can be modified to display specific morphogenetic behaviours (review in(Munjal *et al.* 2014)). During optic cup folding, the increase of actin in expanding cells may be related to a cortical resistance response of cells that undergo area changes (see Figure 30). This resistance behaviour is in contrast to the active recruitment of Myosin *foci* to the cellular vertex, which is potentially responsible for the cellular contractions. In Drosophila follicle cells, little variations of actin at the basal surface are detected, despite the oscillatory behaviour of the cells(He *et al.* 2010). This observation, together with our observations, suggests that actin polymerization *per se* is not the main driving force controlling basal constriction.

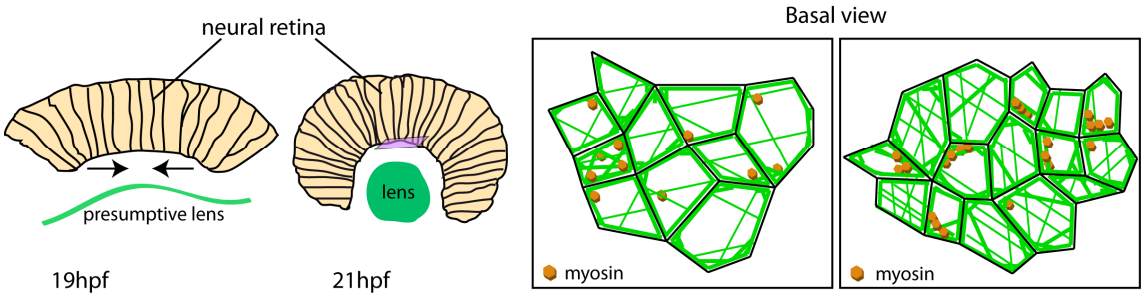

Figure 30.A model for actomyosin network behaviour during optic cup folding. At early stages actin is localized at the cellular cortex and discrete myosin dots are visualized. Later on, during neuroepithelial bending constricting cortical actin recruits myosin *foci* at the basal surface of neuroblast to constrict and neighbouring cells accumulate actin. Contiguous neuroblasts are not in phase.

In our assays, we found that the ventral closure of the retinal epithelium is impaired in blebbistatin-treated embryos, indicating that Myosin dynamicsis required for the contractility of the cells and hence for the folding of the neuroepithelial sheet. Our results show that upon blebbistatin treatment, Myosin *foci* stability increases, while neuroblasts remain in a relaxed state and do not oscillate (see Figure 24 and 25).These results are in concordance with previous works in *Drosophila* showing a decrease in the amplitude of oscillation upon treatment with the ROCK inhibitor Y-27632 either at the apical or the basal surface (Fernandez-Gonzalez *et al.* 2011; He *et al.* 2010). These findings suggest that Myosin recruitment is essential in OC formation.

Previous work in ESC aggregates (Eiraku *et al.* 2012) proposed a relaxation-expansion model by which OC folding proceeds through a mechanism involving the apical actomyosin network. The authors of this work propose that actomyosin accumulates at the hinges (i.e. the transition region between the pigmented epithelium and the NR) and promotes apical constriction of the epithelium. According to the model, the apical constriction of the hinges will be concomitant with a relaxation of the presumptive NR and a tangential expansion of this tissue. These events cause a convex invagination that results in OC folding. Moreover they proposed a model to explain the apical constriction of the hinges as the driving force causing NR invagination. This work is at odds with our results. Our work shows that Myosin is accumulated at the basal side of the presumptive NR and that *foci* appear and disappear in a dynamic fashion during folding, providing an essential tension at the basal surface as happens in other organisms (review in (Munjal *et al.* 2014)). In addition, previous work from our lab has shown that *opo* localisation at the basal feet of neuroblasts is essential for neural retina invagination in medaka embryos. This protein regulates integrin-mediated endocytosis by competing for the recruitment of clathrin adaptor proteins at the basal surface (Bogdanovic *et al.* 2012; Martinez-Morales *et al.* 2009). All these findings support the idea that, at least in teleosts, OC folding proceeds through an active basal constriction, leads by myosin accumulation. This is much in contrasts with the relaxed neuroepithelium state proposed in the ESCs model.

It is possible that specific mechanisms govern OCM in different vertebrate groups. In fact, the authors report different mechanical properties for the tissue when aggregates are

formed from human ESC or in mouse ESC (Eiraku *et al.* 2011; Nakano *et al.* 2012). Furthermore, these observations (not supported by functional experiments in vivo) are inconsistent with previous work in mouse showing a basal accumulation of the actomyosin meshwork (Chauhan *et al.* 2009).

3. Laminin γ Chain Is Essential for the Correct Optic Cup Morphogenesis

As it has been shown in the Introduction, cellular junctions not only transmit tension but also participate in the generation of contractile forces (Harris *et al.* 2014). At the basal surface, integrins attach to a number of ECM components, including Laminins, one of the major component of the basement membrane together with collagens (Hynes 1992). Theses attachments recruit the actomyosin network to the cellular cortex at the basal surface; thus connecting the cytoskeleton to the ECM. Individual cells can transmit forces through these attachments, and in coordination with their neighbours, mediate the morphogenesis of an entire epithelial sheet.

In this study, we used *lamc1*MO to dissect out the role of ECM attachments and more precisely, the function of Laminin γ chain during zebrafish OCM. In our Laminin γ1 knockdown experiments, 50% of morphant retinae failed to fold correctly and showed ventral opening angles greater than 20 degrees. We also quantified the width of the neural retina in morphant embryos, and we detected that over 80% exhibited wider retinae than controls (see Figure 26 and 27 in Results for details). This increase in apico-basal axis length could be caused by the disorganization of the neuroepithelium, as has been shown during zebrafish OVs evagination, where marginal eye field cells appear disorganized and the pseudoestratified morphology of the neuroepithelium is lost when Laminin γ1 chain is disrupted (Ivanovitch *et al.* 2013). Further investigations with apical and basal markers are required to elucidate whether the increase in retina width is associated with the lost of the neuroepithelial organization.

Disruption of either intercellular junction or cell-substrate contacts results in morphogenetic failures, such as neural tube closure defects in *Xenopus* when N-cadherin is depleted (Nandadasa *et al.* 2009). We therefore aimed to analyse whether similar mechanisms act during OC folding. When we quantified *foci* stability, we detected a significant increase in the time that Myosin *foci* are visible at the basal surface in *lamc1*MO-injected embryos (see Figure 28). Our *lamc1*MO injections in Tg(*βactin:Myl12GFP*) show that there is no association between the increase in Myosin intensity at the basal side of the neural retina and any shortening along the apico-basal

axis in morphant embryos, as happens in control retinae. These results indicate that disrupting the attachment to the ECM through Lamininc1 alters *foci* dynamic.

In *Drosophila*, the alignment of actin filaments and ECM fibres functions as a molecular "corset" required to restrict the increase of egg chamber volume. Additionally, this work shows that the interference with integrin-mediated adhesion modifies Myosin recruitment. In this model, knocking down the expression of talin reduces Myosin intensity, in contrast with this, paxillin overexpression enhances cell-ECM contacts and increases myosin intensity (He *et al.* 2010). In medaka, interference with integrin-mediated adhesions indicates that focal contacts are required for OC folding (Martinez-Morales *et al.* 2009). Additionally, most of the previous work addressing focal contacts has focused on the intracellular interactions. In our work, we have used a different approach and disrupt focal adhesion by knocking down Laminin γ chain, part of the ECM, to analyse the relationship of basal FAs with the ECM. This change of experimental focus might explain the increase of Myosin *foci* stability we observed. Myosin is recruited to the basal side by focal adhesions but, as the ECM contact is disrupted, the transmission of tensile forces is impaired and Myosin contractility is slowed down (see Figure 29). The attachment to the ECM provides the balance between stiffness and elasticity required to undergo basal constriction and to keep the shape changes necessary for the final invagination.

In conclusion, we propose that cellular shape changes, controlled by a ratchet-like mechanism, are responsible for the basal constriction required during the invagination of the neural retina. Furthermore, basally localized Myosin *foci* and Laminin γ1 in the ECM are essential for the proper folding of this neuroepithelium. We are therefore providing here the first evidence for the use of a ratchet mechanism during basal constriction in a vertebrate epithelium.

VIII. Conclusions

1. Quantitative analysis reveals no change in neural retina thickness during optic cup folding.

2. Quantitative study of cellular feet area at the basal surface reveals a significant and irreversible reduction between 19 and 20 hpf. This is consistent with a ratchet-like basal constriction mechanism.

3. In contrast, the study of cellular areas at the apical surface of the retina indicates a significant increase between 20 and 21hpf, at later stages of neural retina invagination.

4. Cellular areas from neighbouring cells, both at the basal and apical surfaces, oscillate in an independent fashion during the neuroepithelial folding.

5. Within an individual neuroblast, apical and basal surfaces do not show synchronic oscillations.

6. Mitosis does not promote cellular wedge shape during eye morphogenesis. Thus, proliferation is not a primary force for optic cup folding.

7. The pulsed accumulation of the actin marker Utrophin at the basal surface shows a positive correlation with cell area increase.

8. Myosin is accumulated in *foci* at the basal side of neural retina during optic cup folding.

9. The increase of Myosin *foci* intensity is associated with a decrease of cell area at the basal surface and a transient decrease of the apico-basal axis length.

10. The actomyosin inhibitor blebbistatin causes a reduction in the amplitude of cell oscillations, an increase in myosin *foci* stability, and hence impairs optic cup folding.

11. Knockdown of *lamc1* in zebrafish embryos results in optic cup folding defects. In morphant embryos, myosin foci accumulation is uncoupled from cellular contractility.

IX. Supplementary Material

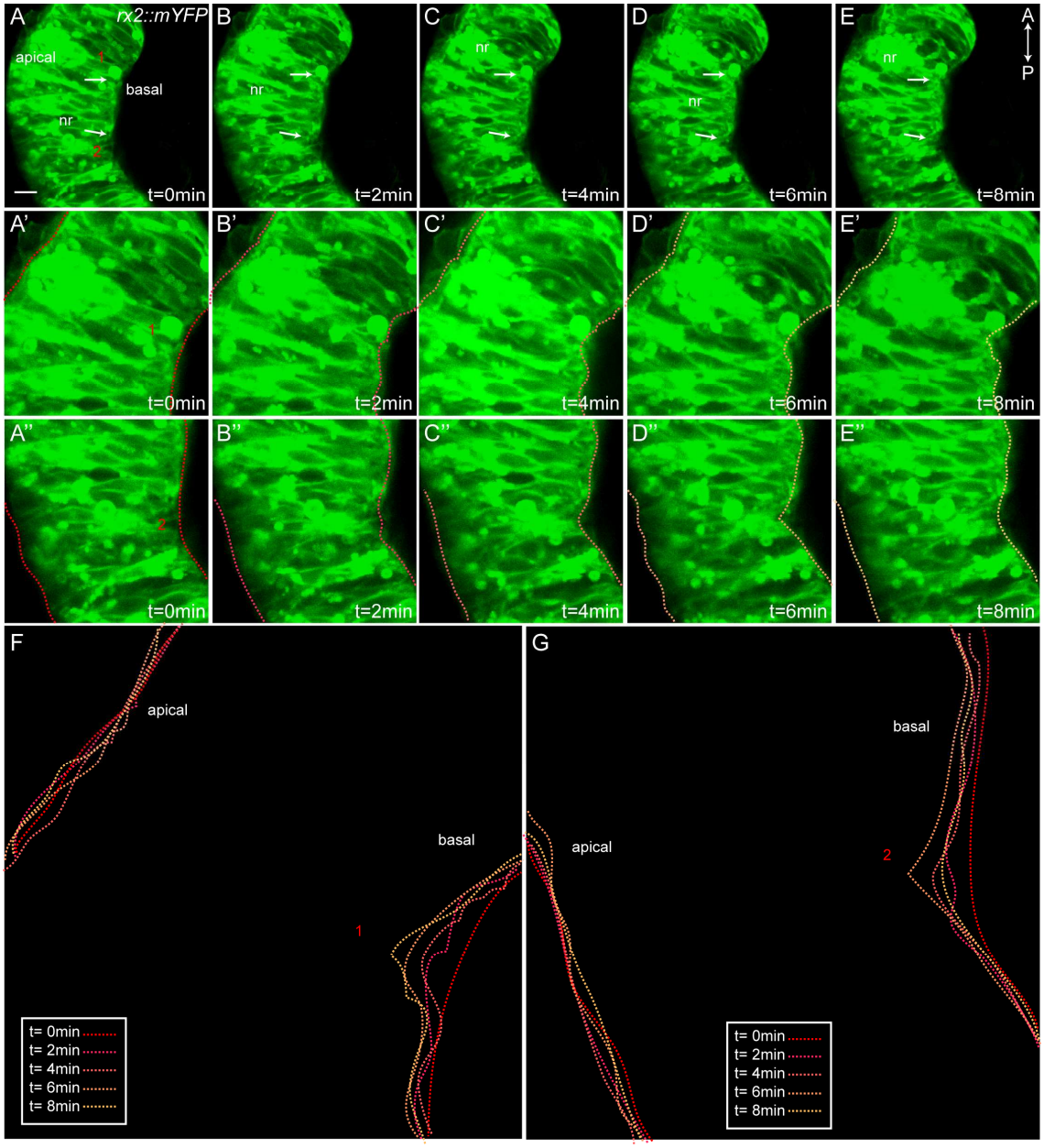

Supple. Figure 1. Cellular displacement at the basal surface during optic cup folding in medaka embryos. A-E) Confocal microscopy time-lapse images showing optic cup folding at stage 22 in retinas labelled with rx::mYFP in medaka embryos. Arrows indicate displacements at the basal surface. Neural retina (nr). Coloured dashed lines mark apical and basal surfaces changes through time. Markers 1 and 2 indicate different displacement. Scale bar: 10 µm. A'-E') are zoom in of marker 1. A''-E'') are zoom in of marker 2. F-G) Charts showing a transient decrease in the apico-basal axis length by superposition of apical and basal outlines from confocal images.

BASAL				
	decrease	constant	increase	n
19hpf	23	7	1	31
20hpf	16	6	2	24
21hpf	11	12	3	26
				81

Supple. Table 1. Cell area changes during optic cup folding at the basal surface. Table showing cells that increase, decrease or remain with the same cell area in each developmental stages analysed.

Basal surfaces during optic cup folding

	<20µm2	≥20<35µm2	≥35µm2	n
19hpf	10	17	4	31
20hpf	15	8	1	24
21hpf	16	10	0	26
				81

Supple. Table 2. Cell areas during optic cup folding at the basal surface. Table showing cell areas in each developmental stage.

APICAL				
	decrease	**constant**	**increase**	n
19hpf	10	9	8	27
20hpf	4	10	9	23
21hpf	9	19	2	30
				80

Supple. Table 3. Cell area changes during optic cup folding at the apical surface. Table showing cells that increase, decrease or remain with the same cell area in each developmental stages analysed.

Apical surfaces during optic cup folding

	<20µm2	≥20<35µm2	≥35µm2	n
19hpf	11	12	4	27
20hpf	8	14	1	23
21hpf	3	21	6	30
				80

Supple. Table 4. Cell areas during optic cup folding at the apical surface. Table showing cell areas in each developmental stage.

Pearson correlation coefficient				
	[1-0,5)	**[0,5,-0,5]**	**(-0,5,-1]**	**n**
n	10	33	0	43
%	23,26	76,74	0,00	

Supple. Table 5. Pearson correlation coefficient for apical areas. Table showing Pearson correlation coefficient for 43 pairs of apical cell areas. More than 76% of cells oscillate independently i.e. with a correlation coefficient between 0,5 and -0,5.

Pearson correlation coefficient				
	[1-0,5)	**[0,5,-0,5]**	**(-0,5,-1]**	**n**
n	3	43	0	46
%	6,52	93,48	0,00	

Supple. Table 6. Pearson correlation coefficient for basal areas. Table showing Pearson correlation coefficient for 46 pairs of cell basal areas. More than 90% of cells oscillate independently.

Pearson correlation coefficient				
	[1-0,5)	**[0,5,-0,5]**	**(-0,5,-1]**	**n**
n	0	10	0	10
%	0,00	100,00	0,00	

Supple. Table 7. Pearson correlation coefficient for transplanted cells. Table showing Pearson correlation coefficient for 10 transplanted cells. All the cells analysed show that the apical and basal surfaces are contracting and relaxing independently.

	untreated	DMSO	Blebbistatin
mean	4,00	4,15	21,50
SD	3,00	1,97	15,26
median	3,25	4,30	17,50

Supple. Table 8. Foci stability in blebbistatin treated embryos. Table shows similar mean and median values for untreated and DMSO treated embryos and significant different values for blebbistatin treated embryos. Standard desviation (SD).

	Retinal opening angle at 24 hpf (% embryos)					
	<20º	>20º≤40º	>40º≤60º	>60º≤80º	>80º	n
wt exp.1	100	0	0	0	0	15
wt exp.2	100	0	0	0	0	13
wt exp.3	100	0	0	0	0	22
Mean	**100**	**0**	**0**	**0**	**0**	**n= 50**
SEM	0	0	0	0	0	
p53 MO exp.1	100	0	0	0	0	18
p53 MO exp.2	100	0	0	0	0	7
p53 MO exp.3	100	0	0	0	0	25
Mean	**100**	**0**	**0**	**0**	**0**	**n= 50**
SEM	0	0	0	0	0	
lamc1 MO exp.1	6,25	18,75	25,00	37,50	12,50	16
lamc1 MO exp.2	73,53	14,71	5,88	2,94	2,94	34
lamc1 MO exp.3	36,00	18,00	20,00	16,00	10,00	50
Mean	**54,76**	**16,35**	**12,94**	**9,47**	**6,47**	**n= 100**
SEM	15,32	1,34	5,76	5,33	2,88	

Supple. Table 9. Retinal opening angles at 24hpf. Data from *lamc1*MO-injected embryos and its respective *p53*MO-injected and un-injected control embryos obtained in three different experiments. Standard error of the mean (Chen *et al.*).

	Normalized retina width at 24hpf (% embryos)				
	0,5≤0,75	>0,75≤1	>1≤1,25	>1,25	n
wt exp.1	6,67	86,67	6,67	0	15
wt exp.2	46,15	53,85	0,00	0	13
wt exp.3	40,91	45,45	13,64	0	22
Mean	**31,24**	**61,99**	**6,77**	**0**	**n= 50**
SEM	12,38	12,57	3,94	0	
p53 MO exp.1	11,11	66,67	22,22	0	18
p53 MO exp.2	28,57	57,14	14,29	0	7
p53 MO exp.3	24,00	72,00	4,00	0	25
Mean	**21,23**	**65,27**	**13,50**	**0**	**n= 50**
SEM	5,23	4,35	5,27	0	
lamc1 MO exp.1	0	6,25	87,50	6,25	16
lamc1 MO exp.2	0	14,71	12	73,53	34
lamc1 MO exp.3	4,00	22,00	20,00	54,00	50
Mean	**1,33**	**14,32**	**39,75**	**44,59**	**n= 100**
SEM	1,33	4,55	23,99	19,98	

Supple. Table 10. Normalized retina width values at 24hpf. Data from *lamc1*MO-injected embryos and its respective *p53*MO-injected and un-injected control embryos obtained in three different experiments. Standard error of the mean (Chen *et al.*).

X. References

Aberle H, Butz S, Stappert J, Weissig H, Kemler R, Hoschuetzky H (1994) Assembly of the cadherin-catenin complex in vitro with recombinant proteins. Journal of cell science 107 (Pt 12):3655-3663

Acehan D, Petzold C, Gumper I, Sabatini DD, Muller EJ, Cowin P, Stokes DL (2008) Plakoglobin is required for effective intermediate filament anchorage to desmosomes. The Journal of investigative dermatology 128:2665-2675

Adelmann HB (1929) Experimental studies on the development of the eye. I. The effect of the removal of median and lateral areas of the anterior end of the urodelan neural plate on the development of the eyes (Triton teniatus and Amblystoma punctatum). Journal of Experimental Zoology 54:249–290

Aigouy B, Farhadifar R, Staple DB, Sagner A, Roper JC, Julicher F, Eaton S (2010) Cell flow reorients the axis of planar polarity in the wing epithelium of Drosophila. Cell 142:773-786

Aranda V, Nolan ME, Muthuswamy SK (2008) Par complex in cancer: a regulator of normal cell polarity joins the dark side. Oncogene 27:6878-6887

Bogdanovic O, Delfino-Machin M, Nicolas-Perez M, Gavilan MP, Gago-Rodrigues I, Fernandez-Minan A, Lillo C, Rios RM, Wittbrodt J, Martinez-Morales JR (2012) Numb/Numbl-Opo antagonism controls retinal epithelium morphogenesis by regulating integrin endocytosis. Dev Cell 23:782-795

Braga VM, Del Maschio A, Machesky L, Dejana E (1999) Regulation of cadherin function by Rho and Rac: modulation by junction maturation and cellular context. Molecular biology of the cell 10:9-22

Braga VM, Machesky LM, Hall A, Hotchin NA (1997) The small GTPases Rho and Rac are required for the establishment of cadherin-dependent cell-cell contacts. The Journal of cell biology 137:1421-1431

Bryant DM, Mostov KE (2008) From cells to organs: building polarized tissue. Nature reviews Molecular cell biology 9:887-901

Calderwood DA, Fujioka Y, de Pereda JM, Garcia-Alvarez B, Nakamoto T, Margolis B, McGlade CJ, Liddington RC, Ginsberg MH (2003) Integrin beta cytoplasmic domain interactions with phosphotyrosine-binding domains: a structural prototype for diversity in integrin signaling. Proceedings of the National Academy of Sciences of the United States of America 100:2272-2277

Carramusa L, Ballestrem C, Zilberman Y, Bershadsky AD (2007) Mammalian diaphanous-related formin Dia1 controls the organization of E-cadherin-mediated cell-cell junctions. Journal of cell science 120:3870-3882

Caswell PT, Norman JC (2006) Integrin trafficking and the control of cell migration. Traffic 7:14-21

Costa M, Wilson ET, Wieschaus E (1994) A putative cell signal encoded by the folded gastrulation gene coordinates cell shape changes during Drosophila gastrulation. Cell 76:1075-1089

Chauhan BK, Disanza A, Choi SY, Faber SC, Lou M, Beggs HE, Scita G, Zheng Y, Lang RA (2009) Cdc42- and IRSp53-dependent contractile filopodia tether presumptive lens and retina to coordinate epithelial invagination. Development 136:3657-3667

Chauhan BK, Lou M, Zheng Y, Lang RA (2011) Balanced Rac1 and RhoA activities regulate cell shape and drive invagination morphogenesis in epithelia. Proceedings of the National Academy of Sciences of the United States of America 108:18289-18294

Chen L, Vicente-Manzanares M, Potvin-Trottier L, Wiseman PW, Horwitz AR (2012) The integrin-ligand interaction regulates adhesion and migration through a molecular clutch. PloS one 7:e40202

Davidson LA, Koehl MA, Keller R, Oster GF (1995) How do sea urchins invaginate? Using biomechanics to distinguish between mechanisms of primary invagination. Development 121:2005-2018

Dawes-Hoang RE, Parmar KM, Christiansen AE, Phelps CB, Brand AH, Wieschaus EF (2005) folded gastrulation, cell shape change and the control of myosin localization. Development 132:4165-4178

Del Bene F, Wehman AM, Link BA, Baier H (2008) Regulation of neurogenesis by interkinetic nuclear migration through an apical-basal notch gradient. Cell 134:1055-1065

Dolez M, Nicolas JF, Hirsinger E (2011) Laminins, via heparan sulfate proteoglycans, participate in zebrafish myotome morphogenesis by modulating the pattern of Bmp responsiveness. Development 138:97-106

Eiraku M, Adachi T, Sasai Y (2012) Relaxation-expansion model for self-driven retinal morphogenesis: a hypothesis from the perspective of biosystems dynamics at the multi-cellular level. Bioessays 34:17-25

Eiraku M, Takata N, Ishibashi H, Kawada M, Sakakura E, Okuda S, Sekiguchi K, Adachi T, Sasai Y (2011) Self-organizing optic-cup morphogenesis in three-dimensional culture. Nature 472:51-56

Ezratty EJ, Bertaux C, Marcantonio EE, Gundersen GG (2009) Clathrin mediates integrin endocytosis for focal adhesion disassembly in migrating cells. The Journal of cell biology 187:733-747

Ezratty EJ, Partridge MA, Gundersen GG (2005) Microtubule-induced focal adhesion disassembly is mediated by dynamin and focal adhesion kinase. Nature cell biology 7:581-590

F.C. Sauer *ea* (1935) Mitosis in the neural tube. The Journal of Comparative Neurology 62:377-405

Fernandez-Gonzalez R, J.A. Z (2011) Oscillatory behaviors and hierarchical assembly of contractile structures in intercalating cells. Phys Biol 8

Fox DT, Peifer M (2007) Abelson kinase (Abl) and RhoGEF2 regulate actin organization during cell constriction in Drosophila. Development 134:567-578

Fuhrmann S (2010) Eye morphogenesis and patterning of the optic vesicle. Current topics in developmental biology 93:61-84

Fuhrmann S, Chow L, Reh TA (2000) Molecular control of cell diversification in the vertebrate retina. Results and problems in cell differentiation 31:69-91

Gallicano GI, Kouklis P, Bauer C, Yin M, Vasioukhin V, Degenstein L, Fuchs E (1998) Desmoplakin is required early in development for assembly of desmosomes and cytoskeletal linkage. The Journal of cell biology 143:2009-2022

Gorfinkiel N, Blanchard GB (2011) Dynamics of actomyosin contractile activity during epithelial morphogenesis. Current opinion in cell biology 23:531-539

Gutzman JH, Graeden EG, Lowery LA, Holley HS, Sive H (2008) Formation of the zebrafish midbrain-hindbrain boundary constriction requires laminin-dependent basal constriction. Mechanisms of development 125:974-983

Hardin J, Keller R (1988) The behaviour and function of bottle cells during gastrulation of Xenopus laevis. Development 103:211-230

Harris AR, Daeden A, Charras GT (2014) Formation of adherens junctions leads to the emergence of a tissue-level tension in epithelial monolayers. Journal of cell science

Harris WA, Hartenstein V (1991) Neuronal determination without cell division in Xenopus embryos. Neuron 6:499-515

He L, Wang X, Tang HL, Montell DJ (2010) Tissue elongation requires oscillating contractions of a basal actomyosin network. Nature cell biology 12:1133-1142

Hendrix RW, Zwaan J (1974) Cell shape regulation and cell cycle in embryonic lens cells. Nature 247:145-147

Hildebrand JD (2005) Shroom regulates epithelial cell shape via the apical positioning of an actomyosin network. Journal of cell science 118:5191-5203

Hohenester E, Yurchenco PD (2013) Laminins in basement membrane assembly. Cell adhesion & migration 7:56-63

Holtfreter J (1943) A study of the mechanics of gastrulation. Part I. J Exp Zool 95:171-212

Hong S, Troyanovsky RB, Troyanovsky SM (2013) Binding to F-actin guides cadherin cluster assembly, stability, and movement. The Journal of cell biology 201:131-143

Hunter MV, Fernandez-Gonzalez R (2013) Gastrulation: cell polarity comes full circle. Current biology : CB 23:R845-848

Hyer J, Kuhlman J, Afif E, Mikawa T (2003) Optic cup morphogenesis requires pre-lens ectoderm but not lens differentiation. Developmental biology 259:351-363

Hynes RO (1992) Integrins: versatility, modulation, and signaling in cell adhesion. Cell 69:11-25

Ivanovitch K, Cavodeassi F, Wilson SW (2013) Precocious acquisition of neuroepithelial character in the eye field underlies the onset of eye morphogenesis. Developmental cell 27:293-305

Kagiyama Y, Gotouda N, Sakagami K, Yasuda K, Mochii M, Araki M (2005) Extraocular dorsal signal affects the developmental fate of the optic vesicle and patterns the optic neuroepithelium. Development, growth & differentiation 47:523-536

Keller PJ (2013) Imaging morphogenesis: technological advances and biological insights. Science 340:1234168

Kimmel CB, Ballard WW, Kimmel SR, Ullmann B, Schilling TF (1995) Stages of embryonic development of the zebrafish. Developmental dynamics : an official publication of the American Association of Anatomists 203:253-310

Kolsch V, Seher T, Fernandez-Ballester GJ, Serrano L, Leptin M (2007) Control of Drosophila gastrulation by apical localization of adherens junctions and RhoGEF2. Science 315:384-386

Kominami T, Takata H (2004) Gastrulation in the sea urchin embryo: a model system for analyzing the morphogenesis of a monolayered epithelium. Development, growth & differentiation 46:309-326

Kovacs M, Toth J, Hetenyi C, Malnasi-Csizmadia A, Sellers JR (2004) Mechanism of blebbistatin inhibition of myosin II. The Journal of biological chemistry 279:35557-35563

Krupke OA, Burke RD (2014) Eph-Ephrin signaling and focal adhesion kinase regulate actomyosin-dependent apical constriction of ciliary band cells. Development 141:1075-1084

Kwan KM, Fujimoto E, Grabher C, Mangum BD, Hardy ME, Campbell DS, Parant JM, Yost HJ, Kanki JP, Chien CB (2007) The Tol2kit: a multisite gateway-based construction kit for Tol2 transposon transgenesis constructs. Developmental dynamics : an official publication of the American Association of Anatomists 236:3088-3099

Kwan KM, Otsuna H, Kidokoro H, Carney KR, Saijoh Y, Chien CB (2011) A complex choreography of cell movements shapes the vertebrate eye. Development 139:359-372

Kwan KM, Otsuna H, Kidokoro H, Carney KR, Saijoh Y, Chien CB (2012) A complex choreography of cell movements shapes the vertebrate eye. Development 139:359-372

Langheinrich U, Elisabeth Hennen, Gordon Stott aGV (2002) Zebrafish as a model organism for the identification and characterization of drugs and genes affecting p53 signalin

Lecuit T, Lenne PF (2007) Cell surface mechanics and the control of cell shape, tissue patterns and morphogenesis. Nature reviews Molecular cell biology 8:633-644

Leptin M, Grunewald B (1990) Cell shape changes during gastrulation in Drosophila. Development 110:73-84

Li Z, Joseph NM, Easter SS, Jr. (2000) The morphogenesis of the zebrafish eye, including a fate map of the optic vesicle. Developmental dynamics : an official publication of the American Association of Anatomists 218:175-188

Locascio A, Nieto MA (2001) Cell movements during vertebrate development: integrated tissue behaviour versus individual cell migration. Current opinion in genetics & development 11:464-469

Loosli F, Del Bene F, Quiring R, Rembold M, Martinez-Morales JR, Carl M, Grabher C, Iquel C, Krone A, Wittbrodt B, Winkler S, Sasado T, Morinaga C, Suwa H, Niwa K, Henrich T, Deguchi T, Hirose Y, Iwanami N, Kunimatsu S, Osakada M, Watanabe T, Yasuoka A, Yoda H, Winkler C, Elmasri H, Kondoh H, Furutani-Seiki M, Wittbrodt J (2004) Mutations affecting retina development in Medaka. Mechanisms of development 121:703-714

Loosli F, Staub W, Finger-Baier KC, Ober EA, Verkade H, Wittbrodt J, Baier H (2003) Loss of eyes in zebrafish caused by mutation of chokh/rx3. EMBO reports 4:894-899

Loosli F, Winkler S, Burgtorf C, Wurmbach E, Ansorge W, Henrich T, Grabher C, Arendt D, Carl M, Krone A, Grzebisz E, Wittbrodt J (2001) Medaka eyeless is the key factor linking retinal determination and eye growth. Development 128:4035-4044

Love NR, Thuret R, Chen Y, Ishibashi S, Sabherwal N, Paredes R, Alves-Silva J, Dorey K, Noble AM, Guille MJ, Sasai Y, Papalopulu N, Amaya E (2011) pTransgenesis: a cross-species, modular transgenesis resource. Development 138:5451-5458

Lowery LA, Sive H (2004) Strategies of vertebrate neurulation and a re-evaluation of teleost neural tube formation. Mechanisms of development 121:1189-1197

Maitre JL, Berthoumieux H, Krens SF, Salbreux G, Julicher F, Paluch E, Heisenberg CP (2012) Adhesion functions in cell sorting by mechanically coupling the cortices of adhering cells. Science 338:253-256

Mammoto T, Ingber DE (2010) Mechanical control of tissue and organ development. Development 137:1407-1420

Martin-Bermudo MD, Brown NH (1999) Uncoupling integrin adhesion and signaling: the betaPS cytoplasmic domain is sufficient to regulate gene expression in the Drosophila embryo. Genes & development 13:729-739

Martin AC, Gelbart M, Fernandez-Gonzalez R, Kaschube M, Wieschaus EF (2010) Integration of contractile forces during tissue invagination. The Journal of cell biology 188:735-749

Martin AC, Kaschube M, Wieschaus EF (2009) Pulsed contractions of an actin-myosin network drive apical constriction. Nature 457:495-499

Martinez-Morales JR, Rembold M, Greger K, Simpson JC, Brown KE, Quiring R, Pepperkok R, Martin-Bermudo MD, Himmelbauer H, Wittbrodt J (2009) ojoplano-mediated basal constriction is essential for optic cup morphogenesis. Development 136:2165-2175

Martinez-Morales JR, Rodrigo I, Bovolenta P (2004) Eye development: a view from the retina pigmented epithelium. BioEssays : news and reviews in molecular, cellular and developmental biology 26:766-777

Martinez-Morales JR, Signore M, Acampora D, Simeone A, Bovolenta P (2001) Otx genes are required for tissue specification in the developing eye. Development 128:2019-2030

Meier S (1978) Development of the embryonic chick otic placode. I. Light microscopic analysis. The Anatomical record 191:447-458

Mierke CT (2013) The role of focal adhesion kinase in the regulation of cellular mechanical properties. Physical biology 10:065005

Mochii M, Mazaki Y, Mizuno N, Hayashi H, Eguchi G (1998) Role of Mitf in differentiation and transdifferentiation of chicken pigmented epithelial cell. Developmental biology 193:47-62

Moreno-Bueno G, Portillo F, Cano A (2008) Transcriptional regulation of cell polarity in EMT and cancer. Oncogene 27:6958-6969

Murciano A, Zamora J, Lopez-Sanchez J, Frade JM (2002) Interkinetic nuclear movement may provide spatial clues to the regulation of neurogenesis. Molecular and cellular neurosciences 21:285-300

Nakano T, Ando S, Takata N, Kawada M, Muguruma K, Sekiguchi K, Saito K, Yonemura S, Eiraku M, Sasai Y (2012) Self-formation of optic cups and storable stratified neural retina from human ESCs. Cell stem cell 10:771-785

Nance J, Munro EM, Priess JR (2003) C. elegans PAR-3 and PAR-6 are required for apicobasal asymmetries associated with cell adhesion and gastrulation. Development 130:5339-5350

Nance J, Priess JR (2002) Cell polarity and gastrulation in C. elegans. Development 129:387-397

Nelson WJ (2003) Adaptation of core mechanisms to generate cell polarity. Nature 422:766-774

Nelson WJ (2009) Remodeling epithelial cell organization: transitions between front-rear and apical-basal polarity. Cold Spring Harbor perspectives in biology 1:a000513

Norden C, Young S, Link BA, Harris WA (2009) Actomyosin is the main driver of interkinetic nuclear migration in the retina. Cell 138:1195-1208

Oda H, Tsukita S (2001) Real-time imaging of cell-cell adherens junctions reveals that Drosophila mesoderm invagination begins with two phases of apical constriction of cells. Journal of cell science 114:493-501

Ozawa M, Baribault H, Kemler R (1989) The cytoplasmic domain of the cell adhesion molecule uvomorulin associates with three independent proteins structurally related in different species. The EMBO journal 8:1711-1717

Ozawa M, Ringwald M, Kemler R (1990) Uvomorulin-catenin complex formation is regulated by a specific domain in the cytoplasmic region of the cell adhesion molecule. Proceedings of the National Academy of Sciences of the United States of America 87:4246-4250

Parsons MJ, Pollard SM, Saude L, Feldman B, Coutinho P, Hirst EM, Stemple DL (2002) Zebrafish mutants identify an essential role for laminins in notochord formation. Development 129:3137-3146

Plageman TF, Jr., Chung MI, Lou M, Smith AN, Hildebrand JD, Wallingford JB, Lang RA (2010) Pax6-dependent Shroom3 expression regulates apical constriction during lens placode invagination. Development 137:405-415

Rembold M, Loosli F, Adams RJ, Wittbrodt J (2006) Individual cell migration serves as the driving force for optic vesicle evagination. Science 313:1130-1134

Rembold M, Wittbrodt J (2004) In vivo time-lapse imaging in medaka--n-heptanol blocks contractile rhythmical movements. Mechanisms of development 121:965-970

Roh-Johnson M, Shemer G, Higgins CD, McClellan JH, Werts AD, Tulu US, Gao L, Betzig E, Kiehart DP, Goldstein B (2012) Triggering a cell shape change by exploiting preexisting actomyosin contractions. Science 335:1232-1235

Rottner K, Hall A, Small JV (1999) Interplay between Rac and Rho in the control of substrate contact dynamics. Current biology : CB 9:640-648

Salbreux G, Charras G, Paluch E (2012) Actin cortex mechanics and cellular morphogenesis. Trends in cell biology 22:536-545

Sauer FC (1935) Mitosis in the neural tube. J Comp Neurol 62:377-405

Sawyer JK, Harris NJ, Slep KC, Gaul U, Peifer M (2009) The Drosophila afadin homologue Canoe regulates linkage of the actin cytoskeleton to adherens junctions during apical constriction. The Journal of cell biology 186:57-73

Sawyer JM, Harrell JR, Shemer G, Sullivan-Brown J, Roh-Johnson M, Goldstein B (2010) Apical constriction: a cell shape change that can drive morphogenesis. Developmental biology 341:5-19

Schoenwolf GC, Franks MV (1984) Quantitative analyses of changes in cell shapes during bending of the avian neural plate. Developmental biology 105:257-272

Solon J, Kaya-Copur A, Colombelli J, Brunner D (2009) Pulsed forces timed by a ratchet-like mechanism drive directed tissue movement during dorsal closure. Cell 137:1331-1342

Sprague J, Clements D, Conlin T, Edwards P, Frazer K, Schaper K, Segerdell E, Song P, Sprunger B, Westerfield M (2003) The Zebrafish Information Network (ZFIN): the zebrafish model organism database. Nucleic acids research 31:241-243

Strathmann RR (1971) The feeding behavior of planktonic echinoderm larvae:mechanisms, regulation, and rates of suspension-feeding. J Exp Mar Biol Ecol 6:109-160

Streuli CH, Schmidhauser C, Bailey N, Yurchenco P, Skubitz AP, Roskelley C, Bissell MJ (1995) Laminin mediates tissue-specific gene expression in mammary epithelia. The Journal of cell biology 129:591-603

Sweeton D, Parks S, Costa M, Wieschaus E (1991) Gastrulation in Drosophila: the formation of the ventral furrow and posterior midgut invaginations. Development 112:775-789

Tamkun JW, DeSimone DW, Fonda D, Patel RS, Buck C, Horwitz AF, Hynes RO (1986) Structure of integrin, a glycoprotein involved in the transmembrane linkage between fibronectin and actin. Cell 46:271-282

Tan JL, Ravid S, Spudich JA (1992) Control of nonmuscle myosins by phosphorylation. Annual review of biochemistry 61:721-759

Thiery JP, Acloque H, Huang RY, Nieto MA (2009) Epithelial-mesenchymal transitions in development and disease. Cell 139:871-890

Tinsley JM, Blake DJ, Roche A, Fairbrother U, Riss J, Byth BC, Knight AE, Kendrick-Jones J, Suthers GK, Love DR, et al. (1992) Primary structure of dystrophin-related protein. Nature 360:591-593

von Hofsten J, Elworthy S, Gilchrist MJ, Smith JC, Wardle FC, Ingham PW (2008) Prdm1- and Sox6-mediated transcriptional repression specifies muscle fibre type in the zebrafish embryo. EMBO reports 9:683-689

Yamada S, Pokutta S, Drees F, Weis WI, Nelson WJ (2005) Deconstructing the cadherin-catenin-actin complex. Cell 123:889-901

Yurchenco PD (2011) Basement membranes: cell scaffoldings and signaling platforms. Cold Spring Harbor perspectives in biology 3

XI. Appendix

Developmental Cell
Article

Numb/Numbl-Opo Antagonism Controls Retinal Epithelium Morphogenesis by Regulating Integrin Endocytosis

Ozren Bogdanovi ́c,[1,5] Mariana Delfino-Machı ́n,[1,5] Marı́a Nicola´s-Pe´rez,[1] Marı́a P. Gavila´n,[2] Inês Gago-Rodrigues,[1] Ana Ferna´ndez-Min˜án,[1] Concepcio´n Lillo,[3] Rosa M. Rı ́os,[2] Joachim Wittbrodt,[4] and Juan R. Martı ́nez-Morales[1,5,*]
[1]Centro Andaluz de Biologı ́a del Desarrollo (CSIC/UPO/JA), 41013 Sevilla, Spain
[2]CABIMER (CSIC), 41092 Sevilla, Spain
[3]INCYL (University of Salamanca), 37007 Salamanca, Spain
[4]University of Heidelberg, Centre for Organismal Studies, 69120 Heidelberg, Germany
[5]These authors contributed equally to this work
*Correspondence: jrmarmor@upo.es
http://dx.doi.org/10.1016/j.devcel.2012.09.004

SUMMARY

Polarized trafficking of adhesion receptors plays a pivotal role in controlling cellular behavior during morphogenesis. Particularly, clathrin-dependent endocytosis ofi ntegrins has long been acknowledged as essential for cell migration. However, little is known about the contribution ofi ntegrin trafficking to epithelial tissue morphogenesis. Here we show how the transmembrane protein Opo, previously described for its essential role during optic cup folding, plays a fundamental role in this process. Through interaction with the PTB domain of the clathrin adaptors Numb and Numbl via an integrin-like NPxF motif, Opo antagonizes Numb/Numbl function and acts as a negative regulator ofi ntegrin endocytosis in vivo. Accordingly, numb/numbl gain-of-function experiments in teleost embryos mimic the retinal malformations observed in opo mutants. We propose that developmental regulator Opo enables polarized integrin localization by modulating Numb/Numbl, thus directing the basal constriction that shapes the vertebrate retina epithelium.

INTRODUCTION

In each metazoan group, stereotyped morphogenetic movements shape embryonic tissues into functional organs. During development and tissue remodeling, precursor cells display a number of characteristic behaviors: cells may move freely, migrate as coordinated clusters and chains, or collectively change their shape to force an epithelial sheet to elongate, protrude, bend, or form a tube (Lecuit and Lenne, 2007 ; Montell, 2008). How cells move and change their shape in a coordinated fashion depends both on the genetic identity ofi ndividual cells and on their microenvironment, which conditions cell signaling and adhesion (Papusheva and Heisenberg, 2010). The cytoskeletal machineries that generate and transmit morphogenetic tensions are locally assembled to drive the asymmetric behavior of the cells. This phenomenon is tightly linked to the regulation of general cell polarity and polarized trafficking of receptors and adhesion molecules (Bryant and Mostov, 2008 ; Nelson, 2009).

During tissue morphogenesis, polarized epithelial sheets bend to form cups, tubes, and cysts, thus providing an important resource for evolutionary plasticity. The best-characterized example among morphogenetic events in animal epithelia is apical constriction (Sawyer et al., 2010). Quantitative imaging studies in Drosophila epithelia have shown that this process is driven by the periodic contractions of the actomyosin network at the cell apex (Martin et al., 2009 ; Solon et al., 2009). In epithelial sheets, bending may also occur toward the basal surface and examples of this behavior are observed in vertebrates during the formation of the midbrain-hindbrain boundary and the folding of the optic cup (Gutzman et al., 2008 ; Martinez-Morales and Wittbrodt, 2009). Basal cell contraction has also been recently described as the driving force directing the elongation of both the egg chamber in Drosophila (He et al., 2010) and the notochord in ascidians (Dong et al., 2011). Together, these studies show that basal constrictions/contractions involve the local recruitment of the actomyosin network. Furthermore, oscillatory actomyosin contractions, similar to those described at the apical surface, have also been recorded at the basal cell surface (He et al., 2010). Although these observations point to common characteristics for the contractile machineries operating at both ends of the apico-basal axis, clear differences also exist. Whereas apical constriction depends on adherens junctions and apical polarity complexes (Kölsch et al., 2007 ; Letizia et al., 2011), it is integrins within focal adhesions that play a pivotal role in basally driven morphogenetic processes. Thus, interference with the adhesive function ofi ntegrins impairs basal actomyosin recruitment and tissue morphogenesis in both vertebrate and invertebrate epithelia (He et al., 2010 ; Martinez-Morales et al., 2009).

The fundamental role off ocal adhesions in tissue morphogenesis has been best characterized in the context of cell migration, where clathrin-dependent trafficking ofi ntegrins along the front-back axis has proven to be essential for directional cell movement (Ezratty et al., 2009). Members of the phosphotyrosine binding (PTB) family of clathrin adaptors (such as Numb, Dab2

Developmental Cell
Numbs/Opo Antagonism Controls Optic Cup Formation

and ARH) interact with integrin- b NPxY/F motifs to regulate their endocytosis rate (Calderwood et al., 2003). Accordingly, both Dab2 and Numb regulate integrin- b turnover and directional cell migration in HeLa cells (Nishimura and Kaibuchi, 2007 ; Teckchandani et al., 2009). Despite the increasing evidence showing that polarized integrin endocytosis is essential for cell polarity and migration (Caswell et al., 2009 ; Nelson, 2009), the role of PTB clathrin adaptors in tissue morphogenesis is just beginning to be understood. Besides its traditional role in asymmetric cell division (Knoblich et al., 1995), the endocytic adaptor protein Numb has also been implicated in the regulation of different cellular processes including cell adhesion and polarity (Rasin et al., 2007 ; Wang et al., 2009). Studies using double-knockout mice for Numb and Numb-like (Numbl) have shown in vivo the redundant role of numb family members during axonal arborization (Huang et al., 2005) spindle orientation (Wu et al., 2010) and chemotaxis (Zhou et al., 2011). In polarized epithelial cells, Numb asymmetrically localizes to the basolateral cortex (Dho et al., 2006). Both in epithelial and migratory cells, as well as during asymmetric cell divisions, the polarized localization of Numb depends on its phosphorylation by aPKC (Smith et al., 2007). In the context of migratory cells, this polarized distribution has been related to a role in integrin recycling and cell motility (Nishimura and Kaibuchi, 2007). In contrast, although the severe neural tube defects observed in Numb $^{-/-}$ mice suggest a role in epithelial morphogenesis (Zhong et al., 2000), the functional significance of Numb polarized localization in epithelial cells is still unclear.

We previously described the essential role of the transmembrane protein Opo, encoded by the gene ojoplano/Ofcc1 , during optic cup morphogenesis. Opo regulates the asymmetric localization off ocal adhesion components to the basal surface of the retina epithelium and consequently, ojoplano loss off unction impairs basal constriction in the teleost retina (Martinez-Morales et al., 2009). To further investigate Opo function, we carried out a yeast two-hybrid screen that identified PTB clathrin adaptors as its interacting partners. Here, we show that Opo interacts with the PTB domain of the adaptors, Numb and Numbl, through a conserved NPxF motifl ocated in the amino terminal end of the protein. Using internalization assays and functional studies in mammalian cells and fish embryos, we demonstrate that Opo and Numb/Numbl act antagonistically to regulate integrin- b trafficking and optic cup morphogenesis. Our data indicate that Opo acts as a negative regulator ofi ntegrin endocytosis at the basal surface of the retina. These findings highlight the key role ofi ntegrin recycling as a developmental mechanism driving basal constriction during epithelial morphogenesis.

RESULTS

Opo Interacts with the PTB Domain of Numb/Numbl through a Conserved NPxF Motif

The morphogenetic gene opo encodes a transmembrane protein (Opo) that regulates the polarized localization off ocal adhesions in the retinal epithelium through a still uncharacterized molecular mechanism (Martinez-Morales et al., 2009). Besides four putative transmembrane passes (Figure 1 A), Opo does not include any annotated protein domains that could suggest its molecular role. To gain insight into Opo molecular function we decided to identify its interacting partners using a yeast two-hybrid approach. As baits, we used the conserved N-terminal (N-Opo) and C-terminal (C-Opo) regions of the protein, both of which face the cytosolic compartment as indicated by topology prediction and also confirmed by epitope tagging (Figure S1 available online). After screening 74 and 64 million interactions, respectively, two members of the PTB family of endocytic adaptors (Numbl and Dab2) were identified as the highest-scoring proteins for the N-terminal bait (Table S1 A), whereas the strongest C-terminal interaction was confirmed as Hsc70/Hspa1l (Table S1 B), a chaperone belonging to the Hsp70s family. Both the PTB family members as well as Hsc70 are known regulators of clathrin-mediated endocytosis (Chang et al., 2002 ; Teckchandani et al., 2009 ; Ungewickell and Hinrichsen, 2007).

Upon closer inspection of the N-Opo sequence, a conserved NPxF motif congruous with the NPxY motif present in integrin-b tails was discovered (Figure 1 B). Biochemical interaction of PTB domain proteins and NPxY/F ligands has been well documented in vivo and in vitro (Calderwood et al., 2003 ; Chen et al., 2006). These observations prompted us to examine the possibility that the Opo NPxF signal might interact with the PTB domain containing proteins: Numb, Numbl, and Dab2, in a similar fashion. To that end, the PTB-containing N-terminal domains of these proteins were recombinantly expressed in bacteria and purified (Figures 1 C and 1D). Glutathione S-transferase (GST) pull-downs of radiolabelled full-length Opo confirmed the biochemical interaction of N-Dab2, N-Numb, and N-Numbl with the Opo protein (Figure 1 D). Similarly, all three tested PTB proteins interacted in vitro, albeit to different extents, with the Integrin-b1 tail bearing the canonical NPxY sequence (Figure 1 D). The converse experiment was also performed, and the immobilized N-Opo was incubated with radiolabelled N-Dab2, N-Numb, and N-Numbl or their corresponding full-length proteins (Figure 1 E). Whereas the interaction of N-Opo with N-Numb/N-Numbl was corroborated in this assay, neither N-Dab2 nor Dab2 were recovered after incubation with immobilized N-Opo, suggesting that additional protein domains might play a role in stabilizing this interaction. Moreover, to test the ability of Opo to interact with PTB domain proteins within a physiological context, either a mammalian Opo-GFP fusion or GFP protein alone control were coexpressed with Myc-tagged N-Numbl (pCS2+:Myc-N-Numbl) in the immortalized retinal pigment epithelial cell line, RPE-1. Western blotting of cellular extracts immunoprecipitated with anti-GFP antibody resulted in a clear signal identified by anti-GFP and anti-Myc antibodies, thereby confirming the biochemical interaction of Opo and Numbl in a mammalian system (Figure 1 F).

These findings are further supported by colocalization experiments performed in HeLa cells where the full-length Opo-GFP fusion was coexpressed with a Numb-Cherry fusion (pCS2+:zNumb:Cherry) and analyzed by confocal microscopy (Figure 1 G). In spite of their differential routing within the cell, Opo is trafficked through the secretory pathway whereas Numb preferentially localizes to the cell cortex (Knoblich et al., 1995); both proteins overlapped locally at the plasma membrane (Figure 1 G).

Finally, to test whether the NPxF sequence present in the Opo N terminus is indeed responsible for the interaction with PTB domain proteins, a point mutagenesis approach was undertaken. It has been previously demonstrated that the tyrosine

Developmental Cell
Numbs/Opo Antagonism Controls Optic Cup Formation

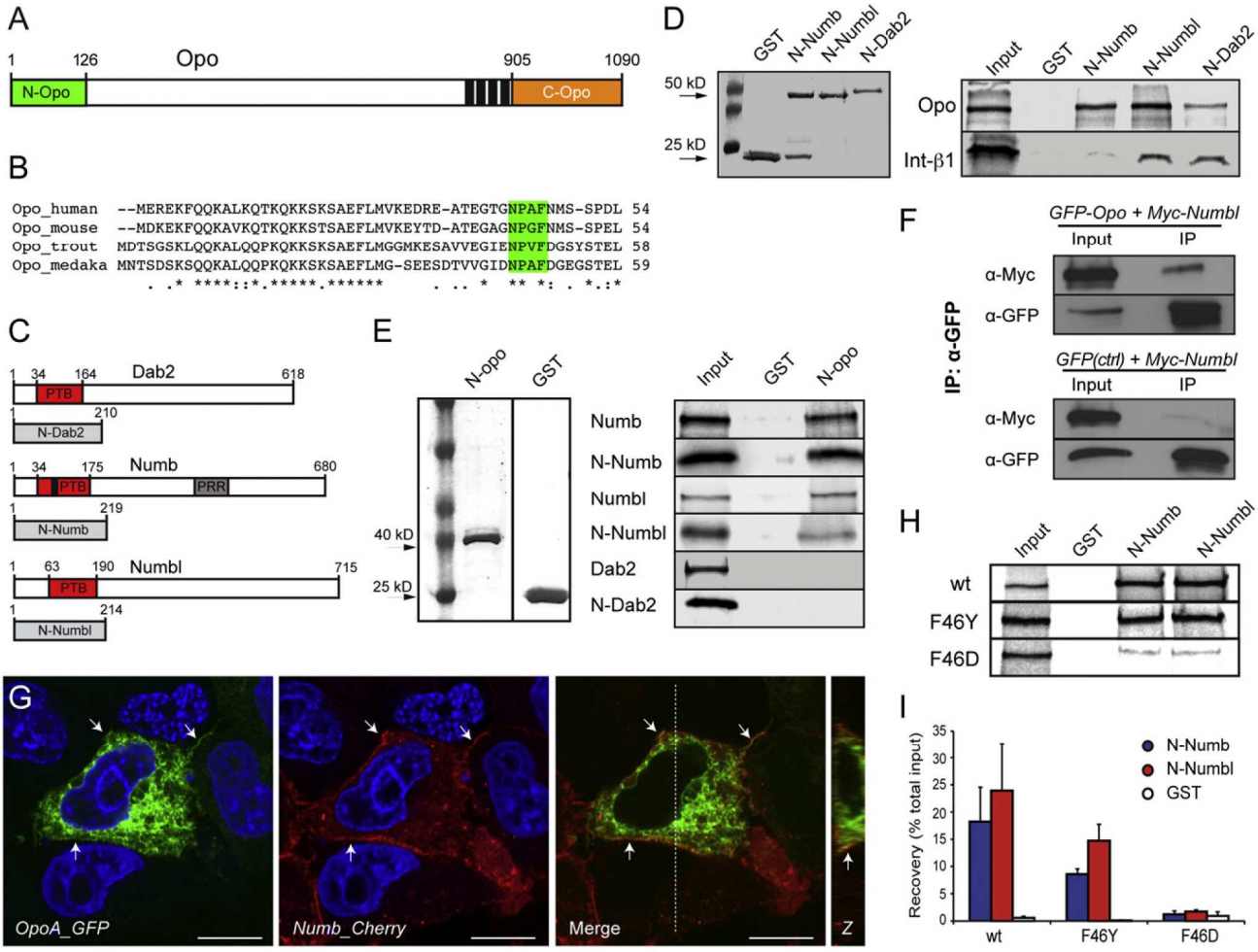

Figure 1. Opo Interacts with Numb/Numbl through a Conserved N-Terminal NPxF Motif

(A) A schematic representation of the medaka Opo protein. The black boxes represent four transmembrane passes.

(B) Conservation of the N-terminal NPxF sequence from teleosts to mammals.

(C) Schematic representation of medaka clathrin adaptors. The PTB containing fragments used for GST pull-downs are indicated.

(D) Coomasie staining (left panel) of recombinantly expressed proteins used for GST pull-downs. Full length Opo interacts with N-Numb, N-Numbl and N-Dab2 in vitro, whereas the Integrin- b1 tail fragment preferentially interacts with Numbl and Dab2 (right panel).

(E) Coomasie staining (left panel) of recombinantly expressed N-Opo used for GST pull-downs of either full length or N-terminal (PTB containing) (S ^{35}) Numb, Numbl and Dab2. Both full length and N-terminal Numb and Numbl interact with N-Opo.

(F) Western blotting of RPE-1 cellular extracts immunoprecipitated with anti-GFP antibody. Staining with anti-GFP and anti-Myc antibodies confirms the interaction of GFP-Opo and Myc-Numbl in RPE-1 cells. GFP alone was used as a negative control in parallel experiments.

(G) Colocalization of Numb_Cherry and OpoA_GFP at the cellular cortex in HeLa cells.

(H) GST pull-downs of S ^{35}-labeled F46Y and F46D Opo mutants shows reduced interaction with N-Numb and N-Numbl.

(I) Quantification of wild-type Opo, F46Y-Opo and F46D-Opo binding to N-Numb/N-Numbl in GST pull-downs. Input lines contain 10% of the input. Error bars represent SEM of three experiments. Scale bar, 20 mm.

See also Figure S1 and Table S1 .

residue present in Integrin NPxY tail sequences is crucial for cell motility and interaction with clathrin adaptors (Chen et al., 2006 ; Filardo et al., 1995). The phenylalanine present in the Opo motif was therefore mutated to either tyrosine or aspartic acid yielding NPAY or NPAD, respectively. The substitution of phenylalanine to tyrosine led to a modest (~2-fold) reduction in PTB domain binding as assayed by GST pull-down, whereas the substitution to aspartate resulted in a severe (>10-fold) loss of protein interactions (Figures 1 H and 1I). Both N-Numb and N-Numbl binding were equally affected by the mutation. Altogether, these data provide evidence for the interaction of Opo with PTB domain proteins and demonstrate the requirement of the NPxF sequence in enabling these interactions.

Opo Localizes to a Subpopulation of Clathrin-Coated Structures

Numb localizes to Ap2 a-positive clathrin-coated structures (CCSs) in HeLa cells, preferentially at the adhesion surface (Nishimura and Kaibuchi, 2007 ; Santolini et al., 2000). To investigate whether Opo shows a similar distribution, we transfected both

Developmental Cell
Numbs/Opo Antagonism Controls Optic Cup Formation

HeLa and RPE-1 cells with either N-terminal (GFP-Opo) or C-terminal (Opo-GFP) fusions (Figures 2 and S2) and examined their subcellular localization. In agreement with our previous observations, Opo localized to different compartments along the secretory pathway including the endoplasmic reticulum, Golgi apparatus, and the plasma membrane, as determined by costaining with BIP, GM130, and F-actin, respectively (data not shown). Opo also colocalized with a subpopulation of Ap2a-positive CCSs both in RPE-1 and HeLa cells, preferentially at the cellular cortex (Figures 2 B–2D and S2).

To investigate the specificity of this colocalization, HeLa cells were transfected with either a carboxy-terminal truncation of the protein (Figures 2 E–2G) or with OpoB, a mouse protein isoform (Mertes et al., 2009) naturally truncated at the amino terminus (Figures 2 H–2J). The truncation of both Opo N- and C terminus resulted in a substantial reduction ofi ts colocalization with Ap2a, suggesting that both protein ends are required for Opo recruitment to CCSs.

Opo Inhibits Integrin Internalization in HeLa Cells

Previous reports in HeLa cells have shown that Numb interacts with the cytoplasmic Integrin -b tails and functions in their endocytosis (Calderwood et al., 2003 ; Nishimura and Kaibuchi, 2007 ; Teckchandani et al., 2009). Here we demonstrate that Opo localizes to a subpopulation of endocytic vesicles and interacts physically with Numb and Numbl. These results suggest that Opo may act as a regulator ofi ntegrin endocytosis. To functionally address this point we carried out internalization assays in HeLa cells (Figure 3). Transfected cells expressing either control GFP , Opo-eGFP , or Numb-Cherry were incubated with anti-Integrin-b1 antibodies for 30 or 40 min to allow its internalization. Cells were then fixed and the relative rate ofi ntegrin endocytosis was calculated as the ratio between neighbor-transfected and nontransfected cells (expressed as a percentage). As expected from the reported role for Numb in endocytosis, Integrin- b1 uptake was significantly enhanced in cells expressing Numb-Cherry (Figures 3 E, 3F, and 3I). In contrast, it was substantially inhibited in cells expressing Opo-GFP (Figures 3 C, 3D, and 3I). Interestingly, cells coexpressing both constructs showed a rate ofi ntegrin endocytosis that was not significantly different from untransfected cells (Figures 3 G–3I) or from cells expressing the control GFP construct (Figures 3 A, 3B, and 3I). These results show that Opo antagonizes Numb and functions as a negative regulator ofi ntegrin endocytosis.

Opo Loss of Function Enhances Integrin Internalization in the Medaka Optic Cup

To further strengthen our observations from HeLa cells, we next set out to investigate the role of Opo in integrin receptor trafficking during optic cup folding. To this end, we carried out in vivo FRAP experiments using the medaka eye-specific transgenic line Vsx3::Integrin b1Tail-GFP (Figure S3 A). Benefiting from the strictly polarized architecture of the retinal epithelium, we bleached equivalent volumes either at the basal or apical side of both wild-type and opo mutant retinae (Figure S3). Fluorescence recovery, which occurred at the expense of the unbleached half of the columnar neuroblasts, was monitored in a central optical section of the bleached volume until it achieved a plateau, reflecting that forward and reverse transport ofl abeled

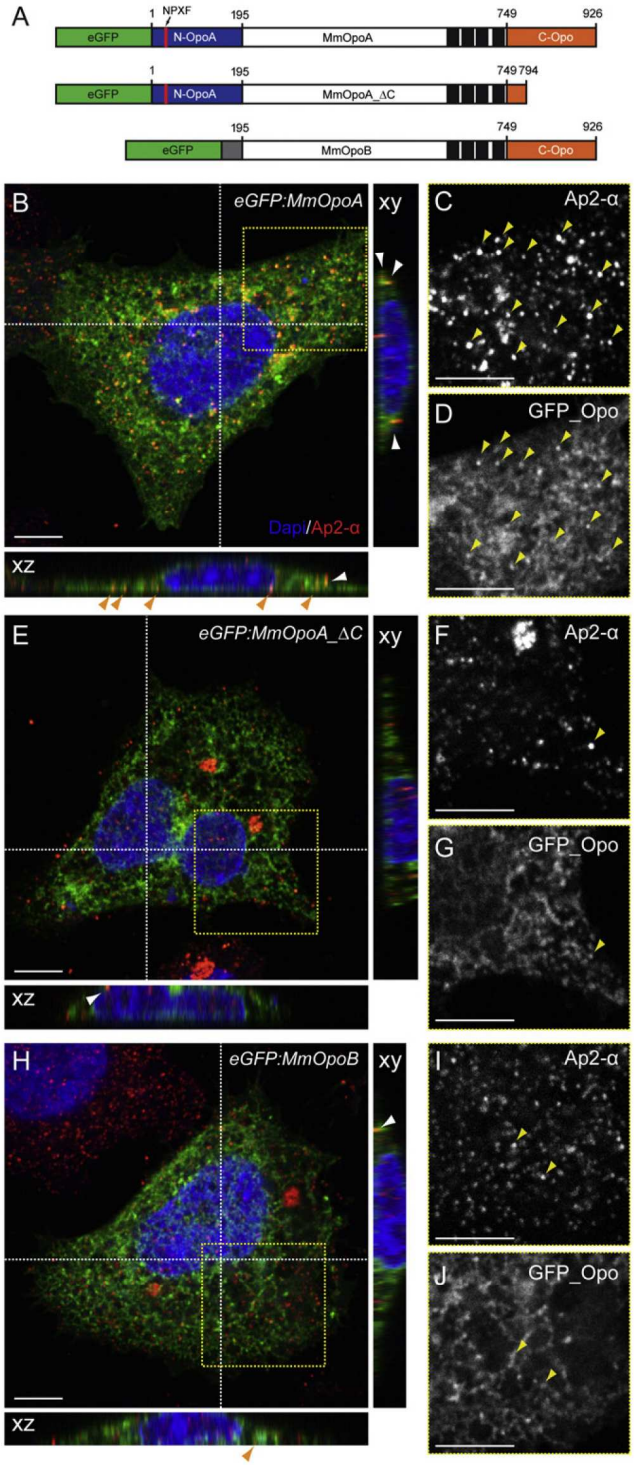

Figure 2. Opo Localizes to Ap2 a-Positive Clathrin-Coated Structures

HeLa cells transfected either with mouse GFP-OpoA or C-terminal and N-terminal Opo truncations (A) were stained with anti- Ap2 a antibodies to detect CCS. Cells transfected with GFP-OpoA (B–D) show colocalization (arrows) at the cellular cortex (arrows in xz and xy projections). This is reduced when GFP-OpoA_ DC (E–G) or GFP-OpoB (H–J) are transfected. Scale bars, 5 mm. See also Figure S2 .

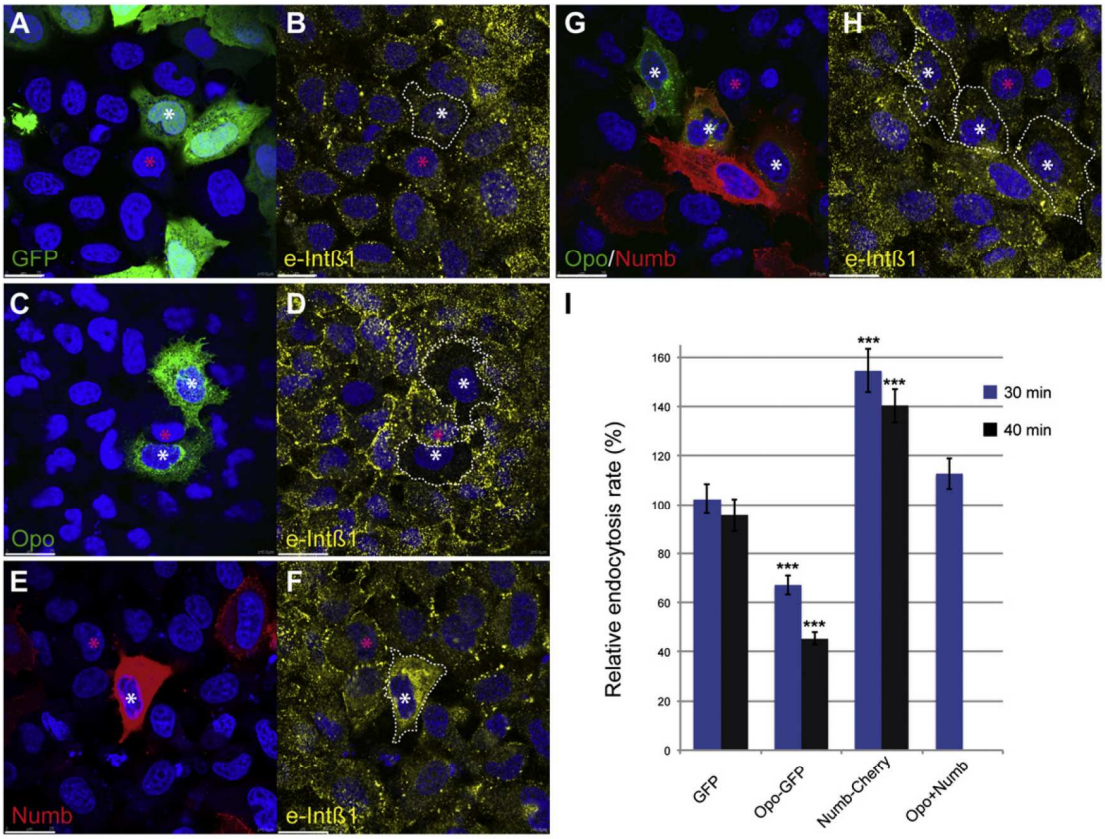

Figure 3. Opo Inhibits Integrin- b1 Internalization in HeLa Cells

(A and B) HeLa cells expressing control GFP (pCS2+:GFP) (A) stained with anti-Integrin- b1 antibodies after the internalization assay (B).

(C and D) Opo-GFP expressing cells (C) stained with anti-Integrin- b1 antibodies after the internalization assay display a significant reduction in Integrin- b1 uptake (D).

(E and F) In contrast to (C) and (D), Integrin- b1 uptake is enhanced in cells expressing Numb-Cherry constructs.

(G and H) Cells coexpressing both constructs. Dotted lines represent areas of measured Integrin- b1 turnover. White and pink asterisks denote equivalent transfected and nontransfected cells respectively.

(I) Relative endocytosis rate is expressed as the transfected/nontransfected ratio (%). Data represent the mean and SEM of 24 cells in each condition. Scale bars, 25 mm.

molecules had reached an equilibrium (Figures S3 A^{0} and S3 A$^{0\prime}$). In wild-type tissues, FRAP analyses consistently revealed higher and faster integrin recovery at the basal rather than at the apical side (Figures 4 A, 4B, and S3 A; Movie S1), thus indicating that integrins are asymmetrically trafficked through the epithelium with a net flux toward the basal side. The analysis off our independent FRAP experiments in mutant tissue showed instead that integrin basal recovery (Figures 4 A, 4B, and S3 A; Movie S1) is significantly reduced when compared to the wild-type. As a control, the recovery rates for the apical tracer Par3-eGFP (Figures 4 C, 4D, and S3 B; Movie S2) are not significantly different from those measured in wild-type tissues. These results suggest that opo function is specifically required for basal, but not apical, transport ofi ntegrins in vivo.

Additionally, electron microscopy (EM) studies also support a role for Opo in trafficking during optic cup morphogenesis. Immunogold analysis of stage 23 Vsx3::eGFP_Opo retinae revealed that Opo is associated to basal endosomes (Figures S3 C and S3D). Furthermore, morphological electron microscopy analysis of stage 23 wild-type and opo mutant retinae revealed a significant accumulation ofi ntracellular vesicles specifically at the basal end of the mutant neuroblasts (Figures 4 E, 4F, S3 E, and S3 F). Although collectively our analyses clearly indicate that Opo acts as regulator ofi ntegrin trafficking during optic cup folding, they cannot discriminate whether this is due to an impaired forward transport or an increased endocytic rate.

To address this question, we performed internalization assays in vivo using the Vsx3::Int b1Tail-GFP line, as the GFP tag of the fusion protein is oriented toward the extracellular space (Figures 4G–4O). To establish the rate ofi ntegrin uptake in both wild-type and opo retinae, dechorionated embryos were incubated with a-GFP antibodies for 30 min before fixation. Fluorescence intensity associated to antibody internalization was then quantified in equivalent areas, both at the basal surface and in medial zones of the retina. We found that in opo Intb1Tail-GFP uptake is significantly enhanced in both areas when compared to wild-type retinae (Figure 4 O), indicating that Opo functions as a negative regulator ofi ntegrin endocytosis also during optic cup folding.

Developmental Cell
Numbs/Opo Antagonism Controls Optic Cup Formation

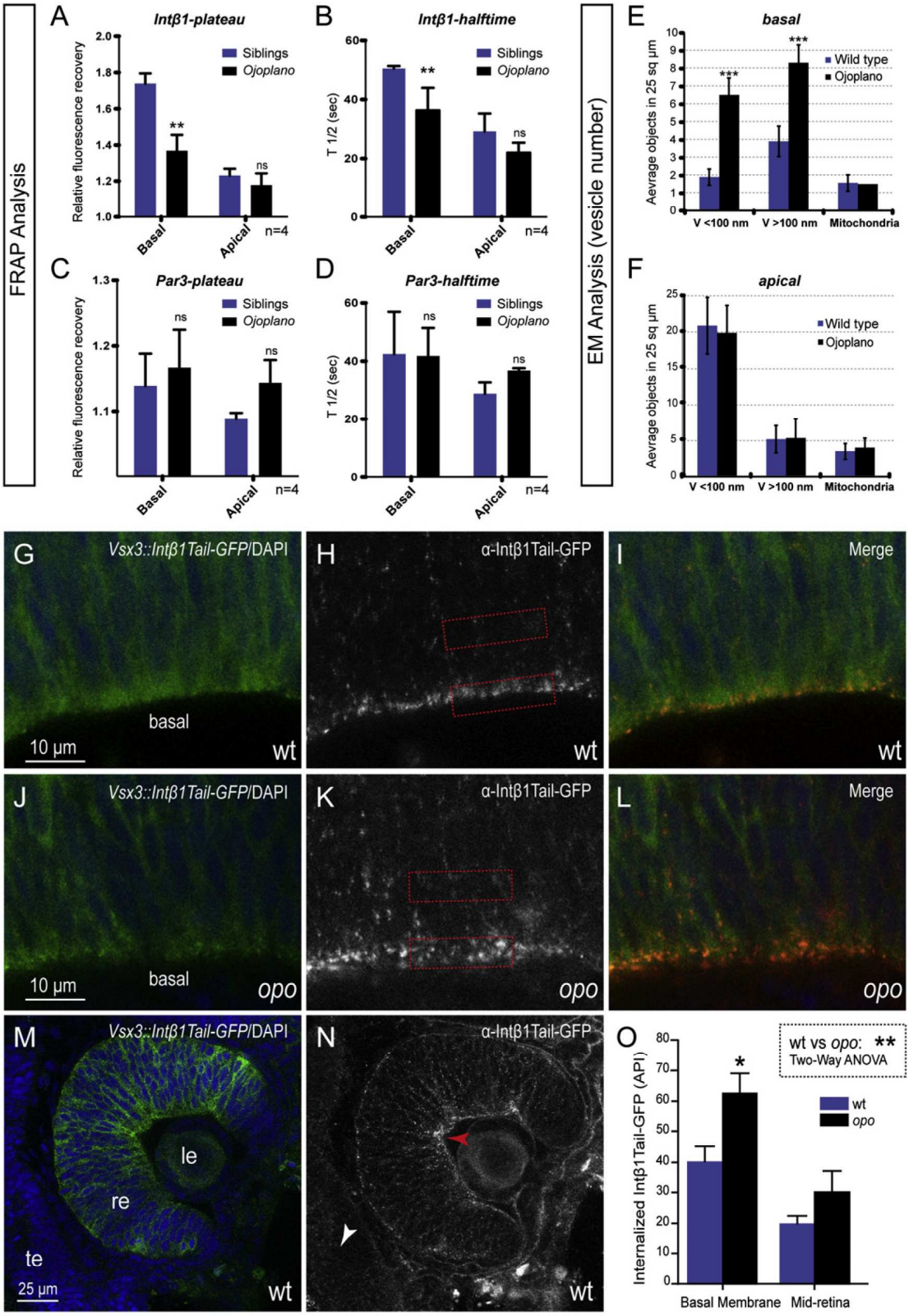

Figure 4. Integrin- b1 Endocytosis Is Enhanced in the opo Retina

In vivo FRAP reveals altered integrin- b1 trafficking in opo mutants. Equivalent areas were bleached from either basal or apical sides, in stage 24 wild-type and opo retinae (see Figure S3 for experimental details).

Developmental Cell
Numbs/Opo Antagonism Controls Optic Cup Formation

Opo and Numb Colocalize to the End Feet of the Neuroepithelial Precursors and Regulate Basal Localization of Integrin- b1

In vertebrates, numb and numbl have been detected in a wide range of tissues and developmental stages (Wakamatsu et al., 1999 ; Zhong et al., 1997). In zebrafish embryos, both transcripts are ubiquitously expressed before neurulation and get progressively restricted to the anterior nervous system and in particular to the retina (Niikura et al., 2006 ; Reugels et al., 2006). The analysis of numb and numbl expression by qPCR and in situ hybridization showed comparable profiles in medaka and confirmed that both genes are expressed in the developing retina (Figures S4 A–S4F). Similarly, both opo transcripts and Opo protein are enriched at the basal side of the retinal epithelium in vertebrates (Figures S4 G–S4J; Martinez-Morales et al., 2009 ; Mertes et al., 2009). To investigate in vivo the distribution of Opo and Numb during the folding of the optic cup (stage 24), we examined the medaka transgenic lines Vsx3::eGFP_Opo and Vsx3::Numb_eGFP (Figures 5 A, 5B, and S4 ; Movies S3 and S4). Confocal microscopy analysis revealed that both proteins are enriched at the basal tip of the neuroblasts in the retina. Numb shows a strong cortical accumulation at the vitreal surface as well as in the baso-lateral cortex of mitotic cells (Figures 5 B and 5C), as previously reported for zebrafish and chick neuroepithelial cells (Reugels et al., 2006 ; Wakamatsu et al., 1999). Finally, the injection of Numb_Cherry RNA into Vsx3::eGFP_Opo embryos at one-cell stage confirmed in vivo the colocalization of both proteins at the basal surface of the retinal epithelium (Figures 5 D–5F). Interestingly, Numb basal localization appeared only mildly reduced in opo mutants as visualized in a Vsx3::Numb_eGFP background (Figures S4 K and S4L), suggesting that its localization does not depend completely on opo function.

It has been shown that Numb regulates Integrin- b turnover in vitro (Nishimura and Kaibuchi, 2007 ; Teckchandani et al., 2009). To determine whether Numb also functions as a regulator off ocal adhesions in the retinal epithelium, we generated retinal clones overexpressing numb and monitored Integrin- b1 localization (Figures 5 G–5P). Integrin- b1 recruitment at the basal side of the neuroepithelium was noticeably reduced in numb gain-of-function clones (Figures 5 K and 5N) but not in control clones expressing only the Lyn_tdTomato tracer (Figure 5 H). These results, together with previous findings on opo function, suggest that Numb and Opo cooperate to regulate focal adhesions turnover during optic cup formation.

Numb/numbl Gain of Function Impairs Optic Cup Morphogenesis

A logical prediction to be drawn from the functional antagonism observed between Numb/Numbl and Opo would be that numb/numbl gain off unction should mimic the embryonic phenotype observed in opo mutants. To confirm this, and to gain insight into the morphogenetic role of numb/numbl during optic cup morphogenesis, we injected medaka numb and numbl RNAs into medaka embryos at the one-cell stage. Injected embryos developed tissue malformations strikingly similar to those observed in opo mutants. The injection of 25 ng/ ml of either numb (Figures 6 A and 6B) or numbl (Figures 6 C and 6D) RNAs resulted in a proportion of the embryos (19%, n = 76 and 12%, n = 102, respectively; Figure 6 E) in which optic cup folding was impaired. The injection of 100 ng/ ml of numb or numbl RNAs resulted in a higher proportion of affected embryos (34.8%, n = 74 and 36%, n = 40, respectively; Figure 6 E). Among the morphologic defects observed, large ventral openings of the optic cups (Figures 6 F and 6G) as well as strong craniofacial malformations (Figures 6 H and 6I) were particularly prominent in hatchlings. Interestingly, a proportion of embryos injected with the highest dose (100 ng/ ml) of numb (8.7%; Figures 6 E and 6J) or numbl (10%; Figures 6 E and 6K) developed complete cyclopia, a condition also observed in strongly affected opo morphants (Martinez-Morales et al., 2009), thus suggesting that Numb and Opo may also cooperate during the bilateralization of the eye field.

To extend our observations to another vertebrate model we also injected numb and numbl RNAs into zebrafish embryos (evolutionary distance 115–200 Myr (Furutani-Seiki and Wittbrodt, 2004). The injection of either 100 ng/ ml of numb (n = 228) or 50 and 200 ng/ ml of numbl RNA (n = 288 and n = 291, respectively) resulted in both a proportion of defects and a phenotypic range of ocular and craniofacial malformations similar to those observed in medaka embryos (Figures S5 A–S5F).

Numb/numbl and opo Interact Genetically

Given the identified association between Opo and Numb/Numbl proteins, we decided to test whether this interaction was also observed at the genetic level. To this end, numbl RNA (25 ng/ml) was injected in the opo background. While the percentage of misshapen eyes observed in the progeny of an opo$^{+/-}$ cross is roughly Mendelian (24 ± 0.1%), and the injection of numbl RNA (25 ng/ ml) into wild-type embryos yields 12% ± 1.1 of retinal defects, when the RNA was injected using the mutant background, ocular malformations increased to 45.8% ± 0.8 (Figure 6 L). This percentage was significantly higher than what

(A–D) Statistical analysis of FRAP experiments. The plateau (A and C) and $t_{1/2}$ (B and D) values for the different FRAP experiments are shown. Quantitative data are expressed as mean ± SEM. Significant differences among groups were evaluated by t tests and indicated when relevant. Notice that when wild-type and opo data are compared, significant differences were observed only for the basal recovery of Intb1Tail-eGFP (A and B) but not for Par3-eGFP (C and D).
(E and F) Electron microscopy analysis of stage 23 wild-type and opo retinas reveals an accumulation ofi ntracellular vesicles at the basal feet of the mutant neuroblasts (see Figure S3 for experimental details). Quantitative data at the basal (E) and apical (F) regions are provided for a 25 mm^2 area (n = 15). Vesicles were classified according to their size. As an internal control mitochondria numbers were also recorded. Significant differences among groups were evaluated by t tests (GraphPad Prism) and indicated when relevant. Error bars represent SEM.
(G–O) In vivo internalization ofi ntegrins in the retina. Optical sections from WT (G–I, M, and N) and opo (J–L) Vsx3::Int1 bTailGFP retinae stained with: DAPI (G, I, J, L, and M) and anti-GFP antibody (H, I, K, L, and N) after Integrin- b1 uptake assays. Anti-Integrin- b1Tail-GFP staining is significantly increased in opo mutants (K, L,and O), indicating an increased endocytic rate. No significant internalization of the antibody was detected in tissues not expressing the construct (compare red and white arrows in N). Dotted lines (H and K) represent areas of measured Integrin- b1 turnover (basal membrane and mid-retina). (O) Relative endocytosis rate is expressed as average pixel intensity (API).
Data represent the mean and SEM of six embryos in each condition. Scale bars, 10 mm. See also Movies S1 and S2 .

Developmental Cell
Numbs/Opo Antagonism Controls Optic Cup Formation

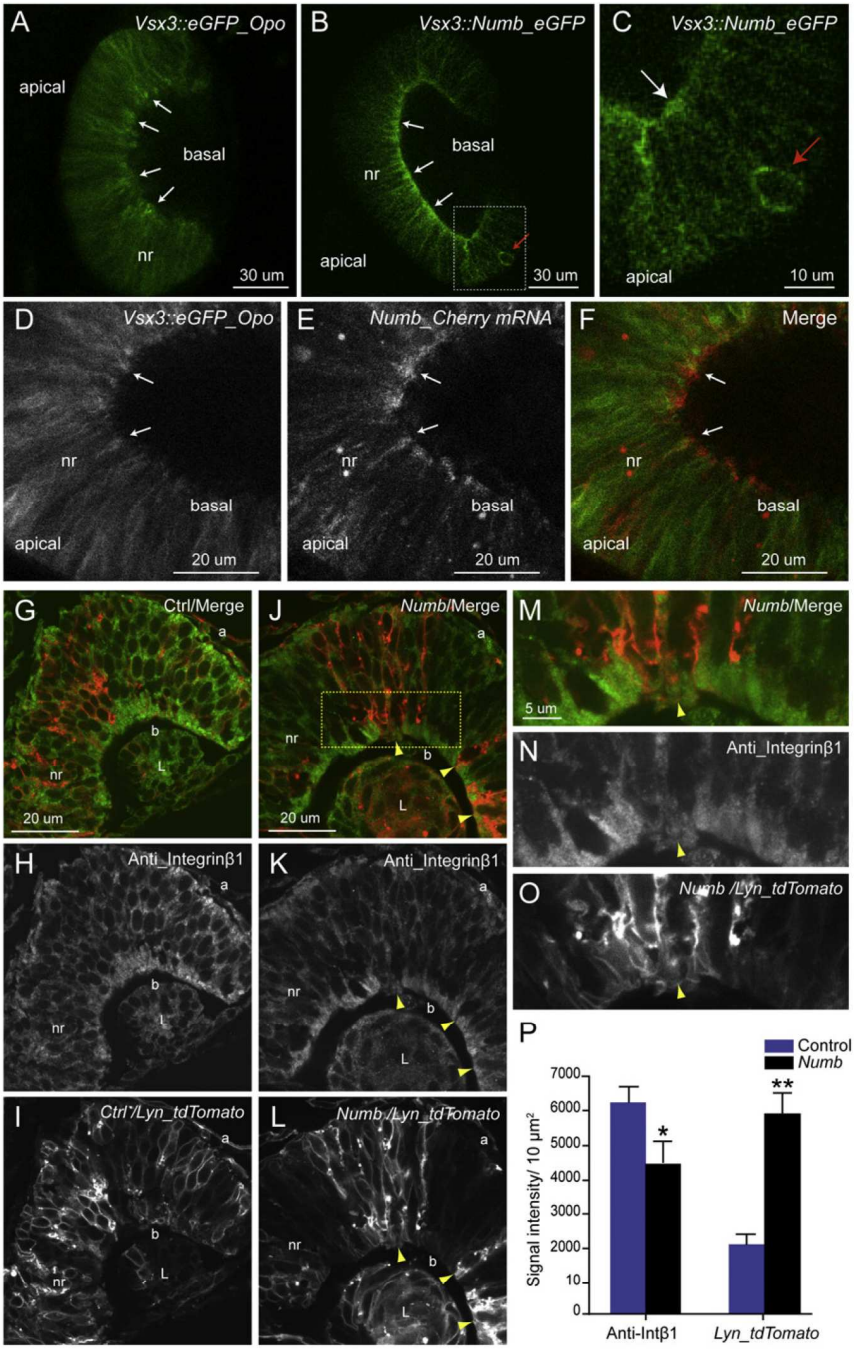

Figure 5. Numb Colocalizes with Opo and Regulates Integrin Recruitment at the Basal Retina

(A and B) Confocal microscopy analysis of transgenic medaka lines Vsx3::eGFP_Opo and Vsx3::Numb_eGFP shows the localization of both proteins at the basal end of the neuroblast.

(C) Numb_eGFP displays strong accumulation both at the basal surface (white arrow) and the baso-lateral cortex of mitotic cells (red arrow).

(D–F) Transient expression of Numb_Cherry RNA in Vsx3::eGFP_Opo embryos shows the in vivo colocalization of Numb and Opo at the basal surface.

(G–P) Stage 24 retinal sections showing different clones overexpressing either the linage tracer Lyn_tdTomato (G–I) or numb together with Lyn_tdTomato (J and L). Higher magnification pictures of (J–L) are shown in (M–O). Note that Integrin-b1 basal enrichment is reduced (yellow arrows) in numb gain-of-function clones as assessed by immunostaining (K and N). Integrin- b1 and Lyn_tdTomato are quantified (n = 5) in 10 mm^2 basal areas and are expressed as mean ± SEM (P).

nr, neural retina; b, basal; L, lens. See also Figure S4 and Movies S3 and S4.

is expected from simple additive effects, as determined after analysis by two-way ANOVA of three independent experiments ($p < 0.0001$; see raw data in Table S2); thus showing a synergistic effect. Moreover, the injection of numbl RNA (25 ng/nl) in the opo context resulted in a small proportion (3.3% ± 1.7) of cyclopic embryos, a phenotype never observed in a wild-type background.

To further expand our analysis we tested whether a partial inactivation of numb/numbl function may alleviate opo ocular phenotype. To this end, we used splicing morpholinos Mo_numbl4E5 and Mo_numbll4E5 to specifically knockdown gene expression (Figures S5 G and S5H). In agreement with the severe defects observed in Numb $^{-/-}$ mice (Zhong et al., 2000), the coinjection of both morpholinos at high concentration (300 nM) caused substantial embryo lethality. To overcome this, morpholinos were injected at a lower concentration (50 and 100 nM, respectively) into one blastomere in four-cell stage embryos, both in wild-type and opo backgrounds. Morpholino coinjection at this concentration did not interfere with optic cup folding. However, it significantly reduced the percentage of embryos (from the expected Mendelian 25% to 15% ± 3) showing the characteristic flattened optic cups observed in opo mutants (Figure 6 M). In addition, a proportion of the injected embryos (11.9% ± 0.9) displayed a partial rescue of optic cup morphology, showing an intermediate bending never observed either in opo mutants or in wild-type siblings (Figures 6 N–6P ^{0}). To support this observation, we measured the folding angles of the retinae and found that rescued embryos showed narrower cup folding angles than mutants (Figures 6 N–6P ^{0}).

Finally, to complement our analyses, we examined optic cup morphogenesis in vivo in wild-type and numbl-injected zebrafish embryos. The folding of the retinal epithelium was recorded by time-lapse microscopy in Vsx3:caaxGFP embryos, either wild-type (Figure 6 Q) or injected with numbl RNA (25 ng/nl; Figure 6 R).

Developmental Cell
Numbs/Opo Antagonism Controls Optic Cup Formation

Using multiposition image acquisition, tissue morphogenesis was simultaneously monitored in control and injected embryos over approximately 4 hr, starting at 20 high-power fields. While a similar mitotic rate was observed in control and numbl-injected retinae, the constriction of the epithelial sheet was retarded in the treated embryos (Figures 6 Q and 6R; Movie S5). Collectively, these data indicate that opo and numb/numbl interact genetically to regulate eye morphogenesis.

DISCUSSION

During organogenesis and tissue remodeling, the regulation of cell adhesive properties determines the morphogenetic behavior of entire epithelial sheets. The basal or baso-lateral localization ofi ntegrin receptors in epithelia has long been described as a common theme in vertebrate and invertebrate tissues (Bateman et al., 2001 ; Schoenenberger et al., 1994). However, the molecular mechanisms controlling the asymmetric turnover of integrin receptors have been poorly explored in the context of epithelial morphogenesis (Schotman et al., 2008).

Taking advantage of the polarized architecture of the vertebrate retina (Figure 7 A), we studied the folding of the optic cup as a model system for epithelial basal constriction (Martinez-Morales et al., 2009). Previously, we described that integrin's adhesive function is required for optic cup folding and that the morphogenetic protein Opo plays an essential role during this process, albeit through a still uncharacterized molecular mechanism (Martinez-Morales and Wittbrodt, 2009). Here we show that Opo binds to clathrin adaptors Numb and Numbl, and functions as a negative regulator ofi ntegrin endocytosis. Our data suggest that Opo plays an important role in the stabilization off ocal contacts at the basal surface. Although it is still unclear how tensional forces are generated and applied during optic cup folding, it is likely that focal contacts are required to transmit tensions basolaterally across the epithelial sheet. A similar requirement has been described during the elongation of the Drosophila egg chamber (He et al., 2010).

The PTB domain proteins Numb, Numbl, and Dab2 have been described as essential adaptors for clathrin-mediated integrin endocytosis (Caswell et al., 2009 ; Teckchandani et al., 2009). Consistently, they belong to the set of proteins recruited to focal adhesions in a Myosin II-dependent manner, as detected by proteomic analysis (Kuo et al., 2011). Our yeast two-hybrid assay has identified the interactions of Opo with Numbl (high confidence) and Dab2 (moderate confidence). Further biochemical analyses confirmed the preferential interaction of Opo with the PTB domains of Numb and Numbl, while showing a much weaker interaction with Dab2. In migratory cells, it has been proposed that Numb and Dab2 may play nonoverlapping roles as integrin endocytosis adaptors; Numb acting at the cell periphery and the leading edge and Dab2 mediating bulk internalization of disengaged integrins (Nishimura and Kaibuchi, 2007 ; Teckchandani et al., 2009). Both Numb and Opo have been described as basolaterally distributed proteins in epithelia (Martinez-Morales et al., 2009 ; Smith et al., 2007). Furthermore, here we show that Numb and Opo colocalize in vivo at the basal surface of the retinal epithelium. In contrast, Dab2 localizes preferentially to the apical surface in epithelia (Collaco et al., 2010). All these observations point to Numb and Numbl, rather than Dab2, as the functional partners of Opo.

The data presented here demonstrate that Opo binding to the PTB domain of Numb/Numbl depends on the conserved NPAF motif. In line with previous findings on the functionality of the integrin NPxF motif (Chen et al., 2006 ; Czuchra et al., 2006), the conservative mutation of the terminal phenylalanine to tyrosine in Opo does not abolish binding to Numb/Numbl. However, the mutation of this residue (1 out of 1090 amino acids) to aspartic acid (NPAD) strongly interferes with this interaction. It has been shown in Drosophila that Numb also binds the endocytic regulator Sanpodo through an amino-terminal conserved NPAF motif (Tong et al., 2010). The parallels between the vertebrate-specific protein Opo and the insect-specific protein Sanpodo can be further extended as both are fast-evolving proteins (O'Connor-Giles and Skeath, 2003), which include four transmembrane passes near their C-termini. Despite these similarities, there is no significant sequence homology between the two proteins, which suggests an independent evolutionary convergence phenomenon.

Our biochemical analyses, presented in the context of previous findings, are summarized in Figure 7 B. Considering the molecular structures of Opo and its identified partners, two tentative hypotheses can be envisioned to explain Opo function as a repressor of clathrin-mediated integrin endocytosis. The first possibility encompasses a simple competitive binding mechanism involving Numb/Numbl sequestration by Opo, which in turn results in an inhibition of the integrin internalization process. The second possible mechanism would rely on the high-confidence interaction detected between the Opo C terminus and the chaperone Hsc70, which has a central role in clathrin disassembly (Sousa and Lafer, 2006). Opo recruitment to integrin clusters at the plasma membrane could therefore mediate the premature disassembly of clathrin structures. These two mechanisms are not mutually exclusive and can operate in parallel to inhibit integrin endocytosis.

The prominent morphogenetic role of polarized receptor trafficking has been acknowledged for both cell-to-cell and cell-to-extracellular matrix contacts (Nelson, 2009 ; Ulrich and Heisenberg, 2009). Although substantial crosstalk between cadherin-mediated and integrin-mediated adhesions has been described (Papusheva and Heisenberg, 2010), they have been classically implicated in distinct morphogenetic phenomena. Thus, whereas the asymmetric internalization of E-cadherin at adherens junctions has been involved in cell intercalation/rearrangement in epithelia (Levayer et al., 2011 ; Shaye et al., 2008), integrin trafficking along the front-rear axis has been primarily studied in migratory cells (Caswell et al., 2009 ; Ezratty et al., 2009). The Opo/Numb-dependent mechanism that we describe here suggests that integrin trafficking along the apicobasal axis also plays an important morphogenetic role in epithelial tissues, particularly in the context of basally driven constrictions.

EXPERIMENTAL PROCEDURES

Transgenic Lines

The medaka lines Rx2::mYFP, Vsx3:Int b1tail_eGFP and Vsx3::eGFP_Opo have been previously described (Martinez-Morales et al., 2009). To generate the

Developmental Cell
Numbs/Opo Antagonism Controls Optic Cup Formation

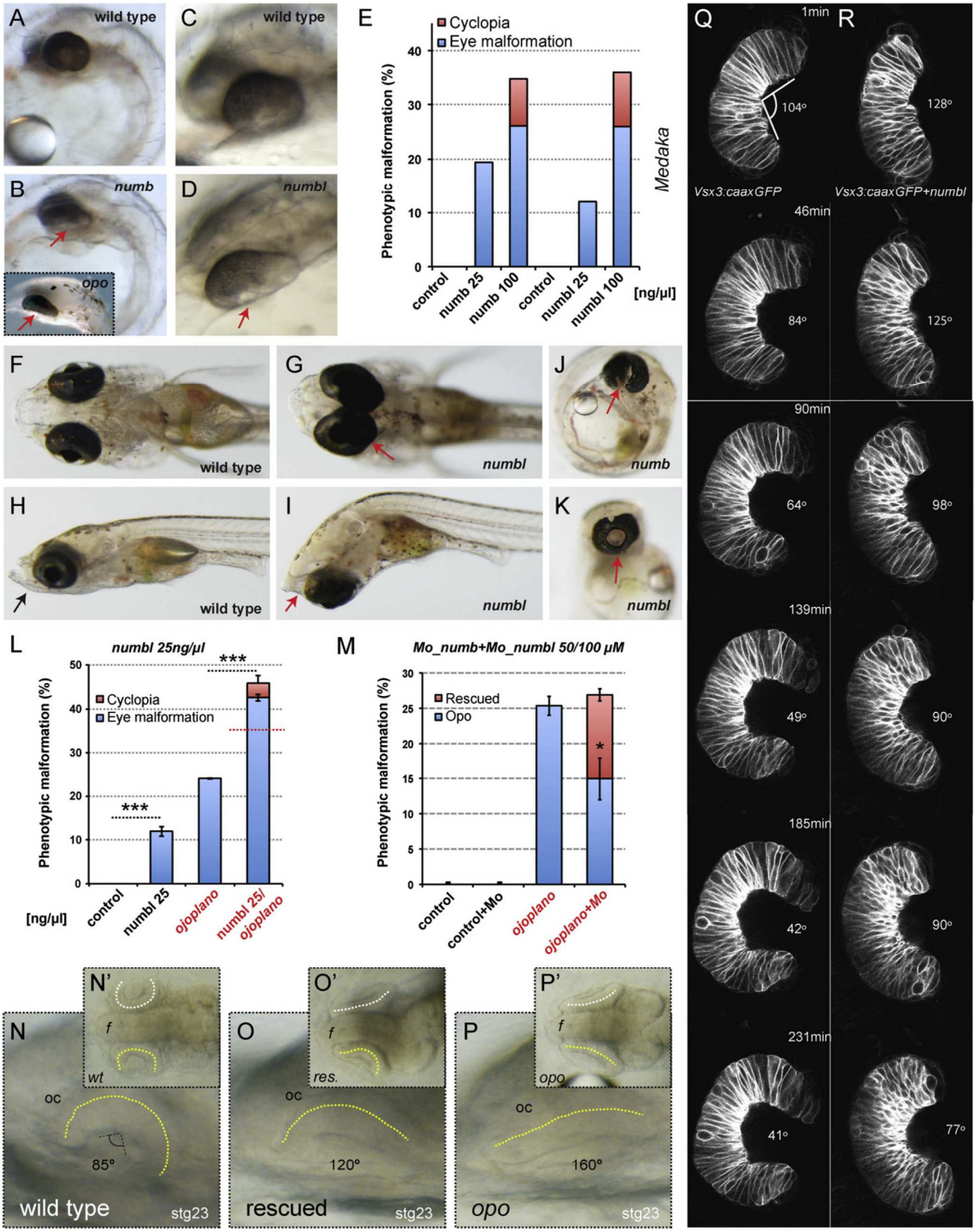

Developmental Cell
Numbs/Opo Antagonism Controls Optic Cup Formation

medaka line Vsx3::zNumb-eGFP , the fusion z Numb(PTBL PRRL): eGFP (Reugels et al., 2006) was cloned into a Vsx3 expression vector. The resulting construct was then injected into one-cell stage embryos following standard protocols (Thermes et al., 2002). Tol2 mediated transgenesis (Kawakami, 2007) in combination with multisite gateway technology (Invitrogen) were used to generate the stable zebrafish line Vsx3::eGFPcaax. The medaka Vsx3 promoter was inserted into a p5E-MCS entry vector and recombined with the Tol2kit vectors pME-EGFPCAAX and p3E-polyA into the Tol2 destination vector (Kwan et al., 2007). For a description of the expression constructs used see Supplemental Experimental Procedures .

Opo Yeast Two-Hybrid Screening

To elucidate Opo biochemical function we performed a yeast two-hybrid screening. The experimental approach used for baits and library construction, the mating methodology employed for screening and the scoring procedure have been previously described (Formstecher et al., 2005 ; Hybrigenics). Briefly, two different baits corresponding to the conserved amino (amino acids 1–126) and carboxy terminus (amino acids 905–1090) of the protein were generated by fusion to LexA in the vector pB29. The resulting fusions, N-OpoN-LexA-C and N-LexA-OpoC-C, were then used to screen a customized medaka cDNA library, cloned into the plasmid pP6 and built from medaka mRNAs (stages 18, 24, 31, and 34). The number of interactions tested was 74.2 million and 64.8 million for the amino and carboxy baits, respectively. The confidence of these interactions was scored using the Predicted Biological Score program to exclude false-positive results and promiscuous interactions.

GST Pull-Downs

Swollen glutathione agarose beads (Sigma, G4510) were incubated with GST fusion proteins in PBS buffer containing 1 mM DTT and 0.1% NP-40. The mixture was left rotating at 4 °C for 3–4 hr with end-to-end mixing. The beads (25 ml) were incubated overnight with 200 ml of pull-down buffer (20 mM HEPES pH 7.9,150 mM NaCl, 0.5 mM EDTA, 10% glycerol, 0.1% Triton X-100, 1 mM DTT), and 20 ml of the S^{35} radiolabeled protein. Beads were washed 3X with pull-down buffer and the bound proteins were eluted in 50 ml Laemmli buffer. The eluted fractions were resolved on a 10% SDS-PA gel. Dried gels were exposed o/n and the signal was quantified with ImageQuant software (GE Healthcare).

Western Blotting and CoIP

Extract preparations, coIP and WB were performed as described (Hurtado et al., 2011). The following antibodies were used: Rabbit polyclonal anti-GFP (ICL); monoclonal anti-c- myc at 1:3000 (9E10, Sigma) and monoclonal anti-GFP at 1:1000 (MAB2003, Abnova).

Site-Directed Mutagenesis

The mutagenesis was performed following the manufacturers' protocol (Agilent, QuikChange Lightning Multi Site-Directed Mutagenesis Kit, 210515-5) with the following primers: ggcatagataacccagccgacgatggagaaggaagcac (t47 g_t48a-NPAD) and gcatagataacccagcctacgatggagaaggaag (t48a-NPAY).

Cell Culture and Immunofluorescence Analysis

HeLa cells and immortalized human pigment epithelial cells RPE-1 (Takara Bio) were cultured at 37 °C in 5% CO2 in DMEM or DMEM/F12 (respectively) supplemented with 10% fetal calf serum. For IF experiments, cells were plated on coverslips the day prior to transfection. Transfections were then performed using Lipofectamine 2000 (Invitrogen) according to the manufacturer's instructions. After 36 hr at 37 °C, cells were fixed in 4% PFA for 20 min and permeabilized (when required) with PBS-0.1%, Tween-0.5%, and Triton X-100 containing 5% FCS for 10 min at room temperature. After PBS washes, cells were sequentially incubated with appropriate dilutions of the primary antibodies (12 hr at 4 °C) and secondary antibodies labeled with Alexa-568 or Alexa-633 (30 min at room temperature). After PBS washing, cells were mounted and confocal images acquired on a Leica TCS SPE or a Leica TCS SP5 confocal systems using HCX PL APO 63x1.4 Oil objectives. Image processing was carried out using Leica (LAS), Adobe Photoshop, and Image J 10.2 software. The following antibodies were used: rabbit polyclonal anti-GFP at 1:500 (A-11122, Invitrogen), mouse anti-Integrin- b1 at 1:300 (MAB1981, Chemicon), and mouse monoclonal anti-alpha adaptin at 1:300 (ab2807, Abcam).

Internalization Assays

The internalization of integrins was studied in HeLa cells as previously described (Nishimura and Kaibuchi, 2007). Briefly, cultures were grown and transfected on PDL-coated coverslips. At 70% confluence live cells were incubated for 30 or 40 min at 37 °C with mouse anti-integrin- b1, diluted 1:300 (MAB1981, Chemicon), to allow internalization. Then cells were rinsed in PBS, fixed in PFA, and permeabilized. Internalized integrins were detected with anti-mouse Alexa633 or Alexa568 secondary antibodies. Parallel negative controls in which cells were treated either without primary antibodies or without permeabilization yielded no significant signal. To quantify integrin internalization, we measured the mean fluorescence intensity per pixel in neighboring transfected and nontransfected cells of the same field (Image J). After background subtraction, relative endocytosis rate was calculated as the transfected/nontransfected ratio (%). Data represent the mean and SEM of 24 cells measured from two independent experiments.

In vivo internalization of integrins in medaka retinae was studied using the transgenic line Vsx3::Int1 bTailGFP . In this construct the GFP tag is fused N-terminal to the 70 C-terminal amino acids of Integrin- b1, including the transmembrane and intracellular domains. Medaka WT and opo retinae expressing Intb1tail:eGFP were dissected in cold PBS 1X. Once the overlying ectoderm was removed to facilitate antibody diffusion, embryos were incubated (30 min at 25 °C) with polyclonal anti-GFP antibodies (ab290, Abcam) diluted 1:300. After fixation and permeabilization, internalized integrins were detected with anti-rabbit Alexa555 secondary antibodies. No significant internalization of the antibody was detected in neighboring tissues lacking Int b1tail:eGFP expression.

Figure 6. Numb/Numbl and Opo Interact Genetically in Medaka Embryos

(A and B) Injection of 25 ng/ ml of numb RNA in medaka embryos results in a flat eye phenotype (red arrows), similar to that observed in opo mutants (inset).
(C and D) Overexpression of numbl RNA (25 ng/ ml) generates similar tissue malformations.
(E) Percentage of phenotypic malformations upon injection of increasing amounts of numb or numbl RNAs in medaka. Note that some of the embryos injected with 100 ng/ml displayed cyclopia.
(F–I) Medaka embryos injected with numbl (100 ng/ml) show large ventral openings of the optic cup and severe cranio-facial malformations (arrows).
(J and K) A small proportion of embryos injected with 100 ng/ ml of numb or numbl developed complete cyclopia.
(L) Statistical analysis showing a synergistic effect when numbl RNA (25 ng/ ml) was injected into an opo mutant background. Note the increased percentage of malformations over the expected 25% from the heterozygous cross.
(M) Statistical analysis showing that coinjection of splicing morpholinos targeting numb and numbl partially rescues ocular malformations observed in opo mutants. (E, L, and M) Error bars represent SEM
(N–P) Ocular morphology in wild-type (N and N^{0}), partially rescued (O and O^{0}), and opo (P and P^{0}) medaka embryos from stage 23. Lateral views (N–P). Dorsal views (N^{0}–P^{0}). Ocular morphology is highlighted with dotted lines both for the left (yellow line) and right (white lines) eyes. Optic cup (oc) folding angle is indicated in N–P. f = forebrain. Folding of the retinal epithelium examined by time-lapse confocal microscopy in Vsx3:caaxGFP transgenic embryos. The basal constriction of the epithelial sheet is significantly impaired in embryos injected with 25 ng/ ml of numbl RNA (Q) when compared to controls (R). Optic cup folding angle is also indicated.
See also Figure S5 , Table S2 , and Movie S5 .

Developmental Cell
Numbs/Opo Antagonism Controls Optic Cup Formation

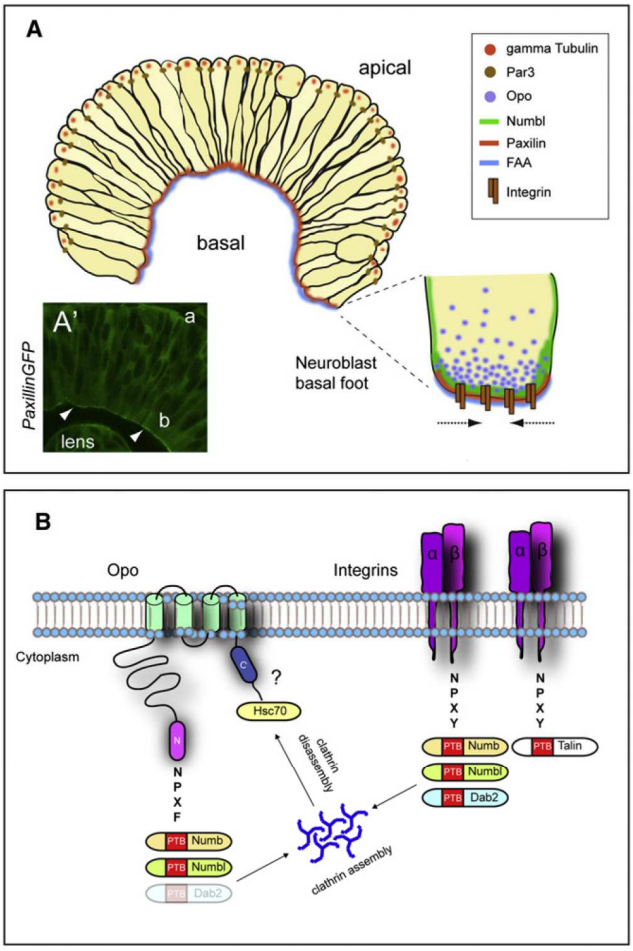

Figure 7. Numb/Numbl and Opo Localization and Function in the Retinal Epithelium

(A) Representation of the polarized retinal organization during morphogenesis. Apical and basal polarity cues are represented. Basal localization of integrins, Opo and Numbl at the basal feet of neuroblast cells is also depicted. Paxillin-eGFP is shown to illustrate the enrichment of focal adhesions (FAA) at the basal retina (A').

(B) Schematic diagram of the molecular interactions between Opo, clathrin adaptors, and integrins. The PTB domains of talin and clathrin adaptors (Numb, Numbl, and Dab2), as well as the NPxF and NPxY motifs of Opo and Integrins.

In Vivo FRAP Analysis

Stage 24 embryos expressing Intb1Tail:eGFP or Par3:eGFP embryos were immobilized and scanned in a Leica SP5 confocal microscope. Retinal cells expressing eGFP-tagged proteins were monitored using the 488 line of the SP5 100 mW argon laser at 20% power and bleached at 100% laser power. The bleaching protocol was as follows: three prebleaching images taken every 3 s; five bleaching pulses taken every 3 s at 100% laser power; 30 postbleaching images taken every 10 s. Equivalent areas in the retina were bleached either at the basal or the apical side of the neuroblasts both for WT and opo retinae. Recovery occurring at expenses of the unbleached side was monitored. The average fluorescence intensity per area in each compartment was plotted over time (LAS AF, Leica). To determine the plateau and $t_{1/2}$ values for the different FRAP experiments (n = 4) regression analyses were carried out using a one-phase exponential association function in GraphPad Prism5. To analyze the relative recovery at the plateau, the fluorescence value after bleaching was normalized to 1.

Electron Microscopy Analyses

For morphological EM analyses, stage 23 and 27 embryos were fixed in 0.05 M sodium cacodylate buffer, pH 7.3, containing 2.5% glutaraldehyde and 2% sucrose for 4 hr at 4 °C. Samples were washed in cacodylate buffer and treated consecutively with osmium tetroxide 2% for 40 min and uranyl acetate 2% for 30 min. After washing in cacodylate buffer, samples were dehydrated in graded (50%, 70%, 80%, 95%, and 100%) ethanol solutions and embedded in Epon. To quantify vesicle number in EM sections, consecutive 25 mm^2 areas in contact with the basal lamina (n = 15) or the apical surface (n = 6) were analyzed in at least three embryos.

RNA Injections

The vectors pCS2+:Numb and pCS2+:Numbl were used to synthesize medaka Numb and Numbl capped RNAs. Similarly, the fusions ASIP/Par-3:eGFP and pEGFPC1-(avian) paxillin WT1-559 (Martinez-Morales et al., 2009) were used to generate capped sense RNAs. After linearization of the vectors, capped sense RNAs were synthesized in vitro using the mMessage Machine Kit (Ambion). Purified RNA (QIAGEN RNeasy) was then injected (25–100 ng/ml) into one-cell stage both in medaka and zebrafish embryos. In clonal analysis experiments, Numb RNA (100 ng/ml) together with the lineage tracer Lyn_tdTomato (100 ng/ml), were coinjected into a single blastomere of four- to eight-cell stage medaka embryos. Mosaic embryos were then fixed in 4% PFA at stage 24, cryo-protected and sectioned as described (Martinez-Morales et al., 2009). Rabbit polyclonal anti-Integrin- b1 antibodies were used at 1:300 (Aviva Systems Biology).

Confocal Time-Lapse Analyses

Control and injected 20hpf Vsx3::caaxGFP embryos were immobilized in E3 (containing 0.01% tricaine) and embedded in 1% low-melting agarose. Time-lapse analyses were performed on a Nikon A1R microscope with a CFI PlanFluor20xMI N.A.0.75 objective and a 488 nm laser line. Samples were imaged as multiposition time-lapses for 3 hr with a time resolution of 3 min. Several central planes, spanning 40 mm, were selected. Movies were put together with single planes from each Z-stack using ImageJ (NIH).

Statistical Analysis

Quantitative data are expressed as mean ± SEM. Significant differences among groups were evaluated either by t tests or two-way ANOVA followed by Bonferroni post hoc tests (GraphPad Prism) and indicated when relevant.

SUPPLEMENTAL INFORMATION

Supplemental Information includes five figures, two tables, five movies, and Supplemental Experimental Procedures and can be found with this article online at http://dx.doi.org/10.1016/j.devcel.2012.09.004.

ACKNOWLEDGMENTS

We thank A. Gonzalez-Reyes, L. Centanin, F. Loosli, J.L. Gomez-Skarmeta, and P. Bovolenta for their critical input; Pam Halley for proofreading; and Rocío Polvillo, Katherina García, and Corín Díaz for their excellent technical assistance. The programs "Intramural/CSIC" 200920I212, Juan de la Cierva, and FCT (Portugal) supported O.B., M.D.-M., and I.G.-R., respectively. This work was supported by grants BFU2008-04362 and BFU2011-22916.

Received: December 13, 2011
Revised: June 4, 2012
Accepted: September 6, 2012
Published online: October 4, 2012

REFERENCES

Bateman, J., Reddy, R.S., Saito, H., and Van Vactor, D. (2001). The receptor tyrosine phosphatase Dlar and integrins organize actin filaments in the Drosophila follicular epithelium. Curr. Biol. 11, 1317–1327.

Bryant, D.M., and Mostov, K.E. (2008). From cells to organs: building polarized tissue. Nat. Rev. Mol. Cell Biol. 9, 887–901.

Developmental Cell
Numbs/Opo Antagonism Controls Optic Cup Formation

Calderwood, D.A., Fujioka, Y., de Pereda, J.M., Garcı´a-Alvarez, B., Nakamoto, T., Margolis, B., McGlade, C.J., Liddington, R.C., and Ginsberg, M.H. (2003). Integrin beta cytoplasmic domain interactions with phosphotyrosine-binding domains: a structural prototype for diversity in integrin signaling. Proc. Natl. Acad. Sci. USA 100, 2272–2277.

Caswell, P.T., Vadrevu, S., and Norman, J.C. (2009). Integrins: masters and slaves of endocytic transport. Nat. Rev. Mol. Cell Biol. 10, 843–853.

Chang, H.C., Newmyer, S.L., Hull, M.J., Ebersold, M., Schmid, S.L., and Mellman, I. (2002). Hsc70 is required for endocytosis and clathrin function in Drosophila. J. Cell Biol. 159, 477–487.

Chen, H., Zou, Z., Sarratt, K.L., Zhou, D., Zhang, M., Sebzda, E., Hammer, D.A., and Kahn, M.L. (2006). In vivo beta1 integrin function requires phosphorylation-independent regulation by cytoplasmic tyrosines. Genes Dev. 20, 927–932.

Collaco, A., Jakab, R., Hegan, P., Mooseker, M., and Ameen, N. (2010). Alpha-AP-2 directs myosin VI-dependent endocytosis of cystic fibrosis transmembrane conductance regulator chloride channels in the intestine. J. Biol. Chem. 285, 17177–17187.

Czuchra, A., Meyer, H., Legate, K.R., Brakebusch, C., and Fa¨ssler, R. (2006). Genetic analysis of beta1 integrin "activation motifs" in mice. J. Cell Biol. 174, 889–899.

Dho, S.E., Trejo, J., Siderovski, D.P., and McGlade, C.J. (2006). Dynamic regulation of mammalian numb by G protein-coupled receptors and protein kinase C activation: Structural determinants of numb association with the cortical membrane. Mol. Biol. Cell 17, 4142–4155.

Dong, B., Deng, W., and Jiang, D. (2011). Distinct cytoskeleton populations and extensive crosstalk control Ciona notochord tubulogenesis. Development 138, 1631–1641.

Ezratty, E.J., Bertaux, C., Marcantonio, E.E., and Gundersen, G.G. (2009). Clathrin mediates integrin endocytosis for focal adhesion disassembly in migrating cells. J. Cell Biol. 187, 733–747.

Filardo, E.J., Brooks, P.C., Deming, S.L., Damsky, C., and Cheresh, D.A. (1995). Requirement of the NPXY motifi n the integrin beta 3 subunit cytoplasmic tail for melanoma cell migration in vitro and in vivo. J. Cell Biol. 130, 441–450.

Formstecher, E., Aresta, S., Collura, V., Hamburger, A., Meil, A., Trehin, A., Reverdy, C., Betin, V., Maire, S., Brun, C., et al. (2005). Protein interaction mapping: a Drosophila case study. Genome Res. 15, 376–384.

Furutani-Seiki, M., and Wittbrodt, J. (2004). Medaka and zebrafish, an evolutionary twin study. Mech. Dev. 121, 629–637.

Gutzman, J.H., Graeden, E.G., Lowery, L.A., Holley, H.S., and Sive, H. (2008). Formation of the zebrafish midbrain-hindbrain boundary constriction requires laminin-dependent basal constriction. Mech. Dev. 125, 974–983.

He, L., Wang, X., Tang, H.L., and Montell, D.J. (2010). Tissue elongation requires oscillating contractions of a basal actomyosin network. Nat. Cell Biol. 12, 1133–1142.

Huang, E.J., Li, H., Tang, A.A., Wiggins, A.K., Neve, R.L., Zhong, W., Jan, L.Y., and Jan, Y.N. (2005). Targeted deletion of numb and numblike in sensory neurons reveals their essential functions in axon arborization. Genes Dev. 19, 138–151.

Hurtado, L., Caballero, C., Gavilan, M.P., Cardenas, J., Bornens, M., and Rios, R.M. (2011). Disconnecting the Golgi ribbon from the centrosome prevents directional cell migration and ciliogenesis. J. Cell Biol. 193, 917–933.

Kawakami, K. (2007). Tol2: a versatile gene transfer vector in vertebrates. Genome Biol. 8 (Suppl 1), S7.

Knoblich, J.A., Jan, L.Y., and Jan, Y.N. (1995). Asymmetric segregation of Numb and Prospero during cell division. Nature 377, 624–627.

Ko¨lsch, V., Seher, T., Fernandez-Ballester, G.J., Serrano, L., and Leptin, M. (2007). Control of Drosophila gastrulation by apical localization of adherens junctions and RhoGEF2. Science 315, 384–386.

Kuo, J.C., Han, X., Hsiao, C.T., Yates, J.R., 3rd, and Waterman, C.M. (2011). Analysis of the myosin-II-responsive focal adhesion proteome reveals a role for b-Pix in negative regulation off ocal adhesion maturation. Nat. Cell Biol. 13, 383–393.

Kwan, K.M., Fujimoto, E., Grabher, C., Mangum, B.D., Hardy, M.E., Campbell, D.S., Parant, J.M., Yost, H.J., Kanki, J.P., and Chien, C.B. (2007). The Tol2kit: a multisite gateway-based construction kit for Tol2 transposon transgenesis constructs. Dev. Dyn. 236, 3088–3099.

Lecuit, T., and Lenne, P.F. (2007). Cell surface mechanics and the control of cell shape, tissue patterns and morphogenesis. Nat. Rev. Mol. Cell Biol. 8, 633–644.

Letizia, A., Sotillos, S., Campuzano, S., and Llimargas, M. (2011). Regulated Crb accumulation controls apical constriction and invagination in Drosophila tracheal cells. J. Cell Sci. 124, 240–251.

Levayer, R., Pelissier-Monier, A., and Lecuit, T. (2011). Spatial regulation of Dia and Myosin-II by RhoGEF2 controls initiation of E-cadherin endocytosis during epithelial morphogenesis. Nat. Cell Biol. 13, 529–540.

Martin, A.C., Kaschube, M., and Wieschaus, E.F. (2009). Pulsed contractions of an actin-myosin network drive apical constriction. Nature 457, 495–499.

Martinez-Morales, J.R., and Wittbrodt, J. (2009). Shaping the vertebrate eye. Curr. Opin. Genet. Dev. 19, 511–517.

Martinez-Morales, J.R., Rembold, M., Greger, K., Simpson, J.C., Brown, K.E., Quiring, R., Pepperkok, R., Martin-Bermudo, M.D., Himmelbauer, H., and Wittbrodt, J. (2009). ojoplano-mediated basal constriction is essential for optic cup morphogenesis. Development 136, 2165–2175.

Mertes, F., Martinez-Morales, J.R., Nolden, T., Spo¨rle, R., Wittbrodt, J., Lehrach, H., and Himmelbauer, H. (2009). Cloning of mouse ojoplano, a reticular cytoplasmic protein expressed during embryonic development. Gene Expr. Patterns 9, 562–567.

Montell, D.J. (2008). Morphogenetic cell movements: diversity from modular mechanical properties. Science 322, 1502–1505.

Nelson, W.J. (2009). Remodeling epithelial cell organization: transitions between front-rear and apical-basal polarity. Cold Spring Harb. Perspect. Biol. 1, a000513.

Niikura, Y., Tabata, Y., Tajima, A., Inoue, I., Arai, K., and Watanabe, S. (2006). Zebrafish Numb homologue: phylogenetic evolution and involvement in regulation ofl eft-right asymmetry. Mech. Dev. 123, 407–414.

Nishimura, T., and Kaibuchi, K. (2007). Numb controls integrin endocytosis for directional cell migration with aPKC and PAR-3. Dev. Cell 13, 15–28.

O'Connor-Giles, K.M., and Skeath, J.B. (2003). Numb inhibits membrane localization of Sanpodo, a four-pass transmembrane protein, to promote asymmetric divisions in Drosophila. Dev. Cell 5, 231–243.

Papusheva, E., and Heisenberg, C.P. (2010). Spatial organization of adhesion: force-dependent regulation and function in tissue morphogenesis. EMBO J. 29, 2753–2768.

Rasin, M.R., Gazula, V.R., Breunig, J.J., Kwan, K.Y., Johnson, M.B., Liu-Chen, S., Li, H.S., Jan, L.Y., Jan, Y.N., Rakic, P., and Sestan, N. (2007). Numb and Numbl are required for maintenance of cadherin-based adhesion and polarity of neural progenitors. Nat. Neurosci. 10, 819–827.

Reugels, A.M., Boggetti, B., Scheer, N., and Campos-Ortega, J.A. (2006). Asymmetric localization of Numb:EGFP in dividing neuroepithelial cells during neurulation in Danio rerio. Dev. Dyn. 235, 934–948.

Santolini, E., Puri, C., Salcini, A.E., Gagliani, M.C., Pelicci, P.G., Tacchetti, C., and Di Fiore, P.P. (2000). Numb is an endocytic protein. J. Cell Biol. 151, 1345–1352.

Sawyer, J.M., Harrell, J.R., Shemer, G., Sullivan-Brown, J., Roh-Johnson, M., and Goldstein, B. (2010). Apical constriction: a cell shape change that can drive morphogenesis. Dev. Biol. 341, 5–19.

Schoenenberger, C.A., Zuk, A., Zinkl, G.M., Kendall, D., and Matlin, K.S. (1994). Integrin expression and localization in normal MDCK cells and transformed MDCK cells lacking apical polarity. J. Cell Sci. 107, 527–541.

Schotman, H., Karhinen, L., and Rabouille, C. (2008). dGRASP-mediated noncanonical integrin secretion is required for Drosophila epithelial remodeling. Dev. Cell 14, 171–182.

Shaye, D.D., Casanova, J., and Llimargas, M. (2008). Modulation ofi ntracellular trafficking regulates cell intercalation in the Drosophila trachea. Nat. Cell Biol. 10, 964–970.

Developmental Cell

Numbs/Opo Antagonism Controls Optic Cup Formation

Smith, C.A., Lau, K.M., Rahmani, Z., Dho, S.E., Brothers, G., She, Y.M., Berry, D.M., Bonneil, E., Thibault, P., Schweisguth, F., et al. (2007). aPKC-mediated phosphorylation regulates asymmetric membrane localization of the cell fate determinant Numb. EMBO J. 26, 468–480.

Solon, J., Kaya-Copur, A., Colombelli, J., and Brunner, D. (2009). Pulsed forces timed by a ratchet-like mechanism drive directed tissue movement during dorsal closure. Cell 137, 1331–1342.

Sousa, R., and Lafer, E.M. (2006). Keep the traffic moving: mechanism of the Hsp70 motor. Traffic 7, 1596–1603.

Teckchandani, A., Toida, N., Goodchild, J., Henderson, C., Watts, J., Wollscheid, B., and Cooper, J.A. (2009). Quantitative proteomics identifies a Dab2/integrin module regulating cell migration. J. Cell Biol. 186, 99–111.

Thermes, V., Grabher, C., Ristoratore, F., Bourrat, F., Choulika, A., Wittbrodt, J., and Joly, J.S. (2002). I-SceI meganuclease mediates highly efficient transgenesis in fish. Mech. Dev. 118, 91–98.

Tong, X., Zitserman, D., Serebriiskii, I., Andrake, M., Dunbrack, R., and Roegiers, F. (2010). Numb independently antagonizes Sanpodo membrane targeting and Notch signaling in Drosophila sensory organ precursor cells. Mol. Biol. Cell 21, 802–810.

Ulrich, F., and Heisenberg, C.P. (2009). Trafficking and cell migration. Traffic 10, 811–818.

Ungewickell, E.J., and Hinrichsen, L. (2007). Endocytosis: clathrin-mediated membrane budding. Curr. Opin. Cell Biol. 19, 417–425.

Wakamatsu, Y., Maynard, T.M., Jones, S.U., and Weston, J.A. (1999). NUMB localizes in the basal cortex of mitotic avian neuroepithelial cells and modulates neuronal differentiation by binding to NOTCH-1. Neuron 23, 71–81.

Wang, Z., Sandiford, S., Wu, C., and Li, S.S. (2009). Numb regulates cell-cell adhesion and polarity in response to tyrosine kinase signalling. EMBO J. 28, 2360–2373.

Wu, M., Smith, C.L., Hall, J.A., Lee, I., Luby-Phelps, K., and Tallquist, M.D. (2010). Epicardial spindle orientation controls cell entry into the myocardium. Dev. Cell 19, 114–125.

Zhong, W., Jiang, M.M., Weinmaster, G., Jan, L.Y., and Jan, Y.N. (1997). Differential expression of mammalian Numb, Numblike and Notch1 suggests distinct roles during mouse cortical neurogenesis. Development 124, 1887–1897.

Zhong, W., Jiang, M.M., Schonemann, M.D., Meneses, J.J., Pedersen, R.A., Jan, L.Y., and Jan, Y.N. (2000). Mouse numb is an essential gene involved in cortical neurogenesis. Proc. Natl. Acad. Sci. USA 97, 6844–6849.

Zhou, P., Alfaro, J., Chang, E.H., Zhao, X., Porcionatto, M., and Segal, R.A. (2011). Numb links extracellular cues to intracellular polarity machinery to promote chemotaxis. Dev. Cell 20, 610–622.

XII. Acknowledgments

Si ahora estoy aquí escribiendo estas palabras es porque después de cinco largos años esta aventura llega a su fin. Como todas las aventuras, esta está llena de anécdotas buenas y no tan buenas, de muchas muchas sonrisas pero también de algunas lágrimas, de peces zebra y medaka, pero sobre todo, está llena de amigos y compañeros sin los cuales este final hubiera sido impensable. Y a todos os dedico estas líneas aunque un "muchas gracias" me sabe a poco para vosotros!

En primer lugar quería dar las gracias a Juan, mi jefe y director de tesis, por acogerme en el laboratorio, depositar su confianza en mí y brindarme la oportunidad de hacerme doctora. Por todo lo que he aprendido en estos años de doctoranda, por tu capacidad de ver soluciones ante las dificultades, por tu cercanía y accesibilidad, y por "tirar" un poco de mí cuando he estado a punto de abandonar el barco. Gracias.

También quiero agradecer aquel paréntesis alemán en Karlsruhe, porque viajar abre la mente y visitar otro laboratorio puede ser una experiencia única. I would also want to thank Félix Loosli, my advisor during my short stay in Karlsruhe, for receiving me in your lab at the KIT, for your patient and your help. Thanks to Clathrin for being always ready to help me. To Sachin, my lab mate, Marika and Pietro for all the great moments I enjoyed there. Gracias también a Inés y José Fernando, por vuestro cariño, por hacerme sentir una más, y por demostrar una vez más que el mundo es un pañuelo y se pueden conocer dos murcianos estando de estancia. Thank you to Michi, my flatmate, for teaching me that a german guy can be an atypical german guy! For your help with my "german", for all the conversations we had about Germany and Spain, the life, the future... and for your friendship.

Gracias a JL Gómez-Skarmeta y a toda la gente de su labo. A Miñán, Eli, Silvia, Juan, Zé y Renata por vuestra ayuda a lo largo de estos cinco años, por enseñarme a pensar y a hacer ciencia. A Ana Neto, por tener siempre una sonrisa que ofrecer, a Royo, por tus consejos, tu alegría y por contagiar el entusiasmo por la ciencia. A Mario, a Carlos y a Ariza por las risas de pasillos, despacho y fishroom, porque reírse de la rutina es la mejor forma de romper con ella.

Y como no, un muchísimas gracias a todos mis compis de labo. A Mariana, por lo que siempre me has ayudado con los lab/fish/dev meetings y en especial, durante la escritura de esta tesis. A Ozren, gracias por las bromas del día a día, por tu sentido crítico, por los "group hugs" y porque a veces has confiado en mí, más que yo misma. A Joaquín, Joaquinillo, porque tu llegada ha sido como una brisa de aire renovado; gracias por tu ayuda, por tus consejos, por estar siempre dispuesto a mirar unos resultados o a preparar una barbacoa, por tu sentido del humor y por tu paciencia con el mío. A Cristina, gracias porque antes de entrar en el labo ya tenías tiempo para escuchar mis historias y darme

algún consejillo. A Javi, Helena, Rosa y a todos los que han pasado por el labo en estos años, en especial a Franz for sharing your physicist opinion and helping me with some analysis of this thesis. A Rocío, gracias por tu amistad, por estar ahí SIEMPRE, por tu sensibilidad para detectar si algo me pasa, por tu preocupación por velar que todo esté bien, por estar siempre dispuesta a ayudar y por la dulzura y serenidad con la que respondes a todo. Eres un cielo. A Inés, mi compañera de tesis, y ante todo mi amiga. Gracias por estar siempre ahí, porque ha sido un placer reír, llorar, viajar y en definitiva crecer contigo en el mundo de la ciencia. Porque has demostrado que el trabajo duro al final obtiene su recompensa. Gracias por tu apoyo y tu cariño.

Gracias también a las otras dos supergirls; Mª Ángeles, por todas las risas que hemos compartido, por escucharme en mis momentos de desesperación, por tu cariño y por transmitirme tus insaciables ganas de superación y tu espíritu luchador. A Adela, por tu paciencia y tu comprensión, por aportar otro punto de vista, por desprender energía positiva donde quiera que vas. A las tres, gracias por las comidas de los martes, las clases de sevillanas, las ferias, los viajes… en resumen, por hacer que mi paso por Sevilla haya sido increíble. Inés, Mª Ángeles y Adela sois las mejores.

Otro gracias a toda la gente del CABD que de una u otra forma ha ayudado a que esta historia se llene de buenos momentos. A David, por tu risa contagiosa, porque nadie dice: "Murcia que hermosa eres!" con tanta gracia y porque eres un gran amigo. A los damianes; Juan Carlos, Ibai y David por ser los fichajes revelación. A Xabi, por tus consejos y tus bromas para levantar el ánimo. A Kathy, Lesly y Corín por vuestra ayuda. Mer, Mario, Manolo por vuestro apoyo y por convertir cualquier momento en un buen rato, gracias.

A Justi, por aguantar mi humor al llegar a casa después de un largo día y sacarme a tomar un algo para despejarme y sacarme una sonrisa.

A Tania y a Alberto, mis compis de piso y mis amigos, gracias por las comiditas de mediodía, por hacer más llevaderos estos últimos meses entre bromas y risas, por compartir sueños, ilusiones y anécdotas.

A Ángel, gracias por los helados de los domingos y por animarme en la última fase.

A Marga y Joaquín, gracias por acogerme como a una más de la familia y estar siempre pendiente de que esté bien por tierras andaluzas.

Y como buena murciana, también me acuerdo de mis murcianos estén donde estén, porque ellos siempre tienen un ratico para mí. Alex, gracias por tu ayuda, por tus ánimos y porque siempre da gusto compartir las penas con alguien que te entiende. Javi y MªTeresa, millones de gracias por las horas de Matlab, por la fundación de UMOC y todas las anécdotas que eso nos ha traído y nos traerá, por estar siempre ahí vaya donde vaya listos para un viaje por la Selva Negra, un fin de semana en Sagres o un Skype, por ironizar ante

las dificultades y convertirlas en risas, y por demostrar que donde caben 2 caben 4! Claudia y Bea, gracias por estar siempre dispuestas a escuchar y por preocuparos por mí y mis progresos semana tras semana.

Y otro gracias enorme a mis biólog@s, porque a pesar de la distancia han vivido esta tesis muy de cerca, porque no importan los kilómetros si se trata de ponernos al día, de organizar un fin de semana de locas o montar una boda. Patri, por los puntazos Patri. Maribel, por las cenitas biologuiles. Rodri, por los momentos de facultad. Juanma, por la ilusión que pones y transmites en todo lo que haces. Aarón, por ser uno más de los nuestros. Santi, por los ratos del aulario que fueron el comienzo de todo y por cómo nos mimas. Clara, por emanar "buen rollo" y porque de fiesta se sale con los labios rojos. Eli, por entender el cariño que hay detrás de "mis sentencias". Cris, por tener siempre un "venga chicas" de ánimo para regalarnos. Isa y Elena, porque fuisteis las últimas incorporaciones, pero da gusto contar con vosotras. Poci, porque mudarse a Israel no cambia las cosas. Ana Tapia, porque eres pura energía y por estar siempre dispuesta a una fiesta biologuil. María, por las llamadas para desahogarnos, por compartir las historias del día a día y por ser una gran amiga. Ana, porque desde que te conozco siempre puedo contar contigo y eso lo dice todo de ti. Mar, por desprender alegría allá donde vas, por no dejar de sorprenderme por mucho que pasen los años y por estar siempre ahí.

Gracias a mis padres y a mi hermano, por vuestro apoyo en este proyecto sin entenderlo muy bien, por empujarme a continuar por difícil que fuera el camino, y por apostar siempre por mi formación.

Y el gracias con mayúsculas es para ti, Manu, mi compañero de aventuras, mi confidente y mi apoyo incondicional. Porque para mí eres el ejemplo de perseverancia y entusiasmo. Por conocerme tanto, porque es inevitable reírse con tu/mi duende hasta llorar y porque esto es sólo el principio.

A todos vosotros, y a los que no he nombrado pero también están ahí:

MUCHAS GRACIAS DE CORAZÓN